



**HAL**  
open science

# Detection of emotions from video in non-controlled environment

Rizwan Ahmed Khan

► **To cite this version:**

Rizwan Ahmed Khan. Detection of emotions from video in non-controlled environment. Image Processing [eess.IV]. Université Claude Bernard - Lyon I, 2013. English. NNT : 2013LYO10227 . tel-01166539v2

**HAL Id: tel-01166539**

**<https://theses.hal.science/tel-01166539v2>**

Submitted on 23 Jun 2015

**HAL** is a multi-disciplinary open access archive for the deposit and dissemination of scientific research documents, whether they are published or not. The documents may come from teaching and research institutions in France or abroad, or from public or private research centers.

L'archive ouverte pluridisciplinaire **HAL**, est destinée au dépôt et à la diffusion de documents scientifiques de niveau recherche, publiés ou non, émanant des établissements d'enseignement et de recherche français ou étrangers, des laboratoires publics ou privés.



THESE DE L'UNIVERSITE DE LYON

Dlivre par

L'UNIVERSITE CLAUDE BERNARD - LYON 1

Ecole Doctorale Informatique et Mathématiques

DIPLOME DE DOCTORAT

P H D T H E S I S

**Détection des émotions à partir de vidéos dans un environnement non contrôlé**

**Detection of emotions from video in non-controlled environment**

Soutenue publiquement (Public defense) le 14/11/2013

par **Rizwan Ahmed KHAN**

Composition du jury (Dissertation committee):

---

*Rapporteurs*

Mr. Renaud SEGUIER      Professor, Supelec, CNRS UMR 6164, Rennes, France  
Mr. Jean-Claude MARTIN      Professor, LIMSI-CNRS, Université Paris-Sud, France

*Examineurs*

Mr. Thomas MOESLUND      Professor, Department of Architecture, Design and Media Technology,  
Aalborg University, Denmark  
Mr. Patrick LAMBERT      Professor, LISTIC - Polytech Annecy-Chambery, France  
Mr. Samir GARBAYA      Associate Professor, Le2i, ENSAM, Chalon sur Saone, France

*Directeur*

Mme. Saida BOUAKAZ      Professor, LIRIS-CNRS, Université Claude Bernard Lyon 1, France

*Co-encadrant*

Mr. Alexandre MEYER      Associate Professor, LIRIS, Université Claude Bernard Lyon 1, France  
Mr. Hubert KONIK      Associate Professor, LaHC, Université Jean Monnet, Saint-Etienne, France



*To my parents, my wife, my kids, my siblings and all of my teachers!*

*A mes parents, ma femme, mes enfants, mes frères et sœurs et tous  
mes enseignants!*

میرے والدین، اہلیہ، بچوں، بہن بھائیوں اور تمام اساتذہ کے نام !!

*and to all who are trying to make this world a better place to live !*





## Acknowledgements

I would like to take this opportunity to thank my thesis supervisors, Prof. Saida Bouakaz, Prof. Alexandre Meyer and Prof. Hubert Konik for their skillful guidance and assistance during the course of thesis. I appreciate their dedication and interest which made possible for me to access the required literature and eventually deliver results of appreciable quality and standard.

Secondly, I would like to thank reporter's of dissertation committee, Prof. Renaud Segurier and Prof. Jean-Claude Martin for their detailed report and their insightful comments and suggestions that certainly have improved the quality of thesis manuscript. I am also thankful to other members of dissertation committee which include Prof. Thomas Moeslund, Prof. Patrick Lambert and Prof. Samir Garbaya for their valuable suggestions while evaluating my research work.

Special thanks to all my friends, colleagues and research staff of Lab. Hubert Curien who spared their valuable time and participated in psycho-visual experiment.

I would also like to thank Région Rhône-Alpes France, for financially supporting this research work. Special thanks to administrative staff of LIRIS for helping me out to complete various administrative tasks.

Last but not the least I would like to extend thanks to all my family members (my parents, my sister, my brothers) specially my ever supporting wife (Sharmeen) and kids (Abdullah and Bilal) without them I wouldn't be able to put all my efforts required to produce the results which can stand in this competitive world.

*Rizwan Ahmed Khan*



# Abstract

Communication in any form i.e. verbal or non-verbal is vital to complete various daily routine tasks and plays a significant role in life. Facial expression is the most effective form of non-verbal communication and it provides a clue about emotional state, mindset and intention.

Generally automatic facial expression recognition framework consists of three step: face tracking, feature extraction and expression classification. In order to built robust facial expression recognition framework that is capable of producing reliable results, it is necessary to extract features (from the appropriate facial regions) that have strong discriminative abilities. Recently different methods for automatic facial expression recognition have been proposed, but invariably they all are computationally expensive and spend computational time on whole face image or divides the facial image based on some mathematical or geometrical heuristic for features extraction. None of them take inspiration from the human visual system in completing the same task. In this research thesis we took inspiration from the human visual system in order to find from where (facial region) to extract features. We argue that the task of expression analysis and recognition could be done in more conducive manner, if only some regions are selected for further processing (i.e. salient regions) as it happens in human visual system.

In this research thesis we have proposed different frameworks for automatic recognition of expressions, all getting inspiration from the human vision. Every subsequently proposed addresses the shortcomings of the previously proposed framework. Our proposed

frameworks in general, achieve results that exceeds state-of-the-art methods for expression recognition. Secondly, they are computationally efficient and simple as they process only perceptually salient region(s) of face for feature extraction. By processing only perceptually salient region(s) of the face, reduction in feature vector dimensionality and reduction in computational time for feature extraction is achieved. Thus making them suitable for real-time applications.

**Keywords:** expression recognition, human visual system, eye-tracker, saliency detection, gaze maps, pyramid histogram of oriented gradients (PHOG), pyramid of local binary pattern (PLBP), supervised learning, SVM, decision tree.

## Résumé

Dans notre communication quotidienne avec les autres, nous avons autant de considération pour l'interlocuteur lui-même que pour l'information transmise. En permanence coexistent en effet deux modes de transmission : le verbal et le non-verbal. Sur ce dernier thème intervient principalement l'expression faciale avec laquelle l'interlocuteur peut révéler d'autres émotions et intentions.

Habituellement, un processus de reconnaissance d'émotions faciales repose sur 3 étapes : le suivi du visage, l'extraction de caractéristiques puis la classification de l'expression faciale. Pour obtenir un processus robuste apte à fournir des résultats fiables et exploitables, il est primordial d'extraire des caractéristiques avec de forts pouvoirs discriminants (selon les zones du visage concernées). Les avancées récentes de l'état de l'art ont conduit aujourd'hui à diverses approches souvent bridées par des temps de traitement trop coûteux compte-tenu de l'extraction de descripteurs sur le visage complet ou sur des heuristiques mathématiques et/ou géométriques. En fait, aucune réponse bio-inspirée n'exploite la perception humaine dans cette tâche qu'elle opère pourtant régulièrement. Au cours de ses travaux de thèse, la base de notre approche fut ainsi de s'inspirer du modèle visuel pour focaliser le calcul de nos descripteurs sur les seules régions du visage essentielles pour la reconnaissance d'émotions. Cette approche nous a permis de concevoir un processus plus naturel basé sur ces seules régions émergentes au regard de la perception humaine. Ce manuscrit présente les différentes méthodologies bio-inspirées mises en place pour aboutir à des résultats qui améliorent généralement l'état de l'art sur les bases de référence.

Ensuite, compte-tenu du fait qu'elles se focalisent sur les seules parties émergentes du visage, elles améliorent les temps de calcul et la complexité des algorithmes mis en jeu conduisant à une utilisation possible pour des applications temps réel.

**Mots clé** : reconnaissance d'émotions, système visuel humain, suivi du regard, oculométrie, émergence, suivi du regard, PHOG, PLBP, apprentissage supervisé, SVM, arbre de décision.





# Contents

<b>Contents</b>	<b>xi</b>
<b>List of Figures</b>	<b>xvii</b>
<b>1 Introduction</b>	<b>1</b>
1.1 Motivation . . . . .	1
1.2 Current approaches . . . . .	3
1.2.1 Challenges . . . . .	4
1.3 Our approach and contributions . . . . .	5
1.3.1 Visual attention and saliency . . . . .	5
1.3.2 Computational efficiency . . . . .	7
1.3.3 Expression recognition on low resolution stimuli . . . . .	7
1.3.4 Recognition of “pain” expression . . . . .	7
1.3.5 Database . . . . .	8
1.4 Application areas . . . . .	8
1.5 Publications . . . . .	10
1.6 Structure of the report . . . . .	11
<b>2 Literature survey</b>	<b>13</b>
2.1 Psychology and cognitive science on facial affect theory . . . . .	14
2.1.1 Ekman’s six basic emotions . . . . .	15
2.1.2 Facial Action Coding System (FACS) . . . . .	17
2.1.2.1 FACS AU combinations and intensity . . . . .	17
2.1.2.2 Drawbacks of Facial Action Coding System (FACS) . . . . .	19
2.1.3 Plutchik’s emotion wheel . . . . .	19

2.1.4	Russell’s circumplex model . . . . .	21
2.2	Databases for facial expression recognition . . . . .	22
2.3	Automatic recognition of facial expressions . . . . .	25
2.3.1	Face detection and tracking . . . . .	25
2.3.1.1	Knowledge-based methods . . . . .	26
2.3.1.2	Feature invariant approaches . . . . .	27
2.3.1.3	Template matching methods . . . . .	28
2.3.1.4	Appearance-based methods . . . . .	30
2.3.2	Feature extraction . . . . .	33
2.3.2.1	Appearance based methods . . . . .	34
2.3.2.2	Geometric feature based methods . . . . .	38
2.3.3	Expression classification / recognition . . . . .	40
2.3.3.1	Template based methods . . . . .	40
2.3.3.2	Support Vector Machines based methods . . . . .	41
2.3.3.3	Boosting based methods . . . . .	42
2.3.3.4	Classification trees . . . . .	44
2.3.3.5	Instance based learning . . . . .	44
2.3.3.6	Naïve Bayes classifiers . . . . .	44
2.4	Drawbacks of the current methods and contributions . . . . .	46
2.4.1	Exploiting visual saliency . . . . .	46
2.4.1.1	Computational simplicity . . . . .	47
2.4.1.2	Adequacy for low resolution stimuli . . . . .	47
2.4.2	Expressions different from six prototypical facial expression .	47
<b>3</b>	<b>Psycho-Visual experiment</b>	<b>49</b>
3.1	Methods . . . . .	50
3.1.1	Participants . . . . .	51
3.1.2	Eye-tracker . . . . .	52
3.1.2.1	Tracker application . . . . .	54
3.1.3	Experiment builder . . . . .	56
3.1.3.1	Features . . . . .	56
3.1.3.2	Organization of events in an experiment . . . . .	56
3.2	Procedure . . . . .	57

3.2.1	Eye movement recording . . . . .	60
3.2.2	Stimuli . . . . .	60
3.3	Psycho-Visual experiment: results and discussion . . . . .	61
3.3.1	Gaze map construction . . . . .	61
3.3.2	Observations from the gaze maps . . . . .	62
3.3.3	Substantiating observations through statistical analysis . . . . .	63
3.4	Conclusion . . . . .	68
<b>4</b>	<b>Facial expression recognition based on brightness and entropy features</b>	<b>71</b>
4.1	Salient region detection . . . . .	73
4.1.1	Biologically based . . . . .	74
4.1.2	Computational models . . . . .	75
4.1.2.1	Frequency-tuned salient region detection (FT) . . . . .	75
4.1.2.2	Graph Based Visual Saliency (GBVS) method . . . . .	76
4.1.2.3	Spectral Residual(SR) approach . . . . .	77
4.1.3	Conclusion . . . . .	79
4.2	Feature extraction . . . . .	79
4.2.1	Brightness calculation . . . . .	81
4.2.2	Entropy calculation . . . . .	83
4.3	Experiments . . . . .	84
4.3.1	Experiment on the extended Cohn-Kanade (CK+) database . . . . .	85
4.3.1.1	Comparison with state-of-the-art methods . . . . .	85
4.3.2	Experiment on the FG-NET FEED database . . . . .	86
4.4	Drawbacks of the proposed algorithm . . . . .	87
<b>5</b>	<b>Facial region shape analysis for recognition of expressions</b>	<b>89</b>
5.1	Proposed framework . . . . .	90
5.2	Feature extraction using PHOG . . . . .	92
5.3	Discriminative strength of PHOG features . . . . .	94
5.4	Expression recognition experiments . . . . .	94
5.4.1	First experiment: CK+ database . . . . .	96
5.4.1.1	Behavior of the classifiers . . . . .	97

5.4.1.2	Comparison with the state-of-the-art methods . . .	98
5.4.2	Second experiment: generalization on the new dataset . . . .	99
5.4.3	Third experiment: low resolution image sequences . . . . .	101
5.5	Conclusion . . . . .	102
<b>6</b>	<b>Recognizing expressions by analyzing texture</b>	<b>105</b>
6.1	PLBP based framework . . . . .	106
6.1.1	Novelty of the proposed descriptor . . . . .	109
6.2	Expression recognition framework . . . . .	110
6.3	Results on universal expressions . . . . .	112
6.3.1	First experiment: posed expressions . . . . .	113
6.3.1.1	Results . . . . .	114
6.3.1.2	Comparisons . . . . .	115
6.3.2	Second experiment: low resolution image sequences . . . . .	118
6.3.3	Third experiment: generalization on the new dataset . . . . .	121
6.3.4	Fourth experiment: spontaneous expressions . . . . .	122
6.4	Pain recognition . . . . .	124
6.4.1	Novelty of proposed approach . . . . .	125
6.4.2	Pain expression database . . . . .	126
6.4.3	Framework . . . . .	126
6.4.4	Experiment . . . . .	128
6.5	Conclusion . . . . .	132
<b>7</b>	<b>Conclusion and perspectives</b>	<b>133</b>
7.1	Contributions . . . . .	133
7.1.1	Exploring human visual system . . . . .	134
7.1.2	Descriptor for low resolution stimuli . . . . .	136
7.1.3	Novel framework for pain recognition . . . . .	137
7.2	Perspectives . . . . .	137
<b>A</b>	<b>Facial expression databases</b>	<b>141</b>
A.1	Cohn-Kanade facial expression database . . . . .	142
A.2	MMI facial expression database . . . . .	143
A.3	FG-NET Facial Expressions and Emotion Database . . . . .	147

A.4	Japanese Female Facial Expression Database . . . . .	147
A.5	AR database . . . . .	149
A.6	CAS-PEAL Database . . . . .	150
A.7	Radboud Faces Databases (RaFD) . . . . .	152
A.8	Pain Expression Database . . . . .	153
A.9	Drawbacks of the current databases . . . . .	155
<b>B</b>	<b>Gaze Maps</b>	<b>157</b>
<b>C</b>	<b>Color space conversion</b>	<b>165</b>
	<b>References</b>	<b>167</b>



# List of Figures

1.1	Generic pipeline for facial expression recognition algorithms. . . . .	3
2.1	Example of expression for the six basic emotions (illustration taken from [Pan09]). Left-to-right from top row: disgust, happiness, sadness, anger, fear, and surprise. . . . .	16
2.2	Some examples of Action Units. Action Units are atomic facial muscle actions described in FACS (Illustration from [Val08]). . . . .	17
2.3	Upper facial Action Units (Illustration taken from [Val08]). . . . .	18
2.4	Lower facial Action Units (Illustration from [Val08]). . . . .	18
2.5	Action Units belonging to neither the upper nor the lower facial area (Illustration from [Val08]). . . . .	18
2.6	Plutchik's emotion wheel (left) and the accompanying emotion cone (right). . . . .	20
2.7	Russells circumplex model of emotions. . . . .	22
2.8	Automatic facial expression recognition system pipeline. . . . .	25
2.9	The image on the left is the Ratio Template (14 pixels by 16 pixels). The template is composed of 16 regions (gray boxes) and 23 relations (arrows). The image on the right is the Spatial Ratio Template. It is a modified version of the Ratio Template by incorporating the Golden Ratio. . . . .	29

2.10	The sum of the pixels within rectangle $D$ can be computed with four array references. The value of the integral image at location 1 is the sum of the pixels in rectangle $A$ . The value at location 2 is $A + B$ , at location 3 is $A + C$ , and at location 4 is $A + B + C + D$ . The sum within $D$ can be computed as $4+1-(2+3)$ . Illustration taken from [VJ01]. . . . .	32
2.11	Schematic depiction of a the detection cascade. A series of classifiers are applied to every sub-window. The initial classifier eliminates a large number of negative examples with very little processing. Subsequent layers eliminate additional negatives but require additional computation. After several stages of processing the number of sub-windows have been reduced radically. Further processing can take any form such as additional stages of the cascade or an alternative detection system. Illustration taken from [VJ01]. . . . .	33
2.12	The left, middle, and right graphics above show the absolute value, and the real and imaginary components of a sample Gabor filter. . .	35
2.13	The basic haar-like feature template. . . . .	36
2.14	Haar-like features extracted from different position and different scale on the face image. . . . .	37
2.15	Demonstration Landmarks on the face. . . . .	39
2.16	Hyperplane through two linearly separable classes. . . . .	42
2.17	$k$ -Nearest Neighbor in a two-dimensional space and where target function is boolean valued. A set of +ve and -ve training examples is shown on the left, along with a query instance $x_q$ to be classified. The 1-Nearest Neighbor algorithm classifies $x_q$ +ve whereas 5-Nearest Neighbor algorithm classifies it as -ve. On the right is the decision surface induced by the 1-Nearest Neighbor algorithm. The convex polygon surrounding each training example indicates the region of instance space closest to that point (i.e. the instance for which 1-Nearest Neighbor algorithm will assign the classification belonging to that training example). . . . .	45



3.1	Observer’s classification on the basis of age group. . . . .	51
3.2	Observer’s classification on the basis of their ethnicity. . . . .	52
3.3	Observer’s classification on the basis of their sex. . . . .	52
3.4	Eyelink II, Eye-tracker used in our experiment. . . . .	53
3.5	EyeLink II Camera Setup Screen. . . . .	55
3.6	EyeLink II Calibration Screen. . . . .	55
3.7	Block diagram of the experiment. . . . .	57
3.8	Hierarchical Organization of the experiment . . . . .	58
3.9	Experiment / eye-tracker setup. First row: tracker being adjusted on the head of an observer. Second row: stimulus display PC (on the left) and the PC connected to the eye-tracker / host PC on the right. Last row: after finalizing the setup stage of the experiment. . . . .	59
3.10	Examples of gaze maps for six universal expressions. Each video sequence is divided in three mutually exclusive time periods. First, second and third columns show average gaze maps for the first, second and third time periods of a particular stimuli respectively. . . . .	61
3.11	Time period wise average percentage of trial time observers have spent on gazing different facial regions. The error bars represent the standard error (SE) of the mean. First time period: initial frames of video sequence. Third time period: apex frames. Second time period: frames which has a transition from neutral face to particular expression. . . . .	63
3.12	Gaze maps for the facial expression of happiness. First, second and third columns show average gaze maps for the first, second and third time periods of stimuli respectively. Each row corresponds to different stimuli/video sequence for “sadness”. . . . .	64
3.13	Gaze maps for the facial expression of surprise. First, second and third columns show average gaze maps for the first, second and third time periods of stimuli respectively. Each row corresponds to different stimuli/video sequence for “sadness”. . . . .	65

3.14	Gaze maps for the facial expression of sadness. First, second and third columns show average gaze maps for the first, second and third time periods of stimuli respectively. Each row corresponds to different stimuli/video sequence for “sadness”.	66
3.15	Gaze maps for the facial expression of disgust. First, second and third columns shows average gaze maps for the first, second and third time periods of stimuli respectively. Each row corresponds to different stimuli/video sequence for “disgust”.	66
3.16	Gaze maps for the facial expression of fear. First, second and third columns show average gaze maps for the first, second and third time periods of stimuli respectively. Each row corresponds to different stimuli/video sequence for “fear”.	67
3.17	Gaze maps for the facial expression of anger. First, second and third columns show average gaze maps for the first, second and third time periods of stimuli respectively. Each row corresponds to different stimuli/video sequence for “anger”.	68
3.18	Summary of the facial regions that emerged as salient for six universal expressions. Salient regions are mentioned according to their importance (for example facial expression of “fear” has two salient regions but mouth is the most important region according to HVS).	69
4.1	Brightness and entropy values from three different facial regions.	73
4.2	Itti’s model architecture [IKN98].	75
4.3	Frequency-tuned salient region detection algorithm [AHES09].	76
4.4	Graph Based Visual Saliency (GBVS) method’s architecture (adopted from poster presentation [JHP06]).	77

4.5	Comparison of automatic detected salient regions with gaze map obtained from psycho-Visual experiment (see Chapter 3 for reference). First row: original image and average gaze map of fifteen observers. Second row: saliency maps obtained from GBVS [JHP06] and Itti methods [IKN98] (shown as heat maps.). Third row: saliency maps obtained from FT [AHES09] and SR methods [HZ07]. . . . .	78
4.6	Salient region detection for different expressions using FT [AHES09]. Each row shows detected salient regions in a complete frame along with the zoom of three facial regions i.e. eyes, nose and mouth. Brightness of the salient regions is proportional to its saliency. First row shows expression of happiness, second row: surprise, third row: sadness, fourth row: anger, fifth row: fear and sixth row: disgust . . . . .	80
4.7	Average entropy value for different facial regions. First time period: initial frames of video sequence. Third time period: apex frames. Second time period: frames which has a transition from neutral face to particular expression. . . . .	81
4.8	Color Coordinate Systems DEF and BCH [BB06]. . . . .	82
5.1	Schematic overview of the proposed framework . . . . .	91
5.2	HOG feature extraction. First row: input stimuli, second row: edge contours at three different pyramid levels, third row: histograms of gradients (HOG) at three respective levels. . . . .	93
5.3	HOG features for different expressions. First row: sadness, second row: surprise, third row: happiness, fourth row: anger and fifth row: disgust. First column shows stimuli and second column shows respective HOG (only mouth facial region) at three levels. . . . .	95
5.4	Evolution of the achieved average recognition accuracy for the six universal facial expressions with the increasing number of folds for the $k$ -fold cross validation technique. . . . .	98

5.5	Example of stimuli with decreasing image resolution. First column shows stimuli in original resolution. Second to fifth column show stimuli in spatial resolution of: 144 x 192, 72 x 96, 36 x 48 and 18 x 24 respectively. . . . .	101
5.6	Robustness of different classifiers for facial expression recognition with decreasing image resolution. . . . .	102
6.1	Pyramid of Local Binary Pattern. First row: stimuli at two different pyramid levels, second row: histograms of LBP at two respective levels, third row: final descriptor. . . . .	107
6.2	Examples of the extended LBP [OPM02]. The pixel values are bilinearly interpolated whenever the sampling point is not in the center of a pixel . . . . .	108
6.3	Schematic overview of the framework. . . . .	111
6.4	Evolution of the achieved average recognition accuracy for the six universal facial expressions with the increasing number of folds for the $k$ -fold cross validation technique. . . . .	116
6.5	Robustness of different methods for facial expression recognition with decreasing image resolution (CK database). PHOG[ICIP] corresponds to framework proposed by Khan et. al [KMKB12b] (framework explained in Chapter 5 and specifically Section 5.4.3), Gabor [CVPRW] corresponds to Tian’s work [Tia04], LBP[JIVC] and Gabor[JIVC] corresponds to results reported by Shan et. al [SGM09] . . . . .	120
6.6	Example of lowest tested facial resolution . . . . .	121
6.7	Examples frames from MMI-Facial Expression Database. The first row is taken from Part V of the database and shows expressions of happiness and disgust. The second row shows expressions of happiness and disgust taken from Part IV of the database. The third row shows four frames of a single sequence in which the participant showed an expression of disgust [VP10]. . . . .	123
6.8	Overview of the framework. . . . .	127

6.9	Results obtained with the proposed framework. Results are presented for four different classifiers, with the first row showing results for “SVM” and “2NN” while the second row showing results for “decision tree” and “random forest”. . . . .	129
6.10	Evolution of the achieved average recognition accuracy for the expression of pain with the increasing number of folds for the $k$ -fold cross validation technique. . . . .	130
7.1	The valence-arousal (V-A) space for emotion analysis. Illustration from [HTKW13]. . . . .	138
A.1	Example of Cohn- Kanade Facial Expression Database. . . . .	143
A.2	Example of MMI Facial Expression Database. . . . .	144
A.3	Examples of static frontal-view images of facial expressions in the MMI Facial Expression Database. . . . .	144
A.4	Examples of apex frames of dual-view image sequences in MMI Facial Expression Database. . . . .	145
A.5	Image captures from the video sequences of the six universal expressions from the FG-NET FEED. . . . .	148
A.6	Example images from the Japanese Female Facial Expression(JAFFE) database. . . . .	149
A.7	AR database. The conditions are (1) neutral, (2) smile, (3) anger, (4) scream, (5) left light on, (6) right light on, (7) both lights on, (8) sun glasses, (9) sun glasses/left light (10) sun glasses/right light, (11) scarf, (12) scarf/left light, (13) scarf/right light. . . . .	150
A.8	Pose variation in the CAS-PEAL database. The images were recorded using separate cameras triggered in close succession. The cameras are each about $22.5^0$ apart. Subjects were asked to look up, to look straight ahead, and to look down. Shown here are seven of the nine poses currently being distributed. . . . .	151
A.9	Illumination variation in the CAS-PEAL database. The images were recorded with constant ambient illumination and manually triggered fluorescent lamps. . . . .	152

A.10	(a) Eight emotional expressions from top left: sad, neutral, anger, contemptuous, disgust, surprise, fear and happiness, (b) Three gaze directions: left, straight and right, (c) Five camera angles at $180^{\circ}$ , $135^{\circ}$ , $90^{\circ}$ , $45^{\circ}$ and $0^{\circ}$ .	153
A.11	Examples of some of the sequences from the UNBC-McMaster Pain Shoulder Archive	154
B.1	Gaze maps for the expression of <b>happiness</b> .	158
B.2	Gaze maps for the expression of <b>surprise</b> .	159
B.3	Gaze maps for the expression of <b>sadness</b> .	160
B.4	Gaze maps for the expression of <b>disgust</b> .	161
B.5	Gaze maps for the expression of <b>fear</b> .	162
B.6	Gaze maps for the expression of <b>anger</b> .	163

# Chapter 1

## Introduction

### Contents

---

<b>1.1</b>	<b>Motivation</b>	<b>1</b>
<b>1.2</b>	<b>Current approaches</b>	<b>3</b>
1.2.1	Challenges	4
<b>1.3</b>	<b>Our approach and contributions</b>	<b>5</b>
1.3.1	Visual attention and saliency	5
1.3.2	Computational efficiency	7
1.3.3	Expression recognition on low resolution stimuli	7
1.3.4	Recognition of “pain” expression	7
1.3.5	Database	8
<b>1.4</b>	<b>Application areas</b>	<b>8</b>
<b>1.5</b>	<b>Publications</b>	<b>10</b>
<b>1.6</b>	<b>Structure of the report</b>	<b>11</b>

---

### 1.1 Motivation

Communication in any form i.e. verbal or non-verbal is vital to complete various daily routine tasks and plays a significant role in life. Facial expression is the most effective form of non-verbal communication and it provides a clue about

emotional state, mindset and intention [EFE72, EF75, Ekm01, Ekm93]. Facial expressions not only can change the flow of conversation [Bul01] but also provides the listeners a way to communicate a wealth of information to the speaker without even uttering a single word [Yng70]. According to [CLFD94, FDWS91] when the facial expression does not coincide with the other communication i.e. spoken words, then the information conveyed by the face gets more weight in decoding information.

The computing environment is moving towards human-centered designs instead of computer centered designs [PPNH06], and human's tend to communicate wealth of information through affective states or expressions. Traditional Human Computer Interaction (HCI) based systems ignores bulk of information communicated through those affective states and just caters for user's intentional input. As mentioned that paradigm is shifting towards human-centered designs, thus analysis of user affective states becomes inevitable. In near future humans will not interact with machines only through intentional inputs but also through their behavior i.e. affective states [ZPRH09, SBR10]. Therefore, computer vision research community has shown a lot of interest in analyzing and automatically recognizing facial expressions. There are lots of application areas that can benefit from a system that can recognize facial expressions i.e. human-computer interaction, entertainment, medical applications e.g. pain detection, social robots, deceit detection, interactive video and behavior monitoring (see Section 1.4 for the description).

Facial expressions are studied since ancient times, as it is one of the most important channel of non-verbal communication [AR92]. Initially facial expressions were studied by great philosophers and thinkers like Aristotle and Stewart. With Darwin, the study of facial expressions became an empirical study. In the computer vision community, the term "facial expression recognition" often refers to the classification of facial features in one of the six so called basic or universal emotions: happiness, sadness, fear, disgust, surprise and anger, as introduced by Ekman in 1971 [Ekm71]. We, the humans, understand various facial expressions everyday without any extra effort. But for computer based systems on the other side, it is still hard to recognize them automatically



due to face appearance changes caused by pose variations, illumination variations and camera quality and angle changes.

## 1.2 Current approaches

There exist two main methodologies to analyze expressions in computer science: a) vision based methods b) audio based methods. Some researchers have found out that the combination of audio and visual signals gives better results [ZHF<sup>+</sup>06]. However, due to the fact that expressions can be emitted by a face without any sound, vision based methods are still the hottest research area in human affection.

Thus, our research work has focused only the *Vision based methods*. Vision based methods for expression analysis operate on images or images sequences. Generally, *Vision based* facial expression recognition system consists of three steps:

1. Face detection and tracking
2. Feature extraction
3. Expression classification / recognition



Figure 1.1: Generic pipeline for facial expression recognition algorithms.

The first step in facial expression analysis is to detect the face in the given image or video sequence. Locating the face within an image is termed as face detection or face localization whereas locating the face and tracking it across the different frames of a video sequence is termed as face tracking.

Extraction of selected features is the second and the most important step to successfully analyze and recognize facial expressions automatically. The optimal

features should minimize within-class variations of expressions while maximize between class variations. Usually, there are two ways to extract facial features: the geometric features and the appearance features. Normally geometric features come from the shapes of the facial components and the location of facial salient points (corners of the eyes, mouth, etc.). Appearance features are extracted by recording appearance changes of the face. *This research work has mainly focused on the second step.*

Third and the last step of automatic expression analysis system is classification. Some systems directly classify expressions while others classify expressions by first recognizing particular action units “AU” [EF78] (see Section 2.1.2 for the description of FACS (facial action coding system) and AU).

### 1.2.1 Challenges

Although different proposed methods for facial expression recognition have achieved good results, there still remains different problems that need to be addressed by the research community.

1. Generally, we have found that all the reviewed methods for automatic facial expression recognition are computationally expensive and usually require dimensionally large feature vector to complete the task. This explains their inability for real-time applications, although they produce good results on different datasets.
2. Smart meeting, video conferencing and visual surveillance are some of the real world applications that require facial expression recognition system that works adequately on low resolution images. There exist lots of methods for facial expression recognition but very few of those methods provide results or work adequately on low resolution images.
3. More research effort is required to be put forth for recognizing more complex facial expressions than the six classical, such as fatigue, pain, and mental states such as agreeing, disagreeing, lie, frustration, thinking as they have numerous application areas.

4. Other problems include expression intensity estimation, spontaneous expression recognition, micro expression recognition (brief, involuntary facial expression, lasts only 1/25 to 1/15 of a second), mis-alignment problem, illumination, and face pose variation.

## 1.3 Our approach and contributions

Recently different methods for automatic facial expression recognition have been proposed [LBF<sup>+</sup>06, ZP07, KZP08, YLM10, VPP05, GL13, ZLY<sup>+</sup>12, WWJ13] but none of them try to mimic or understand human visual system in recognizing them. Rather all of the methods, spend computational time on whole face image or divides the facial image based on some mathematical or geometrical heuristic for features extraction. We argue that the task of expression analysis and recognition could be done in more conducive manner, if only some regions are selected for further processing (i.e. salient regions) as it happens in human visual system [Zha06].

### 1.3.1 Visual attention and saliency

Humans have the amazing ability to decode facial expressions across different cultures, in diverse conditions and in a very short time. Human visual system (HVS) has limited neural resources but still it can analyze complex scenes in real-time. As an explanation for such performance, it has been proposed that only some visual inputs are selected by considering “salient regions” [Zha06], where “salient” means most noticeable or most important.

Visual attention is the ability of a vision system, biological or artificial, to rapidly detect potentially relevant parts of a visual scene, on which higher level vision tasks, such as object recognition, can focus. It is generally agreed today that under normal circumstances human eye movements are tightly coupled to visual attention [JOW<sup>+</sup>05]. William James [Jam90] described Visual attention as the process in which mind takes possession of one out of what seems several simultaneously possible objects. “Focalization, concentration, of consciousness are of its essence. It implies withdrawal from some things in order to deal effectively

with others, and is a condition which has a real opposite in the confused, dazed, scatterbrained state which in French is called distraction, and Zerstreutheit in German”.

Eye fixations describe the way in which visual attention is directed towards salient regions in a given stimuli [RCB02]. In computer vision the notion of saliency was mainly popularized by Tsotsos et al. [TSW<sup>+</sup>95] and Olshausen et al. [OAVE93] with their work on visual attention, and by Itti et al. [IKN98] with their work on rapid scene analysis. Recently, computer vision research community has shown lot of interest in understanding human visual attention phenomenon as it has been shown that such an approach could drastically reduce the need for computational resources without altering the quality of results [Har06].

To determine which facial region(s) is salient according to human vision, we have conducted psycho-visual experiment (see Chapter 3 for details). The experiment has been conducted with the help of an eye-tracking system which records the fixations and saccades. It is known that eye gathers most of the information during the fixations [RCB02] as eye fixations describe the way in which visual attention is directed towards salient regions in a given stimuli. Results of the visual experiment provided the evidence that human visual system either gives importance to one i.e. mouth or to two facial regions i.e. eyes and mouth, while decoding six universal facial expressions (for reference see Section 3.3). In the same manner, we argue that the task of expression analysis and recognition could be done in more conducive manner, if same regions are selected for further processing.

To test and prove our argument we have proposed different algorithms for facial expression recognition, where first part of dividing the face into salient regions is inspired by human vision (refer Chapter 3). Every subsequently proposed addresses the shortcomings of the previously proposed framework (see Chapters 4, 5 and 6). Our proposed frameworks in general, achieve results that exceeds state-of-the-art methods for expression recognition. Secondly, they are computationally efficient and simple as they process only perceptually salient region(s) of face for feature extraction.

### 1.3.2 Computational efficiency

During the course of this research work we have proposed algorithms for facial expression recognition which are based on psycho-visual experimental study (exploiting saliency of different facial regions). Psycho-visual experimental study points to the fact that human visual system is attracted towards only few facial regions while decoding six universal facial expressions (for reference see Section 3.3). The proposed framework(s) extracts features only from the perceptually salient region, thus reducing the length of features vector. This reduction in feature vector length makes the proposed framework suitable for real-time applications due to minimized computational complexity.

### 1.3.3 Expression recognition on low resolution stimuli

We have proposed a novel descriptor for facial features analysis, Pyramid of Local Binary Pattern (PLBP) (refer Chapter 6) that can recognize facial expressions very efficiently and with high accuracy for very low resolution facial images. Proposed framework exceeds state-of-the-art methods for expression recognition on low resolution images, which were derived from Cohn-Kanade (CK+) posed facial expression database. The proposed framework is memory and time efficient as it extracts texture features in a pyramidal fashion only from the perceptual salient regions of the face.

### 1.3.4 Recognition of “pain” expression

In this research work, we are also proposing a novel computer vision system that can recognize expression of pain in videos by analyzing facial features. Usually pain is reported and recorded manually and thus carry lot of subjectivity. Manual monitoring of pain makes difficult for the medical practitioners to respond quickly in critical situations. Thus, it is desirable to design such a system that can automate this task. With our proposed model pain monitoring can be done in real-time without any human intervention. We tested our proposed model on UNBCM McMaster Shoulder Pain Expression Archive Database

[LCP<sup>+</sup>11] (refer Appendix Section A.8) and recorded results that exceeds state-of-the-art.

### 1.3.5 Database

We have tested our proposed frameworks on different databases, which includes Cohn-Kanade (CK+) posed facial expression database (refer Appendix Section A.1), spontaneous expressions of MMI facial expression database (refer Appendix Section A.2) and FG-NET facial expressions and emotions database (FEED) (refer Appendix Section A.3) and obtained very good results.

## 1.4 Application areas

A system that could enable fast and robust facial expression recognition would have many uses in both research and application areas as diverse as behavioural science, education, entertainment, medicine, and security. Following is a list of applications that can benefit from automatic recognition of facial expressions.

1. *Avatars with expressions.* Virtual environments and characters have become tremendously popular in the 21st century. Gaming industry would benefit tremendously if the avatars were able to mimic their user's facial expressions recorded by a webcam and analysed by a facial expression recognition system as the level of immersion and reality in the virtual world would increase. This immersion into virtual world could have many implications i.e. the game could adapt its difficulty level based on information from the facial expressions of the user.
2. *EmotiChat.* Another interesting application has been demonstrated by Anderson and McOwen, called the "EmotiChat" [AM06]. It consists of a chat-room application where users can log in and start chatting. The face expression recognition system is connected to this chat application and it automatically inserts emoticons based on the user's facial expressions.
3. *Smart homes.* As mentioned earlier, computing environment is moving towards human-centered designs instead of computer centered designs

[PPNH06] and this paradigm shift will have far reaching consequences, one of them being smart homes. The houses could be equipped with systems that will record different readings i.e. lighting conditions, type of music playing, room temperatures etc and associate them with the facial expressions of the inhabitants over time. Thus, such system can later control different recorded environment parameters automatically.

4. *Affective/social robots.* For social robots it is also important that they can recognize different expressions and act accordingly in order to have effective interactions [SBR10]. The Social Robots Project at Carnegie Mellon University states its mission as “wanting robots to behave more like people, so that people do not have to behave like robots when they interact with them”. To attain such human-robot interaction, it is of paramount importance for the robot to understand the humans facial expressions.
5. *Detection and treatment of depression and anxiety.* Research based on the FACS has shown that facial expressions can predict the onset and remission of depression, schizophrenia, and other psychopathological afflictions [ER05]. FACS [EF78] has also been able to identify patterns of facial activity involved in alcohol intoxication that observers not trained in FACS failed to note [SSBW92]. This suggests there are many applications for an automatic facial expression recognition system based on FACS.
6. *Pain monitoring of patients.* Pain monitoring of patients is a very complicated but very important task. Currently, this is done manually but it is desirable to design such a system that can automate this task. Manually monitoring of pain has some problems: first, pain cannot be recorded continuously. Secondly, some patients can under report the pain while other can do just opposite. Lastly, the person recording the pain has to make judgment of pain level, which could vary from person to person (subjectivity problem). An automatic facial expression recognition system could solve above mentioned problems. It has been shown that it is possible to derive a measure of pain and to distinguish between different types of pain from a patient’s facial expressions [dCW02]. In this research

work, we have proposed a novel computer vision system that can recognize expression of pain in videos by analyzing facial features (refer Section 6.4 for the details).

## 1.5 Publications

### 1. Peer-reviewed journal articles

- (a) Framework for reliable, real-time facial expression recognition for low resolution images. R.A. Khan, A. Meyer, H. Konik, S. Bouakaz. In Pattern Recognition Letters. Volume 34, Issue 10, Pages 1159-1168. Doi: <http://dx.doi.org/10.1016/j.patrec.2013.03.022> (impact factor: 1.266)

### 2. Peer-reviewed international conferences

- (a) Pain detection through shape and appearance features. R.A. Khan, A. Meyer, H. Konik, S. Bouakaz. In IEEE International Conference on Multimedia and Expo (ICME), San Jose, California, USA 2013. Pages 1-6. Doi: <http://dx.doi.org/10.1109/ICME.2013.6607608> (acceptance rate 30 %).
- (b) Human vision inspired framework for facial expressions recognition. R.A. Khan, A. Meyer, H. Konik, S. Bouakaz. In International Conference on Image Processing (ICIP), Orlando, USA 2012. Pages 2593-2596. Doi: <http://dx.doi.org/10.1109/ICIP.2012.6467429> (acceptance rate 33 %).
- (c) Exploring human visual system: study to aid the development of automatic facial expression recognition framework. R.A. Khan, A. Meyer, H. Konik, S. Bouakaz. In Computer Vision and Pattern Recognition Workshop (CVPRW), Rhode Island, USA 2012. Pages 49-54. Doi: <http://dx.doi.org/10.1109/CVPRW.2012.6239186>
- (d) Facial Expression Recognition using Entropy and Brightness Features. R.A. Khan, A. Meyer, H. Konik, S. Bouakaz. In 11th International



Conference on Intelligent Systems Design and Applications, Còrdoba, Spain 2011. Pages 737-742. Doi: <http://dx.doi.org/10.1109/ISDA.2011.6121744>

### 3. French national conferences

- (a) Une méthode de reconnaissance des expressions du visage basée sur la perception. R.A. Khan, A. Meyer, H. Konik, S. Bouakaz. In Atelier VISAGES (Vidéo-surveillance Intelligente : Systemes et ALgorithmES), Reconnaissance des Formes et l'Intelligence Artificielle (RFIA), Lyon, France. 2012.

### 4. Miscellaneous

- (a) Separating superfluous from essential: which facial region(s) holds the key for expression recognition?. R.A. Khan, H. Konik, . Dinet, A. Meyer, S. Bouakaz. In 16th European Conferences on Eye Movements (ECEM'2011), Marseille, France. 2011. Abstract published in the Journal of Eye Movement Research, Vol.4, Issue 3 2011. URL: <http://www.jemr.org/online/4/3/1>

### 5. Under review: Peer-reviewed journal

- (a) Saliency based framework for facial expression recognition. R.A. Khan, A. Meyer, H. Konik, S. Bouakaz. In Journal of Imaging Science and Technology.

## 1.6 Structure of the report

As mentioned before, generally facial expression recognition framework consists of three step: 1. face detection and tracking 2. feature extraction 3. expression classification / recognition. Chapter 2 presents review of different state-of-the-art methods for all of these three steps and, also provides insight to some of the theories related to facial expressions from the fields of psychology and cognitive science. Chapter 3 presents all the details related to our psycho-visual

experimental study through which we determined which facial region(s) is perceptually salient for a particular expression. Chapter 4 describes detail related to our first proposed descriptor for facial expression recognition. To rectify the drawbacks of this descriptor, we proposed in Chapter 5 second descriptor, that analyzes shape for recognizing expressions. Finally, we proposed in Chapter 6 another descriptor called pyramid of local binary pattern (PLBP) to overcome shortcomings of the previously proposed descriptor/framework for expression recognition. PLBP extends novel texture descriptor local binary pattern (LBP), by creating pyramidal-based spatial representation of LBP descriptor. PLBP works well for both high and low spatial resolution stimuli and also is a part of framework that recognizes expression of “pain”. Chapter 7 describes conclusions of this research work along with the perspectives.

Supplementary details essential to understand this research work is presented in the following appendices:

1. Appendix A (Facial expression databases): presents information related to some of the most famous image/video databases used by the research community to prove effectiveness of their proposed methods for facial expression recognition.
2. Appendix B (Gaze Maps): presents gaze maps recorded during psycho-visual experimental study. It presents five video sequences / expression.
3. Appendix C (Color space conversion): illustrates equations to convert  $XYZ$  color space coordinates to  $L^*a^*b^*$  color space coordinates.

# Chapter 2

## Literature survey

### Contents

---

<b>2.1</b>	<b>Psychology and cognitive science on facial affect theory</b>	<b>14</b>
2.1.1	Ekman’s six basic emotions . . . . .	15
2.1.2	Facial Action Coding System (FACS) . . . . .	17
2.1.3	Plutchik’s emotion wheel . . . . .	19
2.1.4	Russell’s circumplex model . . . . .	21
<b>2.2</b>	<b>Databases for facial expression recognition . . . . .</b>	<b>22</b>
<b>2.3</b>	<b>Automatic recognition of facial expressions . . . . .</b>	<b>25</b>
2.3.1	Face detection and tracking . . . . .	25
2.3.2	Feature extraction . . . . .	33
2.3.3	Expression classification / recognition . . . . .	40
<b>2.4</b>	<b>Drawbacks of the current methods and contributions .</b>	<b>46</b>
2.4.1	Exploiting visual saliency . . . . .	46
2.4.2	Expressions different from six prototypical facial expression . . . . .	47

---

For the last forty years (specifically since 1974 [Par74]), computer vision research community has shown a lot of interest in analyzing and automatically recognizing facial expressions. Initially inspired by the findings of the cognitive

scientists, the computer vision/science research community envisioned to develop such frameworks that can do the job of expression recognition in videos or still images.

Facial expressions are studied simultaneously by different scientists from different domains i.e. cognitive scientists, psychologists, neuroscientists and computer scientists etc. Although the algorithms proposed in this research work fall in the category of “computer vision” but they are based on the psycho-visual study (see Chapter 3). As the psycho-visual study is based on the principles of cognitive science, Section 2.1 provides the overview of facial expression studies from the cognition science literature. Section 2.2 briefly describes characteristics of different databases used for evaluating and benchmarking different facial expression analysis algorithms. Section 2.3 briefly covers core components of a system that recognizes facial expressions automatically. Section 2.4 describes limitations of current algorithms for expression recognition and associated research contributions of this research work.

## 2.1 Psychology and cognitive science on facial affect theory

Different channels contribute to complete the task of conversation, face being the most important channel. Expressions displayed on the face not only shows clue about emotional state but also intentions and mindset [EFE72, EF75, Ekm01, Ekm93]. So, they can not only change the flow of conversation [Bul01] but also provides the listeners a wealth of information without even uttering a single word [Yng70]. According to [CLFD94, FDWS91] when the facial expression does not coincide with the other communication i.e. spoken words, then the information conveyed by the face gets more weight in decoding information. We are used to see face with different expressions every day, but still sometimes we fail to understand them. It is this paradox of the obvious and the mysterious that intrigues people to study the face and facial expressions.

Facial expressions are studied since ancient times, one of the reason is that it is one of the most important channel of non-verbal communication [AR92].

Initially facial expressions were studied by great philosophers and thinkers like Aristotle and Stewart. With Darwin, the study of facial expressions became an empirical study. Darwin's studies created large interest among psychologists and cognitive scientists. The 20th century saw many studies relating facial expression to emotion and inter-human communication. Most notably, Paul Ekman reinvestigated Darwin's work and claimed that there are six universal emotions (see Figure 2.1), which are produced and recognised independently of cultural background [Ekm71].

Facial expressions can either be interpreted in terms of shown affective states (emotions) or in terms of activated facial muscles underlying the displayed facial expression. These two approaches originate directly from the two major approaches to facial expression measurement in psychological research: message and sign judgement [CE05]. Message based approaches infer to what underlies a displayed facial expression, such as affect. Cross-cultural studies by Ekman [Ekm71, Ekm93] and the work by Izard [Iza09] demonstrated the universality and discreteness of subset of facial expressions, which are referred as basic or universal expressions. Generally, physical changes in face shape make the descriptor for sign based approach. The most widely-used approach is that of Ekman and colleagues, known as Facial Action Coding System (FACS) [EF78] (See Subsection 2.1.2 for reference).

Following subsections describe different coding schemes for facial affect theory. Specifically Subsection 2.1.1 describes Ekman's six basic/universal expressions. Subsection 2.1.2 describes Facial Action Coding System (FACS), while Subsection 2.1.3 describes psychologist Robert Plutchik's insight to emotions. Subsection 2.1.4 describes theory of James A. Russell defining emotions in a two-dimensional circular space, containing arousal and valence dimensions.

### 2.1.1 Ekman's six basic emotions

The most commonly used facial expression coding system in the message judgement approach relates to the six basic emotions / expressions proposed by Ekman [Ekm71]. Each of those expressions possess a distinctive content together with a unique facial expression. These six basic emotions are happiness, sadness,

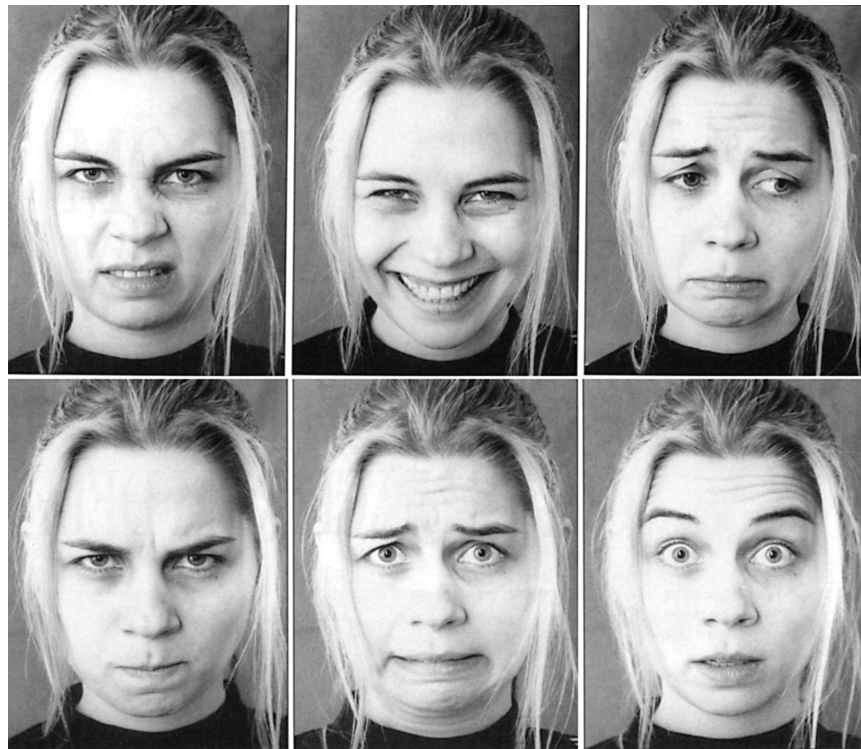


Figure 2.1: Example of expression for the six basic emotions (illustration taken from [Pan09]). Left-to-right from top row: disgust, happiness, sadness, anger, fear, and surprise.

fear, disgust, surprise and anger (see Figure 2.1 for illustration of these expressions). These expressions are also referred as “universal” as they were found to be universal across human ethnicities and cultures.

This theory of expressing emotions through a fixed set of universal emotions was inspired by Darwin’s observations. According to Darwin expression of emotions has evolved in humans from animals. Darwin argued that expressions were unlearned and innate in human nature and were therefore evolutionary significant for survival [Ekm06]. Darwin in his book “The Expression of the Emotions in Man and Animals” [Dar72], concluded that “the young and the old of widely different races, both with man and animals, express the same state of mind by the same movements”. These observations, published in 1872 were left undebated for almost 100 years. Then, in the 1960s, Ekman picked up his research in an effort to validate Darwin’s theories. In this research work,

Ekman’s six basic emotions are used extensively to test various proposed frameworks for automatic recognition of the same.

### 2.1.2 Facial Action Coding System (FACS)

Facial Action Coding System (FACS) [EF78] is the most widely used sign judgement system and it describes the facial expressions in terms of 46 component movements (facial anatomical movements) or action units (AUs)(see Figure 2.2 for examples of AUs), which roughly corresponds to a distinct muscle or muscle group. Figures 2.3, 2.4 and 2.5 shows action units (AUs) in the upper face, in the lower face, and AUs that cannot be classified as belonging to either the upper or the lower face.

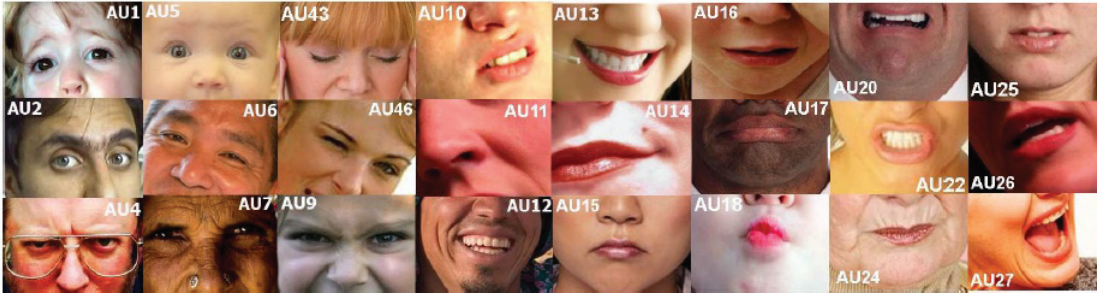


Figure 2.2: Some examples of Action Units. Action Units are atomic facial muscle actions described in FACS (Illustration from [Val08]).

AUs are considered to be the smallest visually discernable facial movements. They are atomic, meaning that no AU can be split into two or more smaller components. Any facial expression can be uniquely described by a combination of AUs.

#### 2.1.2.1 FACS AU combinations and intensity

As AUs represent the “atoms” of facial expressions, multiple AUs often occur simultaneously. Out of 46 AUs 30 AUs are anatomically related to the contractions of specific facial muscles: 12 are for upper face, and 18 are for lower face. When AUs occur in combination they may be additive, in which the combination does not change the appearance of the constituent AUs, or non-additive, in which the





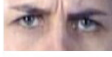



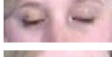


	AU1 Raised inner eyebrow		AU2 Raised outer eyebrow
	AU4 Eyebrows lowered and drawn together		AU5 Raised upper eyelid
	AU6 Raised cheek, compressed eyelids		AU7 Tightened eyelids
	AU43 Eyes closed		AU45 Blink
	AU46 Wink		

Figure 2.3: Upper facial Action Units (Illustration taken from [Val08]).


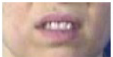


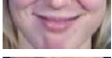


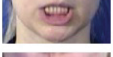

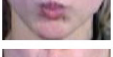

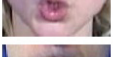
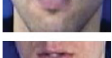

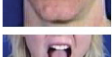

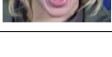
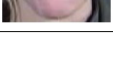
	AU8 Lips towards each other		AU10 Raised upper lip
	AU11 Deepened nasolabial furrow		AU12 Lip corners pulled up
	AU13 Lip corners pulled sharply up		AU14 Dimpler - mouth corners pulled inwards
	AU15 Lip corners depressed		AU16 Lower lip depressed
	AU17 Chin raised		AU18 Puckered lips
	AU20 Mouth stretched horizontally		AU22 Lip funneled and protruded
	AU23 Lips tightened		AU24 Lips pressed
	AU25 Lips parted		AU26 Jaw dropped
	AU27 Mouth stretched open		AU28 Lips sucked into the mouth

Figure 2.4: Lower facial Action Units (Illustration from [Val08]).

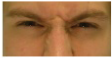




	AU9 Nose wrinkler		AU21 Neck thightened
	AU31 Jaw clenched		AU38 Nostril wings flared out (left is neutral, right active)
	AU39 Nostril wings compressed (left is neutral, right active)		

Figure 2.5: Action Units belonging to neither the upper nor the lower facial area (Illustration from [Val08]).



appearance of the constituents does change [TKC01]. So far, about 7000 valid AU combinations have been identified within the FACS framework.

Further relationships among multiple AUs exist as well. For instance, in certain AU combinations, the dominant AU may completely mask the presence of another, subordinate action unit. For certain such combinations, special rules have been added to FACS so that the subordinate AU is not scored at all [Val08].

In addition to determining which AUs are contained within the face, the intensity of each AU present must also be ascertained. Intensity is rated on a scale from A (least intense) through E (most intense). Criteria for each intensity level are given in the FACS Manual for each AU.

### 2.1.2.2 Drawbacks of Facial Action Coding System (FACS)

1. FACS codes often reveal unnecessary details that can hamper facial expression recognition approaches. The sheer number of combinations (7000 AU combinations) can lead to a bad generalization performance as it is virtually impossible to have access to a training database that covers all possible AU combinations while featuring a sufficient number of instances of specific facial expressions [FMGP04].
2. Secondly, the problem with using FACS is the time required to code every frame of the video. FACS was envisioned for manual coding by FACS human experts. It takes over 100 hours of training to become proficient in FACS, and it takes approximately two hours for human experts to code each minute of video [LBL07].

Above mentioned drawbacks of FACS make it impractical for real life scenarios.

### 2.1.3 Plutchik's emotion wheel

While Ekman proposed that there are six basic emotions, psychologist Robert Plutchik on the other hand, proposed a model of human emotions with eight primary emotions. The emotions are organized in pairs of opposites: joy versus sadness; trust versus disgust; fear versus anger and anticipation versus surprise [Plu80]. Every other emotion can be produced by mixing the primary ones. The

model resulted in a circumplex where emotions and variations are represented by different colors and hues (see Figure 2.6). The three dimensional circumplex model describes the relationships between concepts of emotion with each emotion smoothly flowing into another when we traverse a path on the surface of the 3-dimensional cone.

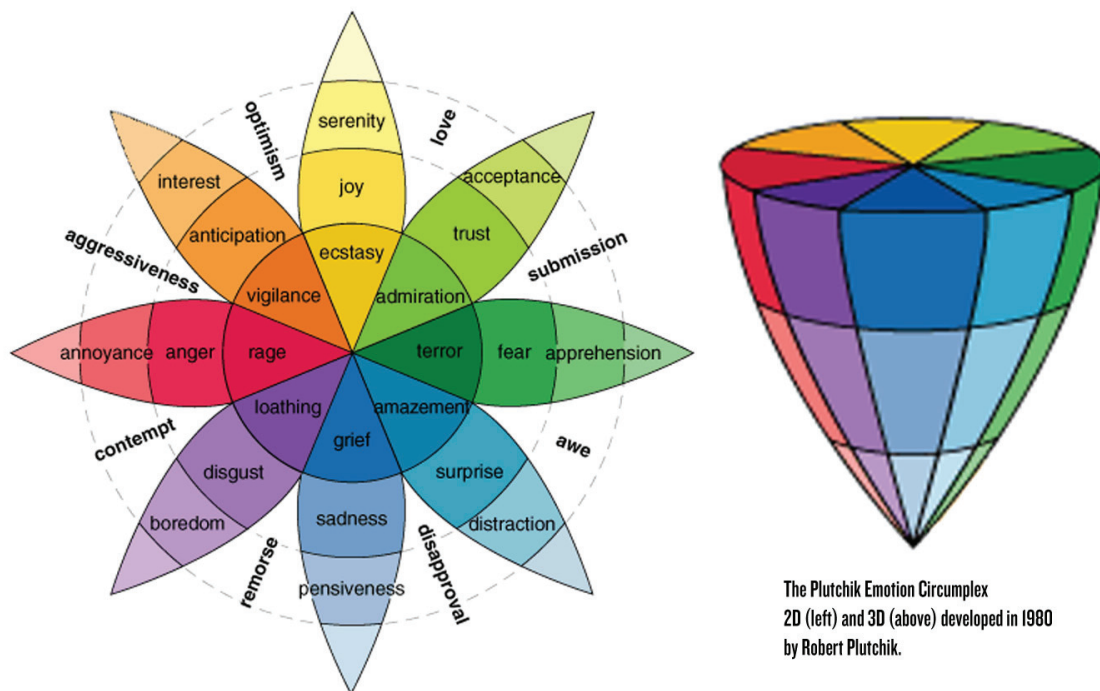


Figure 2.6: Plutchik's emotion wheel (left) and the accompanying emotion cone (right).

The cone's vertical dimension represents the intensity of the emotion and the position on the circle defines in what basic emotion sector we are. The eight sectors are designed to indicate that there are eight primary emotion dimensions, formed by four pairs of opposites. Secondary emotions are produced by combinations of primary emotions that are adjacent on the emotion wheel. For instances, Plutchik characterises love as a combination of joy and acceptance, whereas submission is a combination of acceptance and fear.

The reason for inclusion of the eight primary emotions is that they all have a direct relation to adaptive biological processes. For instance, when we gain a valued object, the cognitive process is that we possess and thus we feel joy. The

associated action would be to retain this state or repeat the process, gaining more valued objects and thereby feeling joy again. The theory is very much based on our inner state, i.e. on the way we actually feel.

On the contrary, it is often inadequate to describe emotions of every-day life by mixtures of basic emotions as these are assumed to be full-blown, and in everyday life, full-blown emotions occur very rarely i.e. love = joy + acceptance. So, the description secondary emotions is dubious. Secondly, Plutchik's system does not explain how emotions can be systematized so categorically without taking into account all of the overlaps and crossovers from one to the other. These problems contributes to non utilization of this model in computer vision research community.

#### 2.1.4 Russell's circumplex model

Many cognitive scientists oppose the theory of a set of discrete, basic emotions [Man84, Rus95]. Some of these opponents instead take a dimensional view of the problem [SBR10]. In their view, affective states are not discrete and independent of each other, instead they are systematically related to one another [CB94, MR73].

Perhaps the most influential of the scientists who proposed this systematic view is James A. Russell. He proposed a system of two bipolar continui, namely valence and arousal [Rus80]. Valence roughly ranges from sadness to happiness while arousal ranges from boredom or sleepiness to frantic excitement. According to Russell, emotions lie on a circle in this two dimensional space (see Figure 2.7), and are characterized by fuzzy categories clustered on axes such as valence, arousal, or dominance.

While a continuous space could possibly represent all possible facial expressions, this is not guaranteed by Russell's theory and indeed has not been shown. It is unclear how a facial expression should be mapped to the space or, vice versa, how to define regions in the valence/arousal space that correspond to a certain facial expression. Being a judgement system that is based on feeling, it is again problematic to use this system to describe non-emotional communicative signals. All this leads to the conclusion that this system is not suitable for computer vision community [Val08].

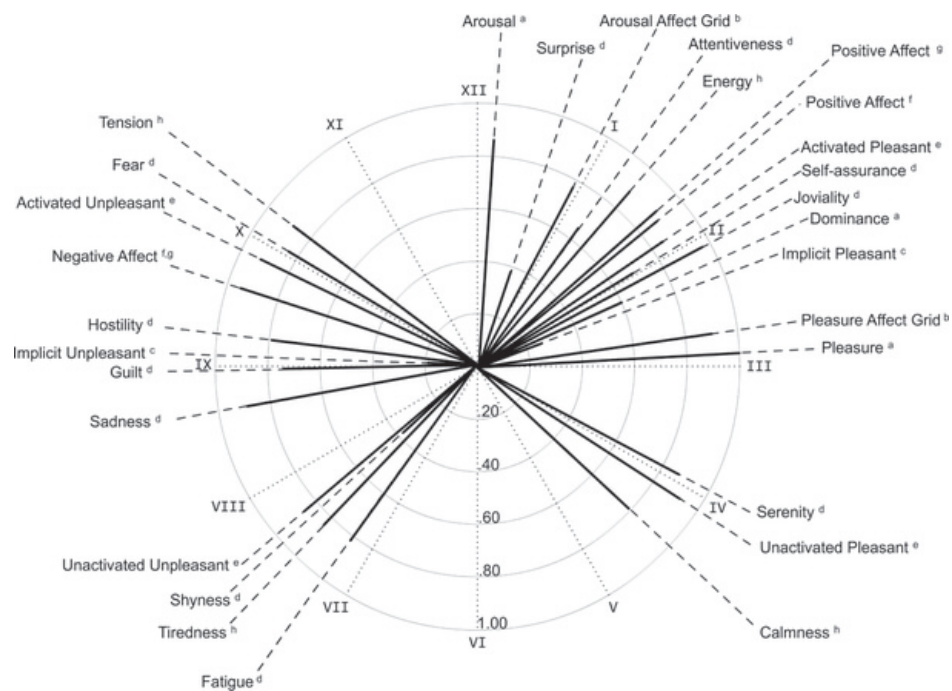


Figure 2.7: Russells circumplex model of emotions.

In this research work, Ekman’s six basic emotions are used extensively to test various proposed frameworks for automatic recognition of expression. This is due to the fact that Ekman’s six basic emotions are well suited for the computer vision application (classifying in discrete classes) and most of the state-of-the-art methods show their results on it.

Recently affect analysis research is moving from recognizing discrete classes of emotion to continuum emotion recognition. The rationale behind this shift is that the full spectrum of human emotion cannot be expressed by a few discrete classes. Emotion is better represented by continuous values on multiple attribute axes such as valence, activation or dominance [MKH<sup>+</sup>07]. This point is discussed in detail in Section 7.2.

## 2.2 Databases for facial expression recognition

Generally, for evaluating and benchmarking different facial expression analysis algorithms, standardised databases are needed to enable a meaningful

comparison. In the absence of comparative tests on such standardised databases it is difficult to find relative strengths and weaknesses of different facial expression recognition algorithms. Cohn-Kanade(CK) database, which is also known as the CMU-Pittsburg AU coded database [KCT00] has somehow emerged as that standardised database. This is a fairly extensive database and has been widely used by the face expression recognition community. Refer to Appendix Section A.1 for more information on CK database.

For explanation of different databases refer to Appendix A. Some of the databases that are described in the appendix are used during the course of this thesis. Few of the characteristics that create difference between databases are [TKCis].

1. **Individuality of subjects.** Face shape, skin texture, facial hairs, whether subjects wear eye glasses/sun glasses, sex, ethnicity and age group of subjects are some of the factors that differentiate databases. Some databases use only females as a subject, for example Japanese Female Facial Expression Database (JAFFE) contains images of only Japanese females.
2. **Deliberate versus spontaneous expression.** Most face expression databases have been collected by asking subjects to perform a series of expressions i.e. CK, JAFFE, AR etc (for discussion on different database refer to Appendix A). These directed facial action tasks may differ in their characteristics, temporal dynamics and timings from spontaneously occurring behavior [ER05]. The same has been proved by Bartlett et al. [BLB<sup>+</sup>02].

Recently efforts are growing towards automatic analysis of spontaneous expressions but research needs to be done to recognize wide array of spontaneous expressions. For example MMI Facial Expression Database contain spontaneous emotive content (see Appendix Section A.2 for more information). Another database that is recently used for spontaneous expression analysis is RU-FACS database [BLF<sup>+</sup>06] but this database is not available publically.

3. **Image sequence resolution.** Most of the existing state-of-the-art systems for expressions recognition report their results on high resolution images without reporting results on low resolution images. But there are many real world applications that require expression recognition system to work amicably on low resolution images. Smart meeting, video conferencing and visual surveillance are some examples of such applications. In this thesis I have worked on the problem of low resolution input image sequences but those low resolution input image sequences were created by subsampling the original high resolution images from CK database. There is a need of a standard database which contains stimuli in low resolution so that different methods can be compared in more systematic way.
4. **Head/face Orientation.** Face orientation with respect to camera influences the performance of different algorithms for expression recognition. In literature, not much effort is done on developing algorithms for facial expression recognition that are invariant to camera angle. There exist some databases that contain emotive content having different camera angles i.e. MMI facial expression database [PVRM05] and FERET [MP98].
5. **Background clutter.** Image sequence recorded in a complex background makes the task of automatic facial expression recognition even more difficult as the complex background influences accuracy of automatic face detection, feature tracking, and expression recognition. Most of the available database have a neutral or very persistent background.
6. **Varying illumination.** It is desired that algorithms for automatic expression recognition should be invariant to lighting conditions. Very few publically available databases record stimuli in varying illumination. One of such database is CAS-PEAL [GCS<sup>+</sup>04]. The CAS-PEAL (pose, expression, accessory, lighting) Chinese face database was collected at the Chinese Academy of Sciences (CAS) between August 2002 and April 2003. For more information on this database, refer to Appendix Section A.6.

## 2.3 Automatic recognition of facial expressions

The general approach to automatic facial expression analysis consists of three steps (refer Figure 2.8): face detection and tracking, feature extraction and expression classification / recognition. Face detection stage processes stimuli to automatically find the face region from the input images or sequences. After face is located, the next step is to extract meaningful or discriminative information caused by facial expressions. Facial expression recognition is the last stage of the systems. The facial changes can be identified either as prototypic emotions or facial action units (refer Sections 2.1.1 and 2.1.2 for details). In the following subsections (Section 2.3.1: face detection, Section 2.3.2: feature extraction and Section 2.3.3: expression classification), I will briefly cover the literature on all of the above mentioned three steps.

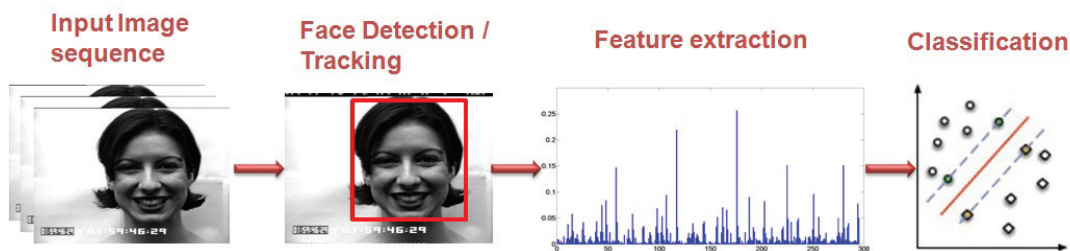


Figure 2.8: Automatic facial expression recognition system pipeline.

### 2.3.1 Face detection and tracking

The first step in facial expression analysis is to detect the face in the given image or video sequence. Locating the face within an image is termed as face detection or face localization whereas locating the face and tracking it across the different frames of a video sequence is termed as face tracking. Research in the fields of face detection and tracking has been very active and there is exhaustive literature available on the same. It is beyond the scope of this thesis report to introduce and survey all of the proposed methods.



Methods for face detection can be grouped into four categories [YKA02]: knowledge-based methods, feature invariant approaches, template matching methods, and appearance-based methods.

### 2.3.1.1 Knowledge-based methods

Knowledge-based methods use pre-defined rules to determine a face based on human knowledge. Usually, the rules capture the relationships between facial features. It is trivial to find simple rules to describe the features of a face and their relationships. For example, face appears in an image with two eyes (usually), a nose and a mouth. To describe relationship between features, distance and relative position are good metric.

Yang and Huang used a hierarchical knowledge-based method to detect faces [YH94]. They proposed three level system, where at first level all possible face candidates are found. The rules at a higher level are general descriptions of what a face looks like while the rules at lower levels rely on details of facial features. Motivated by the simplicity of the approach proposed by Yang and Huang [YH94], Kotropoulos and Pitas [KP97] proposed face detection algorithm which extends their method. Kotropoulos's method [KP97] makes computationally complex algorithm of Yang's [YH94] much simpler. Mekami and Benabderrahmane proposed [MB10] algorithm that not only detects face but also its inclination. They used Adaboost learner for face detection. For the calculation inclination, they used an eyes detector. Then the line passing through the two eyes is identified, and the angle to horizon is calculated.

Problem with this approach is the difficulty in translating human knowledge into rules. If the rules are detailed (i.e., strict), they may fail to detect faces that do not pass all the rules. If the rules are too general, they may give many false positives. Moreover, it is difficult to extend this approach to detect faces in different poses since it is challenging to enumerate all the possible cases. On the other hand, heuristics about faces work well in detecting frontal faces in uncluttered scenes.



### 2.3.1.2 Feature invariant approaches

Feature invariant approaches aim to find face structure features that are robust to pose and lighting variations. These methods use primitives physical properties of the face and rely on numerous heuristics for the proper choice of the data patterns extracted from the image. Usually these methods perform low level analysis (or early vision) on stimuli to find and extract discriminative features. Based on the extracted features, a statistical model is built to describe their relationships and to verify the existence of face. Different extracted features are often specific to the context at hand, and are constructed empirically on colour, edge or texture cues.

**Facial features:** Sirohey proposed method to detect face from a cluttered background [Sir93]. The method uses an edge map (Canny detector) and heuristics to remove and group edges so that only the ones on the face contour are preserved. Leung et al. developed a probabilistic method to locate a face in a cluttered scene based on local feature detectors and random graph matching [LBP95]. Han et al. developed a morphology-based technique to extract “eye-analogue segments” for face detection [HMHY<sup>+</sup>97]. They argue that eyes and eyebrows are the most salient and stable features of human face and, thus, useful for detection. They define eye-analogue segments as edges on the contours of eyes.

**Skin color:** human skin color has been used and proven to be an effective feature in many applications from face detection to hand tracking. Saxe and Foulds proposed an iterative skin identification method that uses histogram intersection in HSV color space [SF96]. First an initial patch of skin color is selected by the user and then iteratively algorithms find similar patch. Similarity is measured by histogram intersection of two color patches. Huang et al. [HAL09] proposed system to detect face based on skin tone filter. Zhang et al. [ZZH09] proposed system to detect multiple faces in a video using centroids of image in RGB color space. Khandait and Thool [KT09] has also proposed an algorithm to detect faces using color information. They have proposed a hybrid

approach that first detects skin pixels in different color spaces (i.e. modified RGB, YCbCr and HSV) and then combines them to localize face.

**Texture:** texture can be defined as the visual or tactile surface characteristics and appearance. Thus, human face has a very discriminative texture that separates it from the other objects in an stimuli. Augusteijn and Skufca developed a method that infers the presence of a face through the identification of face-like textures [AS93]. Dai and Nakano [DN96] incorporated color information with the face-texture model.

Problem with these feature-based algorithms is that the image features can be severely corrupted due to illumination, noise, and occlusion. Feature boundaries can be weakened for faces, while shadows can cause numerous strong edges which together render perceptual grouping algorithms useless [YKA02].

### 2.3.1.3 Template matching methods

Template matching methods use pre-stored face templates (parametric face model) to judge if an image is a face. Given an input image, the correlation values with the standard patterns are computed for the face contour, eyes, nose, and mouth independently. The existence of a face is determined based on the correlation values.

**Predefined templates:** the Ratio Template Algorithm was proposed by Sinha in 1996 for the cognitive robotics project at MIT [Sin95]. Scassellati used it to develop a system that located the eyes by first detecting the face in real time [Sca98]. In 2004, Anderson and McOwen modified the Ratio Template by incorporating the “Golden Ratio” (or Divine Proportion, *in mathematics, two quantities are in the golden ratio if the ratio of the sum of the quantities to the larger quantity is equal to the ratio of the larger quantity to the smaller one*) into it. They called this modified version as the Spatial Ratio Template tracker [AM04]. This modified detector was shown to work better under different illuminations. Anderson and McOwen suggest that this improvement is because of the incorporated Golden Ratio, which helps in describing the structure of the

human face more accurately. The Ratio Template and the Spatial Ratio Template are shown in Figure 2.9.

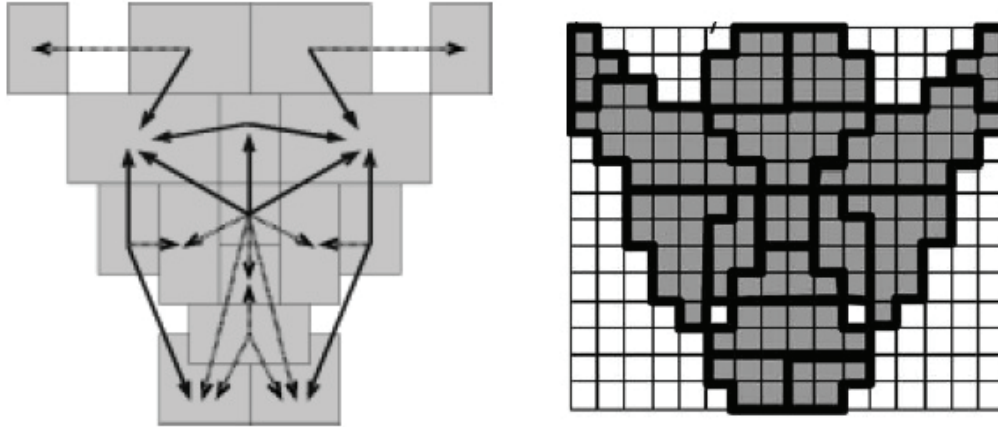


Figure 2.9: The image on the left is the Ratio Template (14 pixels by 16 pixels). The template is composed of 16 regions (gray boxes) and 23 relations (arrows). The image on the right is the Spatial Ratio Template. It is a modified version of the Ratio Template by incorporating the Golden Ratio.

**Deformable templates:** the technique of deformable template has gained a lot of interest for face detection and tracking. Generally deformable model based methods work in two phases. The first phase is the creation of model/template, which can be used to generate a set of plausible representations in terms of shape and/or texture of the face. The second phase (segmentation phase) is to find the optimal parameters of variation of the model, in order to match the shape and/or the texture of the face in an unknown stimuli.

The active shapemodels (ASM), introduced by Cootes and Taylor [CHTH94], are deformable models which depict the highest level of appearance of the face features. Once initialized near a facial component, the model modifies its local characteristics (outline, contrast) and evolves gradually in order to take the shape of the target feature i.e. face. One disadvantage of ASM is that it only uses shape constraints (together with some information about the image structure near the landmarks), and does not take advantage of all the available information. The active appearance models (AAM) are an extension of the ASM by Cootes et al. [CET98]. The use of third dimension, namely the temporal one, can lead to a real-

time 3D deformable face model varying according to morphological parameters during a video sequence.

Generally, the drawback of predefined and deformable template methods for face detection are their inadequacy for dealing with variation in scale, pose, and shape. Secondly, the problem of AAM is that it fails to register face when either the initial shape estimate of face is too far off and / or the appearance model fails to direct search toward a good match. Another limitation of AAM is the computational complexity associated with the training phase of it [LBHW07].

#### 2.3.1.4 Appearance-based methods

Unlike template-matching method which rely on a predefined template or model, appearance-based methods use large numbers of examples (images of faces and or facial features) depicting different variations (face shape, skin color, eye color, open closed mouth, etc). Face detection in this case can be viewed as a pattern recognition problem with two classes: face and nonface [MB10]. In general, appearance-based methods rely on techniques from statistical analysis and machine learning to find the relevant characteristics of face and nonface images [YKA02]. Seminal work in appearance-based methods for face detection are based on eigenfaces [TP91], neural networks [RBK96], support vector machines [OFG97] and hidden Markov models [NH98].

Adaboost (proposed by Freund and Schapire [FS95]) has also been used by several researchers to create robust system for detection of objects in real time [KT04a]. Papageorgiou et al. in [POP98] have used this algorithm to detect pedestrians using the Haar wavelet to extract discriminating features. Inspired by the algorithm proposed by Papageorgiou et al. in [POP98], Paul Viola and Michael Jones [VJ01] proposed algorithm for face detection.

In this research work, we have used Viola-Jones object detection algorithm for detecting face / salient facial regions as it is the most cited and considered the fastest and most accurate pattern recognition method for face detection [KT04b]. Viola-Jones object detection algorithm is explained below.

**Viola and Jones algorithm.** Viola and Jones method combines incorporate following four key concepts:

1. *Haar-like features*: The first contribution of Viola and Jones algorithm is computational simplicity for feature extraction. The features used by their method are called Haar-like features. Haar-like features are explained in Section 2.3.2.1.
2. *Integral image*: To rapidly compute Haar-like features Viola and Jones proposed intermediate representation for the image, called integral image. The integral value for each pixel location  $(x, y)$  is the sum of all the pixels above it and to the left of  $(x, y)$  inclusive (refer Equation 2.1):

$$ii(x, y) = \sum_{x' \leq x, y' \leq y} i(x', y') \quad (2.1)$$

where  $ii(x, y)$  is the integral image and  $i(x, y)$  is the original image.

Using the integral image any rectangular sum can be computed in four array references (see Figure 2.10). Clearly the difference between two rectangular sums can be computed in eight references. Since the two-rectangle features defined above involve adjacent rectangular sums they can be computed in six array references, eight in the case of the three-rectangle features, and nine for four-rectangle features [VJ01].

3. *AdaBoost machine-learning method*: Viola and Jones have chosen a variant of training algorithm called *AdaBoost*, first proposed by Freund and Schapire [FS95]. This training algorithm is used to determine the presence Haar-like feature by setting threshold levels. Threshold value is used to determine the presence of a Haar-like feature (the sum of pixels values in the shaded rectangle is subtracted from the white rectangle). If the difference is above a threshold, that feature is said to be present.

Secondly, within any image subwindow the total number of Haar-like features is very large, far larger than the number of pixels. In order to ensure fast classification, the learning process must exclude a large majority of the available features, and focus on a small set of critical features. To achieve this goal, the weak learning algorithm is proposed by Viola Jones which selects the single rectangle feature which best separates

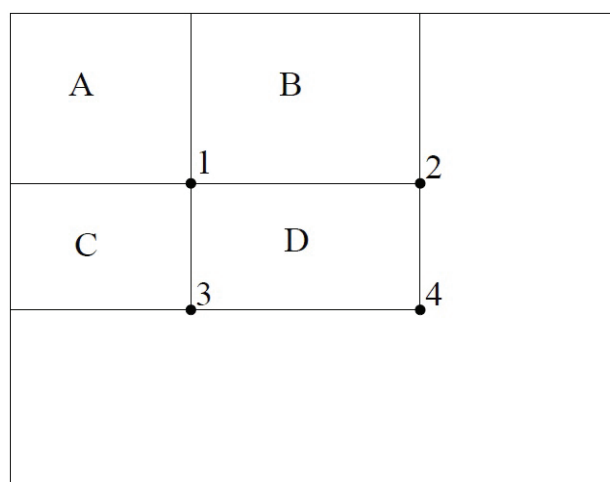


Figure 2.10: The sum of the pixels within rectangle  $D$  can be computed with four array references. The value of the integral image at location 1 is the sum of the pixels in rectangle  $A$ . The value at location 2 is  $A + B$ , at location 3 is  $A + C$ , and at location 4 is  $A + B + C + D$ . The sum within  $D$  can be computed as  $4 + 1 - (2 + 3)$ . Illustration taken from [VJ01].

the positive and negative examples. For each feature, the weak learner determines the optimal threshold classification function, such that the minimum number of examples are misclassified [VJ01].

Learning algorithm combines many *weak* classifiers to create one *strong* classifier. *Weak* here means the classifier only gets the right answer a little more often than random guessing would. Then, this learning algorithm selects a set of weak classifiers to combine and assigns a weight to each. This weighted combination is the strong classifier.

4. *Cascades of classifiers*: Viola and Jones introduced a method for combining successively more complex classifiers in a cascade structure for increased detection performance while radically reducing computation time. The rationale behind this is to construct boosted classifiers which reject many of the negative sub-windows while detecting almost all positive instances. Simpler classifiers are used to reject the majority of subwindows before more complex classifiers are called upon to achieve low false positive rates [VJ01]. Each stage is only required to eliminate slightly more than 50% of

false detection as long as it kept the positive hit rate close to 100%. An illustration of such cascaded structure is shown in Figure 2.11.

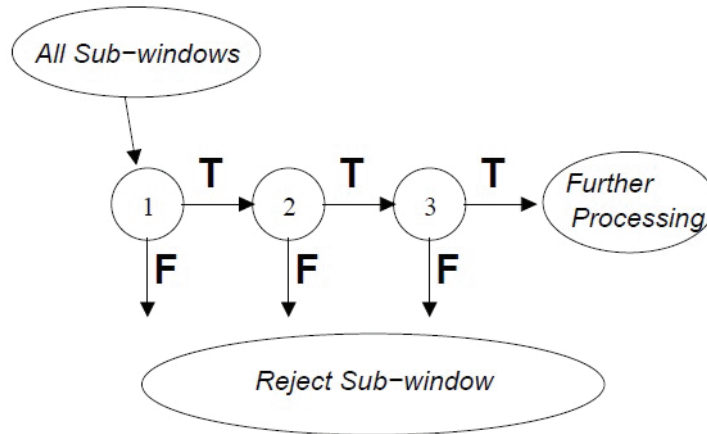


Figure 2.11: Schematic depiction of a the detection cascade. A series of classifiers are applied to every sub-window. The initial classifier eliminates a large number of negative examples with very little processing. Subsequent layers eliminate additional negatives but require additional computation. After several stages of processing the number of sub-windows have been reduced radically. Further processing can take any form such as additional stages of the cascade or an alternative detection system. Illustration taken from [VJ01].

### 2.3.2 Feature extraction

After detecting face in input stimuli, feature selection is one of the most important step to successfully analyze and recognize facial expressions automatically. The optimal features should minimize within-class variations of expressions while maximize between class variations. If inadequate features are used, even the best classifier could fail to achieve accurate recognition [SGM09]. In literature, various methods are employed to extract facial features and these methods can be categorized either as appearance based methods or geometric feature based methods. Geometric features present the shape and locations of facial components (including mouth, eyes, brows, nose), while the appearance features present the appearance (skin texture) changes of the face, such as wrinkles and furrows [TKCis].

### 2.3.2.1 Appearance based methods

Different methods that are usually employed to extract appearance information are:

1. Gabor Features
2. Haar-like features
3. Local Binary Pattern (LBP) features

Brief overview of the above mentioned features are given below.

**Gabor Features:** the Gabor decomposition of an image is computed by filtering the input image with a Gabor filter, which can be tuned to a particular frequency  $k_0 = (u, v)$ , where  $k = \|k_0\|$  is the scalar frequency and  $\varphi = \arctan\left(\frac{u}{v}\right)$  is the orientation. Gabor filters accentuate the frequency components of the input image which lie close to  $k$  and  $\varphi$  in spatial frequency and orientation, respectively. A Gabor filter can be represented in the space domain using complex exponential notation as:

$$F_{k_0} = \frac{k_0^2}{\sigma^2} \exp\left(-\frac{k_0^2 x^2}{2\sigma^2}\right) \left( \exp(ik_0 \cdot x) - \exp\left(-\frac{\sigma^2}{2}\right) \right) \quad (2.2)$$

where  $x = (x, y)$  is the image location and  $k_0$  is the peak response frequency [LVB<sup>+</sup>93]. An example of a Gabor filter is given in Figure 2.12, which shows the absolute value (left), real component (middle), and imaginary component (right) of the filter in the space domain.

For expression analysis, often a filter bank of multiple Gabor filters tuned to different characteristic frequencies and orientations is used for feature extraction. The combined response is called a jet. Filter banks typically span at least 6 different orientations and have frequencies spaced at half-octaves. Prior to classification, the extracted features are usually converted into real numbers by calculating the magnitude of the complex filter response.

Examples of different methods that uses Gabor features are [LBF<sup>+</sup>06, Tia04, DBH<sup>+</sup>99]. Littlewort et al. [LBF<sup>+</sup>06] has shown a high recognition accuracy (93.3% for Cohn-Kanade facial expression database



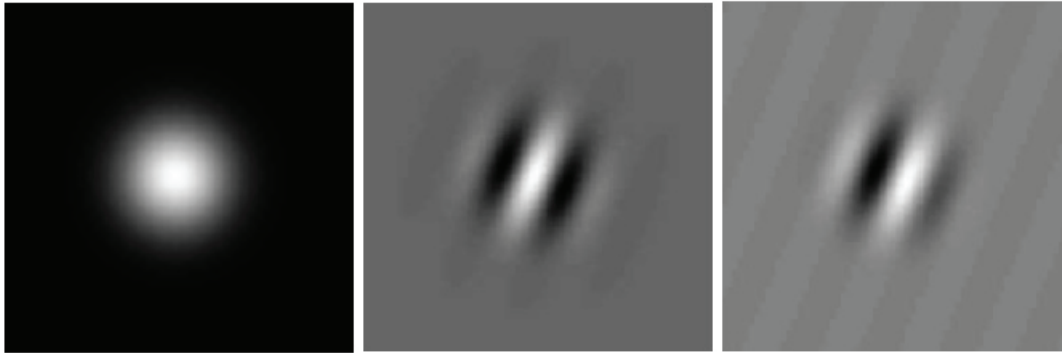


Figure 2.12: The left, middle, and right graphics above show the absolute value, and the real and imaginary components of a sample Gabor filter.

[KCT00]) using Gabor features. They proposed to extract Gabor features from the whole face and then selected the subset of those features using AdaBoost method. Tian [Tia04] has used Gabor wavelets of multi-scale and multi-orientation at the “difference” images. The difference images were obtained by subtracting a neutral expression frame from the rest of the frames of the sequence. Donato et al. [DBH<sup>+</sup>99] has employed the technique of dividing the facial image into two: upper and lower face to extract finer Gabor representation for classification. Generally, the drawback of using Gabor filters is that it produces extremely large number of features and it is both time and memory intensive to convolve face images with a bank of Gabor filters to extract multi-scale and multi-orientational coefficients [SGM09].

**Haar-like features:** Viola and Jones face detector [VJ01] introduced Haar-like features due to their computational simplicity for feature extraction. Haar-like features owe their name to their intuitive similarity with Haar wavelets. Haar wavelets are single wavelength square waves (one high interval and one low interval). In two dimensions, a square wave is a pair of adjacent rectangles - one light and one dark. The actual rectangle combinations used for visual object detection are not true Haar wavelets. Instead, they contain rectangle combinations better suited to visual recognition tasks. Because of that difference, these features are called Haar-like features, rather than Haar wavelets.

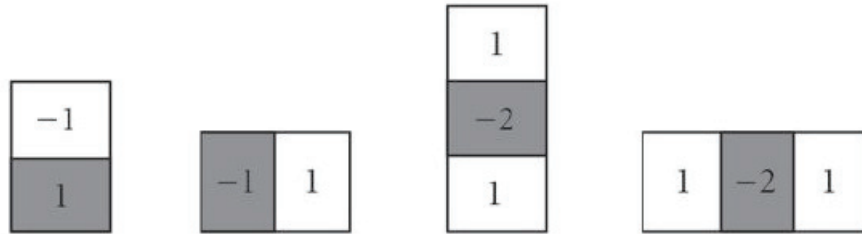


Figure 2.13: The basic haar-like feature template.

In the Figure 2.13, the basic Haar-like feature templates are displayed. And the process of Haar-like feature extraction on a face image is shown in the Figure 2.14. The key advantage of a Haar-like feature over most other features is its calculation speed [PS10]. Due to the use of integral images (see Section 2.3.1 for details), a Haar-like feature of any size can be calculated in constant time [VJ01]. Because of this advantages of Haar-like feature, researchers also applied it on facial expression analysis [YLM10, WO06] and got promising performance. Yang et al. [YLM10] extracted Haar-like features from the facial image patches (49 sub-windows). Compositional features based on minimum error based optimization strategy were build within the Boosting learning framework. The proposed method was tested on Cohn-Kanade facial expression database [KCT00] and it achieved average recognition accuracy of 92.3% on the apex data (last three frames of the sequence) and 80% on the extended data (frames from onset to apex of the expression).

**Local Binary Pattern (LBP) features:** LBP features were initially proposed for texture analysis [OPH96], but recently they have been successfully used for facial expression analysis [ZP07, SGM09]. The most important property of LBP features are their tolerance against illumination changes and their computational simplicity [OP99, OPH96, OPM02]. The operator labels the pixels of an image by thresholding the 3 x 3 neighbourhood of each pixel with the center value and considering the result as a binary number. Then the histogram of the labels can be used as a texture descriptor. Formally, LBP operator takes the form:



Figure 2.14: Haar-like features extracted from different position and different scale on the face image.

$$LBP(x_c, y_c) = \sum_{n=0}^7 s(i_n - i_c) 2^n \quad (2.3)$$

where in this case  $n$  runs over the 8 neighbours of the central pixel  $c$ ,  $i_c$  and  $i_n$  are the grey level values at  $c$  and  $n$  and  $s(u)$  is 1 if  $u \geq 0$  or 0 otherwise.

Shan et al. [SGM09] applied the LBP features on facial expression recognition and also got promising performance. Zhao et al. [ZP07] proposed to model texture using volume local binary patterns (VLBP) an extension to LBP, for expression recognition. Average FER accuracy of 96.26% was achieved for six universal expression with their proposed model on Cohn-Kanade facial expression database [KCT00]. Due to both spacial and temporal information is considered in VLBP, it got better result comparing with the traditional LBP.

Inspired by Shan's and Zhao's work we also used LBP features in a novel fashion (See Chapter 6 for details). We extended LBP descriptor to Pyramid LBP (PLBP). PLBP is a *pyramidal-based spatial* representation of local binary pattern (LBP) descriptor. PLBP represents stimuli by their local texture (LBP) and the spatial layout of the texture. The spatial layout is acquired by tiling the

image into regions at multiple resolutions. We obtained very good results using our novel approach on different databases and the proposed descriptor performed much better than other state-of-the-art descriptors on low resolution images.

### 2.3.2.2 Geometric feature based methods

As mentioned earlier, geometric features present the shape and locations of facial components (including mouth, eyes, brows, nose). Thus, the motivation for employing a geometry-based method is that facial expressions affect the relative position and size of various facial features, and that, by measuring the movement of certain facial points, the underlying facial expression can be determined [ZJ05, PP06, VPP05, BGJH09, PPNH06, VP06]. In order for geometric methods to be effective, the locations of these fiducial points must be determined precisely; in real-time systems, they must also be found quickly. The exact type of feature vector that is extracted in a geometry-based facial expression recognition systems depends on

1. which points on the face are to be tracked,
2. whether 2-D or 3-D locations are used,
3. the method of converting a set of feature positions into the final feature vector.

Active shape models (ASMs) [CHTH94] are statistical models of the shape of objects which iteratively deform to fit to an example of the object in a new image. One disadvantage of ASM is that it only uses shape constraints (together with some information about the image structure near the landmarks), and does not take advantage of all the available information: the texture across the target. Therefore, active appearance model (AAM) [CET98] which is related to ASM is proposed for matching a statistical model of object based on both shape and appearance to a new image. Like the ASM, AAM is also built during a training phase: on a set of images, together with coordinates of landmarks that appear in all of the images, is provided to the training supervisor. AAM could be looked as the hybrid methods based on both geometric and appearance features.

The typical examples of geometric-feature-based methods are those of Pantic and her colleagues [PPNH06, VP06], who used a set of facial characteristic points around the mouth, eyes, eyebrows, nose, and chin. Figure 2.15 shows the landmarks in Pantic’s work, and through tracking these landmarks, the motion information is obtained to do expression recognition.

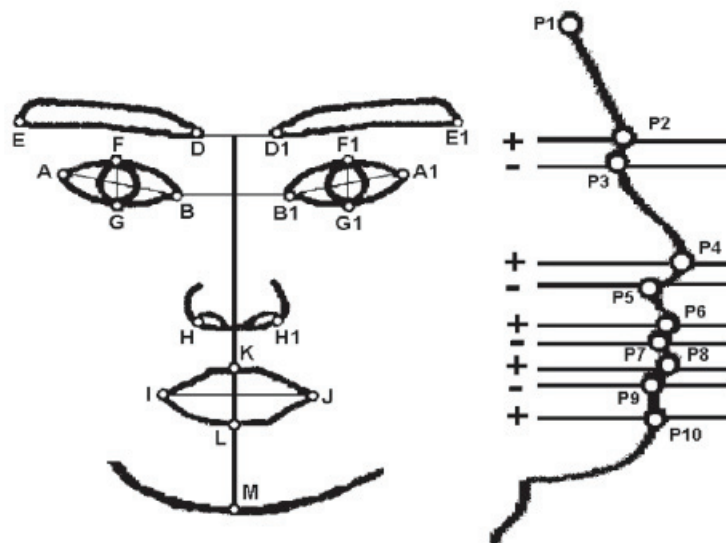


Figure 2.15: Demonstration Landmarks on the face.

Zhang et al. [ZJ05] measured and tracked the facial motion using Kalman Filters. To achieve the expression recognition task they have also modeled the temporal behaviors of the facial expressions using Dynamic Bayesian networks (DBNs). In [VPP05] authors have presented Facial Action Coding System’s (FACS) [EF78] Action Unit (AU) detection scheme by using features calculated from the “Particle Filter” tracked fiducial facial points. They trained the system on the MMI-Facial expression database [PVRM05] and tested on the Cohn-Kanade database [KCT00] and achieved recognition rate of 84%. Bai et al. [BGJH09] extracted only shape information using Pyramid Histogram of Orientation Gradients (PHOG) and showed the “smile” detection accuracy as high as 96.7% on Cohn-Kanade database [KCT00]. PHOG is a spatial shape descriptor and it describes object appearance and shape by the distribution of

intensity gradients or edge directions. More information on PHOG is given in Chapter 5.

Research has been done with success in recent times to combine features extracted using appearance-based methods and geometric feature-based methods [KZP08, DAGG11]. The key problem with geometric methods is to precisely locate the landmark and track it. In the real applications, due to the pose and illumination variations, small resolution input images, and the noise from the background, it is still very hard to precisely locate the landmarks.

### 2.3.3 Expression classification / recognition

Last step of automatic expression analysis system is classification. Some system directly classify expressions while others classify expressions by first recognizing particular action units “AU” [EF78] (see Section 2.1.2 for description of FACS (facial action coding system) and AU). According to [Mit97] classification deals with labelling new sample/data on the basis of a training data containing observations (or instances) whose category membership is known (supervised learning).

Some of the most frequently used classification techniques are:

1. Template based methods
2. Support Vector Machines based methods
3. Boosting based methods
4. Classification Trees
5. Instance Based Learning
6. Naive Bayes Classifiers

#### 2.3.3.1 Template based methods

The template-based techniques are simple face representation and classification methods. They just compare the new images with the learned template which normally is the average of the images in the same category. These methods have

limited recognition capabilities, because the averaging process always causes smoothing of some important individual facial details, and misalignment of the faces also impacts the template. Another problem is the inability of this technique to cope with large inter-personal expression differences [Yan11]. Due to all of these problems template based classification methods are not used much in facial expression analysis now. Examples of facial feature analysis systems that reported their recognition accuracy using this technique are [EP95, AHP04, SGM09].

### 2.3.3.2 Support Vector Machines based methods

Support Vector Machines (SVMs) are state-of-the-art large margin classifiers which have recently gained popularity within visual pattern recognition. In this section, a brief review of the theory behind this algorithm is presented, for more details we refer reader to [Vap98].

We have  $L$  training points, where each input  $X_i$  has  $D$  attributes (i.e. is of dimensionality  $D$ ) and is in one of two classes  $y_i = -1$  or  $+1$ , i.e our training data is of the form:

$$\{x_i, y_i\} \text{ where } i = 1 \dots L, y_i \in \{-1, 1\}, x \in \mathbb{R}^D$$

Here we assume the data is linearly separable, meaning that we can draw a line on a graph of  $x_1$  vs  $x_2$  separating the two classes when  $D = 2$  and a hyperplane on graphs of  $x_1, x_2 \dots x_D$  for when  $D > 2$ .

This hyperplane can be described by  $w \cdot x + b = 0$  where:

1.  $w$  is normal to the hyperplane.
2.  $\frac{b}{\|w\|}$  is the perpendicular distance from the hyperplane to the origin.

Support Vectors are the examples closest to the separating hyperplane and the aim of Support Vector Machines (SVM) is to orientate this hyperplane in such a way as to be as far as possible from the closest members of both classes.

Referring to Figure 2.16, implementing a SVM boils down to selecting the variables  $w$  and  $b$  so that our training data can be described by:

$$w \cdot x + b \geq +1 \text{ for } y_i = +1 \tag{2.4}$$

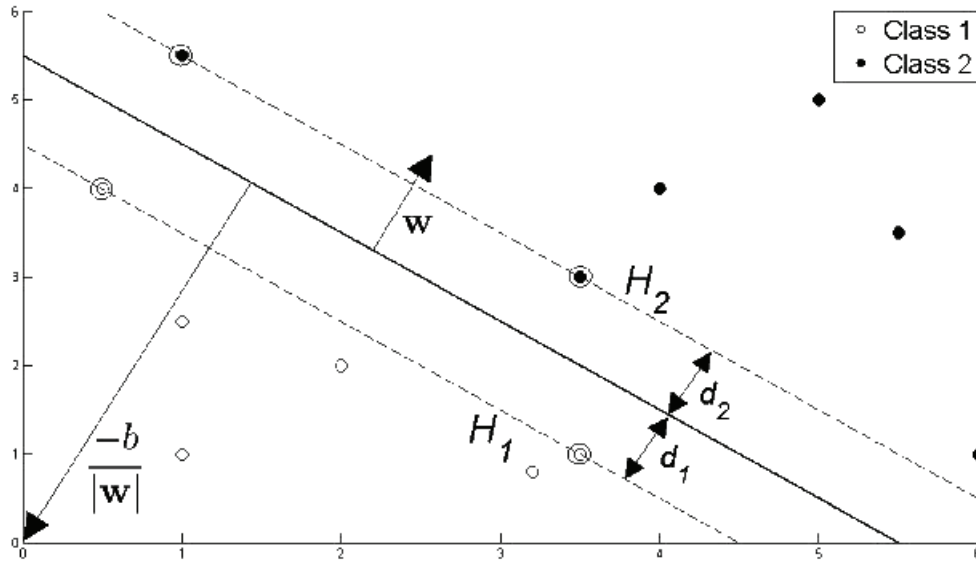


Figure 2.16: Hyperplane through two linearly separable classes.

$$w \cdot x + b \leq -1 \text{ for } y_i = -1 \quad (2.5)$$

These equations can be combined into:

$$y_i(w \cdot x + b) - 1 \geq 0 \quad \forall i \quad (2.6)$$

In this thesis we have used the SVM implementation available in WEKA, open source data mining software in Java [HFH<sup>+</sup>09]. As SVM proves to be highly powerful for classification tasks, it is considered to be the state-of-the-art method and is used in almost all of the latest/reviewed frameworks for expression recognition, i.e. [KBP08, KZP08, DAGG11, SGM09, ZP07, KMKB12b, JVP11, LFCY06, LBL07].

### 2.3.3.3 Boosting based methods

Boosting refers to the general problem of learning accurate prediction rule by combining moderately weak learners or weak hypothesis. A weak learner means the classifier only gets the right answer a little more often than random guessing



would. Then, Boosting based learning algorithm linearly combines weak classifiers to obtain a strong classifier that generalizes well over the target domain (reduced cumulative error). Research has shown improved generalization performance of ensemble of classifiers (linear combination of classifiers) in many machine learning problem over single classifier [Leo96].

In the domain of facial expression recognition very often, the dimension of features extracted from face image is very high, and it is almost impossible to directly use the high dimension features to train classifier, as in Gabor features (see Section 2.3.2.1). Therefore, feature selection and dimension reduction must be done as preprocessing. These problems have been addressed by boosting based classification methods as during the building of strong classifier it can do feature selection at the same time because the weak classifier is directly relative to the corresponding feature [Yan11].

AdaBoost (Adaptive Boosting) [FS95], as proposed in the seminal work of Freund et al., is probably the most popular boosting algorithm. AdaBoost adjusts adaptively to the errors of the weak hypotheses and subsequent classifiers built are tweaked in favor of those instances misclassified by previous classifiers. Due to this advantage AdaBoost has also been employed for facial expression recognition tasks.

Littlewort et al. [LBF<sup>+</sup>06] has used the power of AdaBoost method to select the subset of most discriminant features. They extract Gabor features from the whole face and then selected the subset of those features. Their proposed system achieved recognition accuracy of 93.3% for Cohn-Kanade facial expression database [KCT00]. Yang et al. [YLM10] also used the power of boosting classifier to extract compositional features. They extracted Haar-like features (see section 2.3.2.1 for reference) from the facial image patches (49 sub-windows). Compositional features based on minimum error based optimization strategy were built within Boosting learning framework. The proposed method was tested on Cohn-Kanade facial expression database [KCT00] and it achieved average recognition accuracy of 92.38% on the apex data (last three frames of the sequence) and 80% on the extended data (frames from onset to apex of the expression).

### 2.3.3.4 Classification trees

A Classification Tree is a classifier composed by nodes and branches which break the set of samples into a set of covering decision rules. In each node, a single test is made to obtain the partition. The starting node is called the root of the tree. In the final nodes or leaves, a decision about the classification of the case is made. In this research work, we have used C4.5 paradigm [Qui93]. Random Forest (RFs) are collections of Decision Trees (DTs) that have been constructed randomly. RFs generally performs better than DT on unseen data.

### 2.3.3.5 Instance based learning

$k$ -NN classifiers are instance-based algorithms taking a conceptually straightforward approach to approximate real or discrete valued target functions. The learning process consists in simply storing the presented data. All instances correspond to points in an  $n$ -dimensional space and the nearest neighbors of a given query are defined in terms of the standard Euclidean distance. The probability of a query  $q$  belonging to a class  $c$  can be calculated as follows:

$$p(c | q) = \frac{\sum_{k \in K} W_k \cdot 1_{(kc=c)}}{\sum_{k \in K} W_k} \quad (2.7)$$

$$W_k = \frac{1}{d(k, q)} \quad (2.8)$$

$K$  is the set of nearest neighbors,  $kc$  the class of  $k$  and  $d(k, q)$  the Euclidean distance of  $k$  from  $q$ .

Figure 2.17 illustrates the operation of the  $k$ -Nearest Neighbor algorithm for the case where the instances are points in a two-dimensional space and where the target function is boolean valued.

### 2.3.3.6 Naïve Bayes classifiers

Bayesian classifiers are statistical classifiers and are based on Bayes theorem. They can predict class membership probabilities, such as the probability that a given sample belongs to a particular class. Naïve Bayesian (NB) classifiers assume that

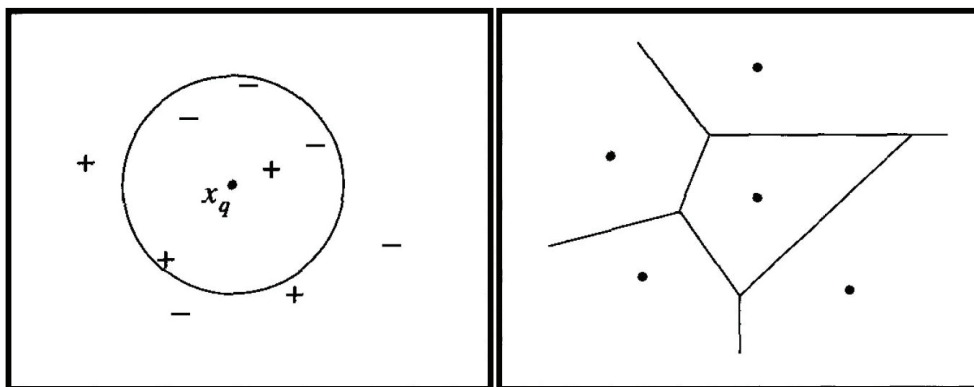


Figure 2.17:  $k$ -Nearest Neighbor in a two-dimensional space and where target function is boolean valued. A set of +ve and -ve training examples is shown on the left, along with a query instance  $x_q$  to be classified. The 1-Nearest Neighbor algorithm classifies  $x_q$  +ve whereas 5-Nearest Neighbor algorithm classifies it as -ve. On the right is the decision surface induced by the 1-Nearest Neighbor algorithm. The convex polygon surrounding each training example indicates the region of instance space closest to that point (i.e. the instance for which 1-Nearest Neighbor algorithm will assign the classification belonging to that training example).

the effect of an attribute value on a given class is independent of the values of the other attributes. This assumption is called class conditional independence. It is made to simplify the computation involved and, in this sense, is considered “naïve”.

To classify a new sample characterized by  $d$  genes  $X = (X_1, X_2, \dots, X_d)$ , the NB classifier applies the following rule:

$$C_N - B = \arg \max_{c_j \in C} p(c_j) \prod_{i=1}^d p(x_i | c_j) \quad (2.9)$$

where  $C_N - B$  denotes the class label predicted by the Naive-Bayes classifier and the possible classes of the problem are grouped in  $C = \{c_1, \dots, c_l\}$ .

In this section we presented a survey of different state-of-the-art methods that exist for three sub-components (face detection and tracking, feature extraction and expression classification) of facial expression recognition systems. Frameworks that are proposed (for reference see Chapters 4, 5 and 6) during the course of this research have used some of these methods. Next section (Section 2.4) describes

the drawbacks of current methods for expression analysis and our contributions in this regard.

## 2.4 Drawbacks of the current methods and contributions

### 2.4.1 Exploiting visual saliency

We have found one main shortcoming in all of the reviewed methods for automatic facial expression recognition that none of them tries to mimic the human visual system in recognizing them. Rather all of the methods, spend computational time on whole face image or divides the facial image based on some mathematical or geometrical heuristic for features extraction. We argue that the task of expression analysis and recognition could be done in more conducive manner, if only some regions are selected for further processing (i.e. salient regions) as it happens in human visual system. Thus, our contributions in this regard are twofold:

1. We have statistically determined which facial region(s) is salient according to human vision for six basic expressions by conducting psycho-visual experiment. The experiment has been carried out using eye-tracker which records the fixations and saccades of human observers as they watch the collection of videos showing facial expressions. Salient facial regions for specific expressions have been determined through the analysis of the fixation data (for reference see Chapter 3).
2. We have illustrated that human visual system inspired frameworks can achieve high facial expression recognition (FER) accuracy (results that exceeds state-of-the-art methods). Highly discriminative feature space is created by extracting features only from the perceptually salient facial regions. For reference read Chapters 5 and 6.

As a consequence of studying the human visual system and using this knowledge in proposed frameworks, we achieved the following two objectives.

### **2.4.1.1 Computational simplicity**

Generally, we have found that all the reviewed methods for automatic facial expression recognition are computationally expensive and usually require a dimensionally large feature vector to complete the task. This explains their inadequacy for real-time applications, although they produce good results on different datasets. Our proposed algorithms are based on the phenomenon of visual saliency, thus reduction in feature vector dimensionality is inherited. This reduction in computational complexity makes our proposed algorithms suitable for real-time applications.

### **2.4.1.2 Adequacy for low resolution stimuli**

There exist lots of methods for facial expression recognition but very few of those methods provide results or work adequately on low resolution images. In this research thesis, we have proposed a facial expression recognition system that caters for illumination changes and works equally well for low resolution as well as for good quality / high resolution images. For reference see Section 6.3.

### **2.4.2 Expressions different from six prototypical facial expression**

More research effort is required to be put forth for recognizing facial expressions such as fatigue, pain, and mental states such as agreeing, disagreeing, lie, frustration, thinking as they have numerous application areas. In this work, we are proposing a novel computer vision system that can recognize expression of pain in videos by analyzing facial features. For reference see Section 6.4.



# Chapter 3

## Psycho-Visual experiment

### Contents

---

<b>3.1</b>	<b>Methods . . . . .</b>	<b>50</b>
3.1.1	Participants . . . . .	51
3.1.2	Eye-tracker . . . . .	52
3.1.3	Experiment builder . . . . .	56
<b>3.2</b>	<b>Procedure . . . . .</b>	<b>57</b>
3.2.1	Eye movement recording . . . . .	60
3.2.2	Stimuli . . . . .	60
<b>3.3</b>	<b>Psycho-Visual experiment: results and discussion . . .</b>	<b>61</b>
3.3.1	Gaze map construction . . . . .	61
3.3.2	Observations from the gaze maps . . . . .	62
3.3.3	Substantiating observations through statistical analysis	63
<b>3.4</b>	<b>Conclusion . . . . .</b>	<b>68</b>

---

There has long been interest in the nature of eye movements and fixation behavior following early study by Buswell [Bus35]. Eye fixations describe the way in which visual attention is directed towards salient regions in a given stimuli [RCB02], where “salient” means most noticeable or most important. In computer vision the notion of saliency was mainly popularized by Tsotsos et al. [TSW+95]

and Olshausen et al. [OAVE93] with their work on visual attention, and by Itti et al. [IKN98] with their work on rapid scene analysis.

Recently, computer vision research community has shown lot of interest in understanding human visual attention phenomenon as it has been shown that such an approach could drastically reduce the need for computational resources without altering the quality of results [Har06]. Various computer vision applications have benefited by understanding human visual attention phenomenon. Such applications are adaptive content delivery, smart resizing, adaptive region-of-interest based compression and image quality analysis [MZ03, STR<sup>+</sup>05, AS07, LQI11, GMK02, Itt04, KKD10, QL08, IKN98]. This motivates to understand underlying mechanisms of human visual attention when decoding facial expressions.

This chapter presents all the details related to psycho-visual experimental study, which we have conducted in order to study human visual attention mechanisms when it decodes facial expressions. The experiment was conducted with the help of an eye-tracking system which records fixations and saccades. We segmented eye fixation data as it is known that eye gathers most of the information during the fixations [RCB02]. Results deduced from the experiment serves as the basis to determine salient facial regions which are algorithmically processed to extract features for automatic analysis of expressions. Sections 3.1 and 3.2 presents details related to hardware equipment, observers, stimuli, software while the results of the study are presented in Section 3.3.

## 3.1 Methods

Eye movements of human observers were recorded as subjects watched a collection of 54 videos selected from the extended Cohn-Kanade (CK+) database (Refer Appendix Section A.1), showing one of the six universal facial expressions [Ekm71]. Then saccades, blinks and fixations were segmented from each subject's recording. Each video showed a neutral face at the beginning and then gradually developed into one of the six facial expression.



### 3.1.1 Participants

Fifteen observers volunteered for experiment. They include both male and female aging from 20 to 45 years with normal or corrected to normal vision. Most of the participants / observers are graduate students while some are faculty members.

All observers were naive to the purpose of the experiment. They were given only a short briefing about the apparatus and about the expected time required to complete the whole experiment.

Figure 3.1 shows observers classification on the basis of age groups. Subjects/observers were classified in five age groups i.e. 20-25, 25-30,30-35, 35-40 and 40-45. Figure 3.2 shows classification of observers on the basis of their ethnicity, while Figure 3.3 shows classification of observers on the basis of their sex.

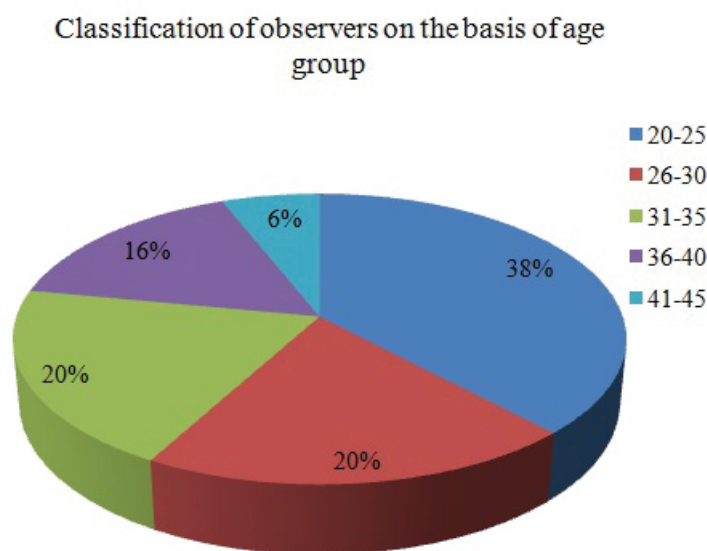


Figure 3.1: Observer’s classification on the basis of age group.

Figure 3.1 shows that observers presented a good mix of different age groups while Figures 3.2 and 3.3 show that the observers came from different ethnic backgrounds with no gender bias. These figures emphasize the fact that experimental study is not biased to one ethnic background, sex or one age group, as these biases are proved to impact on the judgment of expressions [EA02, HBK00].

Classification of observers on the basis of ethnicity

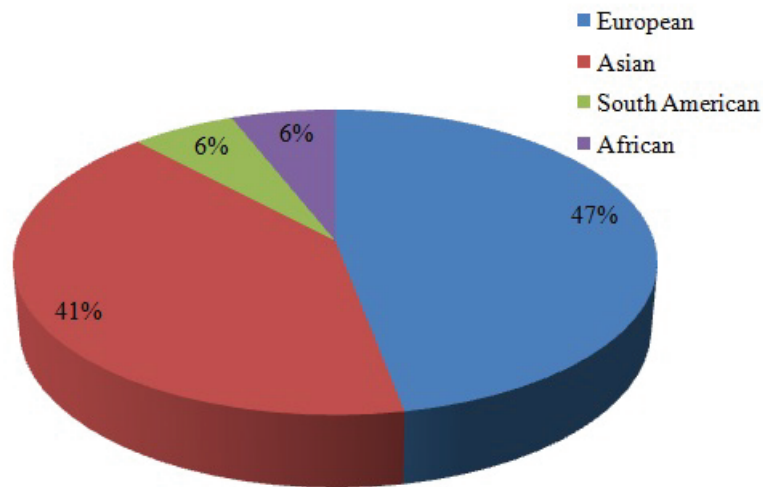


Figure 3.2: Observer's classification on the basis of their ethnicity.

Classification of observers on the basis of sex

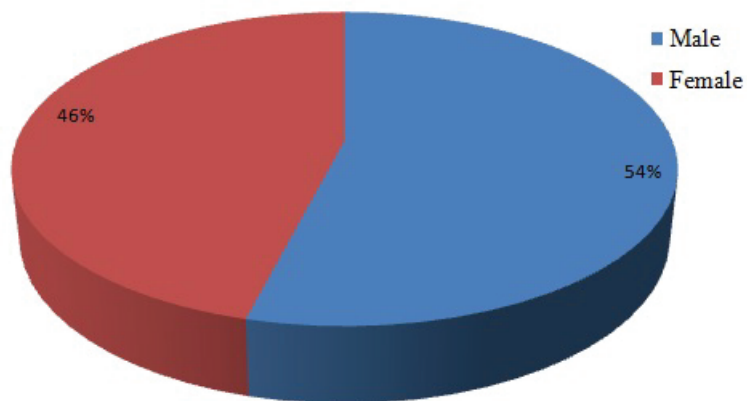


Figure 3.3: Observer's classification on the basis of their sex.

### 3.1.2 Eye-tracker

A video based eye-tracker (Eyelink II system from SR Research, Canada) was used to record eye movements (see Figure 3.4 for reference). The system consists of three miniature infrared cameras.

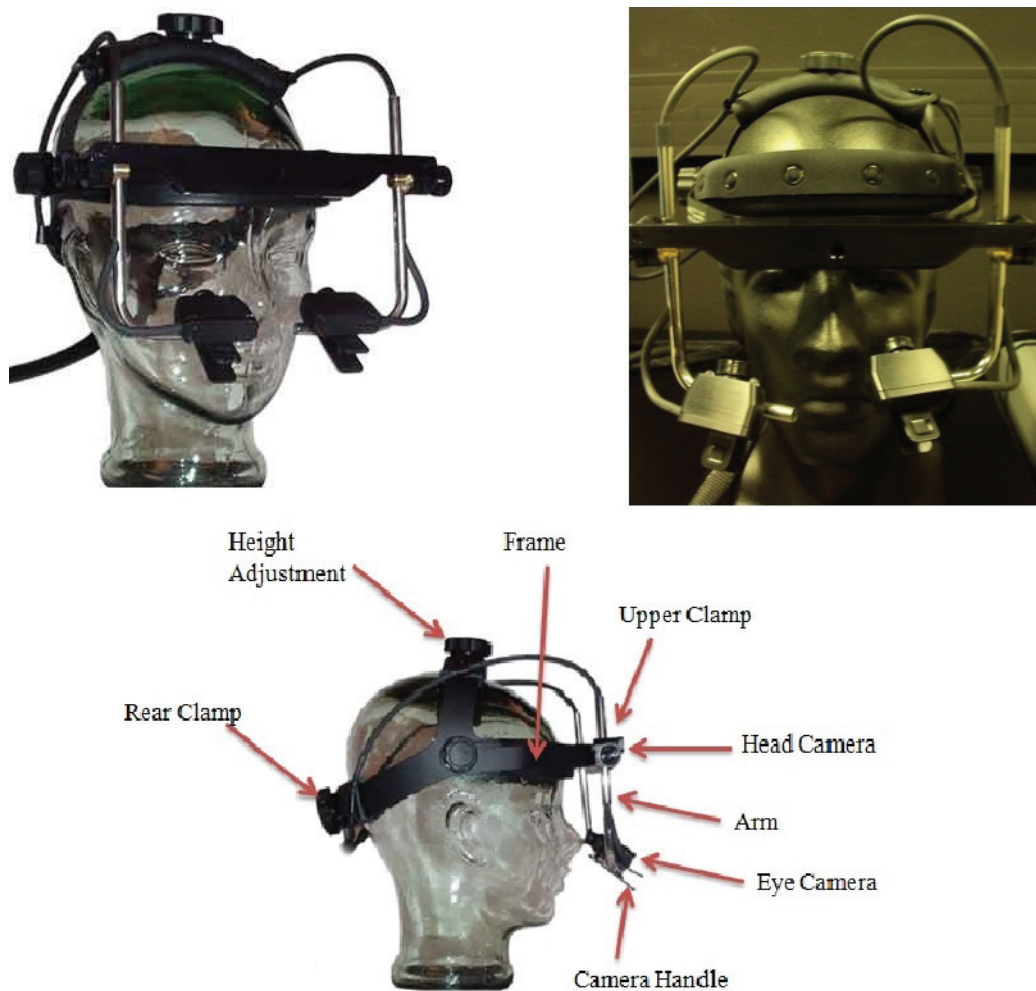


Figure 3.4: Eyelink II, Eye-tracker used in our experiment.

The EyeLink II headband has two eye cameras for binocular tracking or instant selection of eye to be tracked as well as an optical head tracking camera with exceptionally low angular noise. The headband also contains these key features:

1. Off-axis illumination and high-contrast cameras for maximum compatibility with eyeglasses and contact lenses.
2. Lightweight headband ( $\sim 420\text{g}$ ) has a low center of mass for stability, is well balanced and has low rotational inertia. This reduces neck muscle tremor and permits long periods of use without fatigue.

3. Leather-padded headband provides excellent grip on skin with low pressure, and is not affected by skin oils.
4. No mirrors used for lightweight and robustness.
5. All mechanical adjustments and sliding parts have been wear-tested to ensure long lifetime with no maintenance.

The Eyelink II system allows determination and tracking of subject's dominant eye without any mechanical configuration. Each camera has a built-in infrared illuminator (925 nm IR, IEC-825 Class 1,  $<1.2 \text{ mW/cm}^2$ ) . As the eye-tracker system used for experiment was head mounted, the observers were allowed to move their heads normally during experiment.

### 3.1.2.1 Tracker application

EyeLink II Tracker Application was used during the experiment for camera set-up, calibration, validation, and drift correction, as explained below:

1. Camera set-up. The first step for the experiment execution is to set-up eye and head tracking cameras. Eye(s) to be tracked, tracking mode and options are to be set. Then calibration, validation, and drift correction are performed. Figure 3.5 shows the screen shot of the set-up screen.
2. Calibration. Calibration is used to collect fixations on target points, in order to map raw eye data to gaze position. Targets are presented for the observers to fixate on the Display PC while feedback graphics are presented to the experimenter on this display. The calibration is then checked, and diagnostics are provided. Calibration was performed after camera setup and before validation. Figure 3.6 shows the calibration screen.
3. Validation. The validation of the calibration was achieved by measuring the difference between the computed fixation positions and the locations of the target points. Such a difference reflects the accuracy of the eye movement recording. A threshold error of  $1^\circ$  has been selected as the greatest divergence that could be accepted.

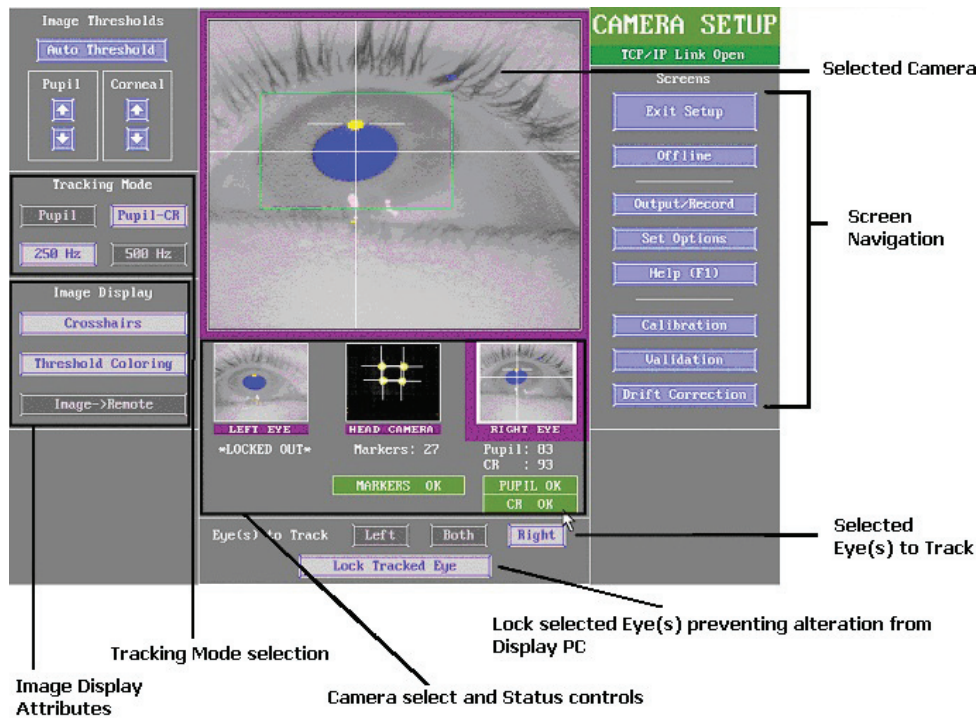


Figure 3.5: EyeLink II Camera Setup Screen.

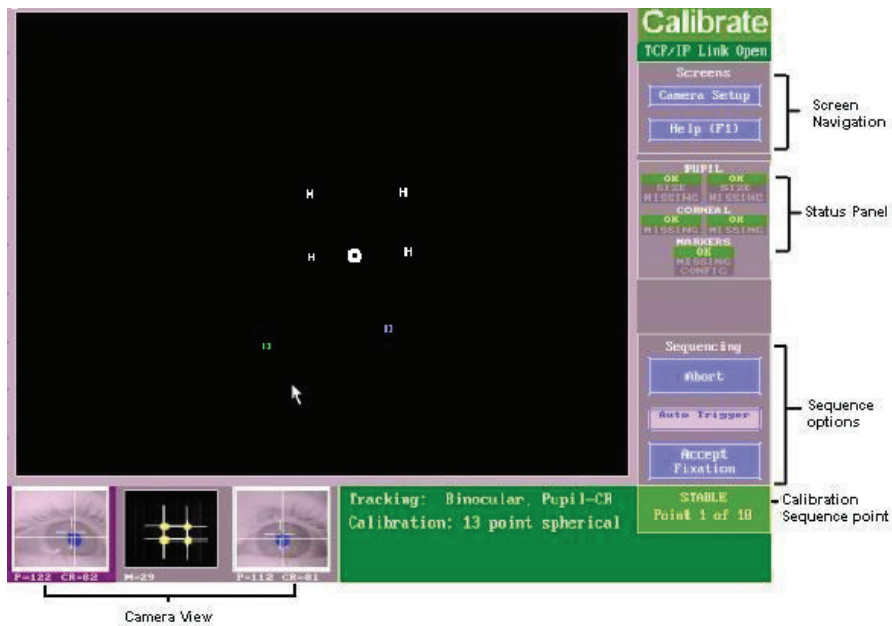


Figure 3.6: EyeLink II Calibration Screen.

4. Drift correction. The drift correction process displays a single target to the participant and then measures the difference between the computed fixation position during calibration / validation and the target. This error reflects headband slippage or other factors, which are then corrected for by the measured error.

### **3.1.3 Experiment builder**

The SR Research Experiment Builder (SREB) is a visual experiment creation tool. When used in combination with the SR Research EyeLink eye tracking system, the SREB provides seamless integration into the EyeLink hardware and software platform. As a convenient tool for creating eye-tracking experiments, the Experiment Builder is fully integrated with the EyeLink eye tracker.

#### **3.1.3.1 Features**

We created experiments in the Experiment Builder by dragging and dropping experiment components into a workspace and configuring the properties of the added components. There are two main classes of experiment components in the Experiment Builder: Actions and Triggers. Actions tell the computer to do something, like displaying a set of graphics on the screen or playing a sound. Triggers define the conditions that must be met before an action can be performed. Examples of Triggers are keyboard events and eye (Fixation, Saccade, and Invisible Boundary) events. Our experiment is categorized in the first category i.e actions. Figure 3.7 shows the graphical/block diagram of our experiment.

#### **3.1.3.2 Organization of events in an experiment**

Our experiment can be dissected into several levels along a hierarchy of Experiment, Blocks, Trials, Trial Runtime / Recording. All of the events within each level of this hierarchy are conveniently wrapped in a loop (called sequence or sub-graph in Experiment Builder). This allows the whole sequence to be connected to other objects as a unit and be repeated several times in a row. Figure 3.8 illustrates our experiment architecture.

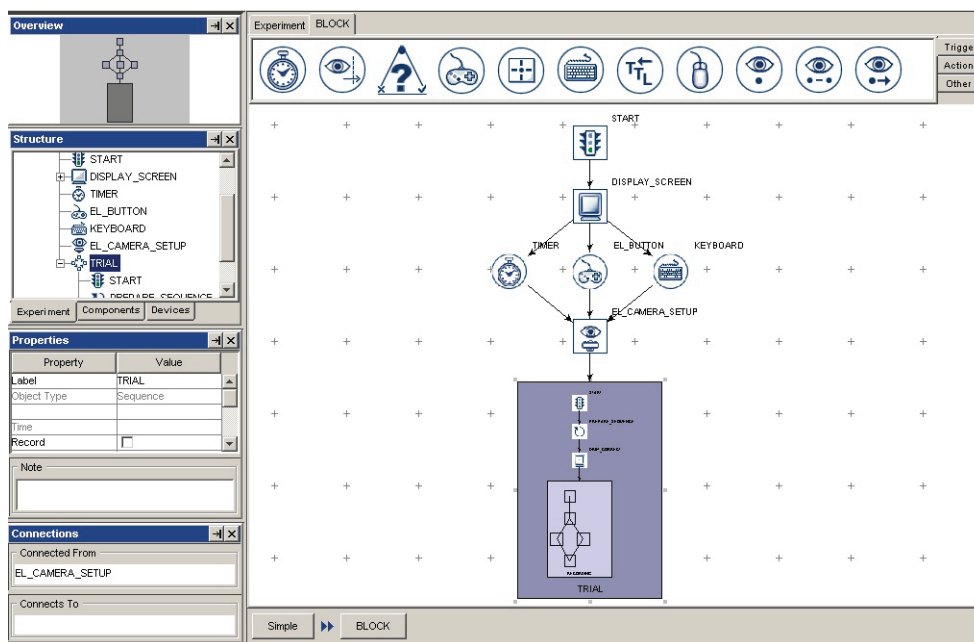


Figure 3.7: Block diagram of the experiment.

The top-most level of the experiment (Experiment Sequence) contains a greeting message/instruction screen followed by a sub-sequence representing blocks of trials (Block Sequence), and then a goodbye or debriefing message at the end of the experiment. Within each repetition of the Block Sequence, the user/observer first performs a camera adjustment, calibration and validation, and then runs several trials (Trial Sequence containing different videos). Every iteration of the Trial Sequence starts with pre-recording preparations (e.g. video resources, sending some simple drawing graphics to the tracker screen, flushing log file) and drift correction followed by the trial recording (Recording Sequence). The Recording Sequence is responsible for collecting the eye data and is where visual and auditory stimuli are presented.

## 3.2 Procedure

The experiment was performed in a dark room with no visible object in observer's field of view except stimulus. The participants were seated on an adjustable height chair. The height of the chair was adjusted in order that the eyes of all subjects



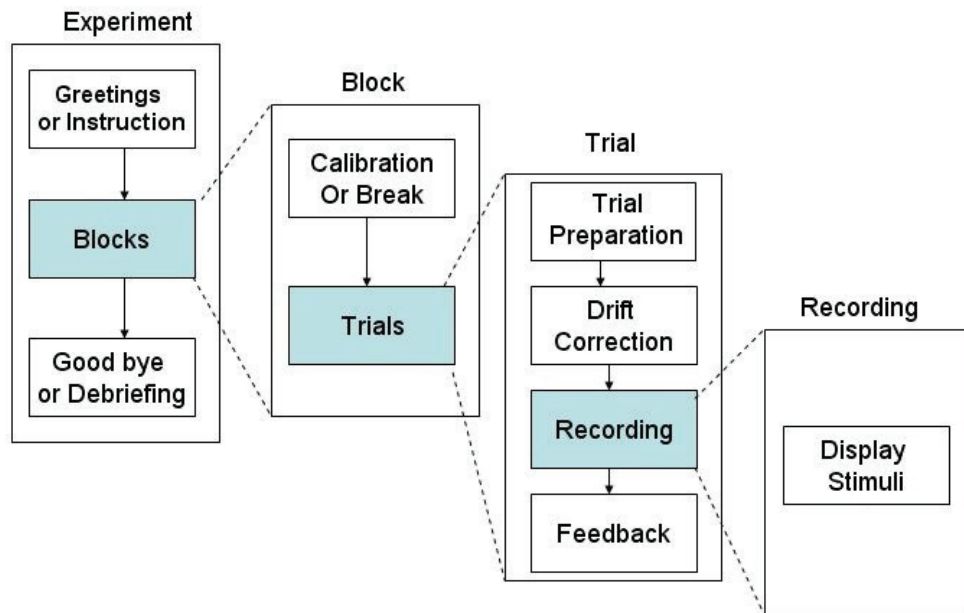


Figure 3.8: Hierarchical Organization of the experiment

would align with the center of the screen. Stimuli (videos) were presented on a 19 inch CRT monitor with a resolution of 1024 x 768, 32 bit color depth, and a refresh rate of 85 Hz. A viewing distance of 70 cm was maintained resulting in a  $29^{\circ} \times 22^{\circ}$  usable field of view as done by Jost et al [JOW<sup>+</sup>05]. Refer Figure 3.9 for the setup of the experiment.

Every participant has completed two sessions of experiment with at least one day of gap between them. Both sessions were identical and same stimuli were presented in random order. The aim of repeating the same experiment at different times for every participant was to check the cross-correlation and the repeatability of the recorded data.

The experiment has been designed carefully so that it should not exceed 25 minutes including calibration stage, in order to prevent observer's lose of interest or disengagement from experiment over time.



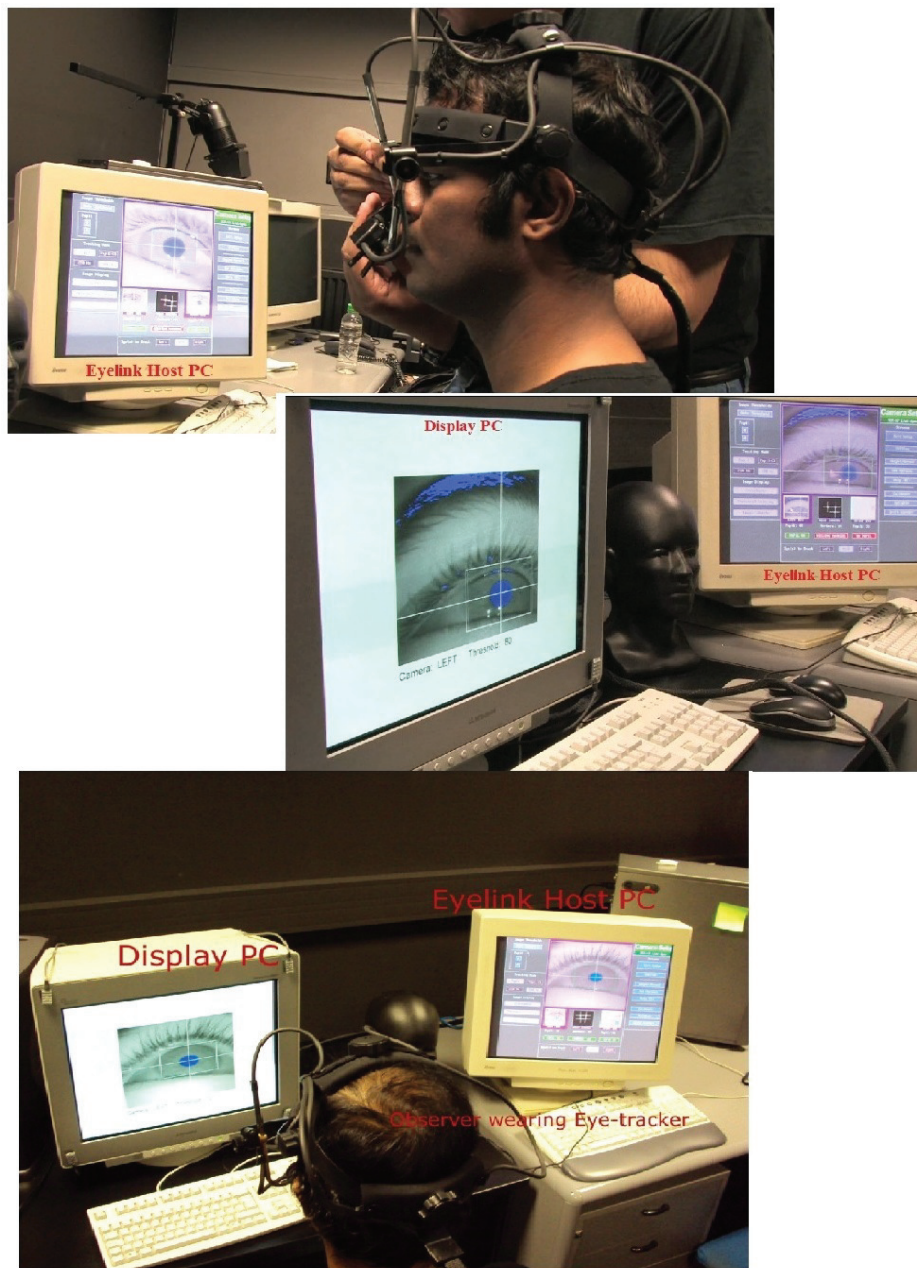


Figure 3.9: Experiment / eye-tracker setup. First row: tracker being adjusted on the head of an observer. Second row: stimulus display PC (on the left) and the PC connected to the eye-tracker / host PC on the right. Last row: after finalizing the setup stage of the experiment.

### 3.2.1 Eye movement recording

Eye position was tracked at 500 Hz with an average noise (RMS value)  $<0.01^\circ$ . Fixations were estimated from a comparison between the center of the pupil and the reflection of the IR illuminator on the cornea. Before starting a session of experiment, the eye-tracker was calibrated with a set of random points on 3 x 3 matrix (see Figure 3.6 for reference). For the observer, the calibration stage simply consisted of fixating the gaze at the nine points displayed sequentially and randomly at different locations on the screen. The validation of the calibration was achieved by measuring the difference between the computed fixation positions and the locations of the target points. Such a difference reflects the accuracy of the eye movement recording. A threshold error of  $1^\circ$  has been selected as the greatest divergence that could be accepted.

Head mounted eye-tracker allows flexibility to perform experiment in free viewing conditions as the system is designed to compensate for small head movements. Then the recorded data is not affected by head motions and allows observers to view stimuli normally with no restrictions on the head movements. Severe restrictions in head movements has been shown to alter eye movements and can lead to noisy data acquisition and corrupted results [CSE<sup>+</sup>92].

### 3.2.2 Stimuli

For the experiment, we used the videos from the extended Cohn-Kanade (CK+) database [LCK<sup>+</sup>10]. CK+ database contains 593 sequences across 123 subjects which are FACS [EF78] coded at the peak frame. Out of 593 sequences only 327 sequences have emotion labels. This is because these are the only ones that fit the prototypic definition. Database consists of subjects aged from 18 to 50 years old, of which 69% were female, 81% Euro-American, 13% Afro-American and 6% others. Each video (without sound) showed a neutral face at the beginning and then gradually developed into one of the six facial expressions. We selected 54 videos for the Psycho-Visual experiment (see section A.1 for more details about the database). Videos were selected with the criteria that videos should show both male and female subjects, experiment session should complete within 20 minutes and posed facial expression should not look unnatural. Another consideration

while selecting the videos was to avoid such sequences where the date/time stamp is not recorded over the chin of the subject [PVRM05].

### 3.3 Psycho-Visual experiment: results and discussion

#### 3.3.1 Gaze map construction



Figure 3.10: Examples of gaze maps for six universal expressions. Each video sequence is divided in three mutually exclusive time periods. First, second and third columns show average gaze maps for the first, second and third time periods of a particular stimuli respectively.

The most intuitively revealing output that can be obtained from the recorded fixations data is to obtain gaze maps. For every frame of the video and each subject  $i$ , the eye movement recordings yielded an eye trajectory  $T^i$  composed of the coordinates of the successive fixations  $f_k$ , expressed as image coordinates  $(x_k, y_k)$ :

$$T^i = (f_1^i, f_2^i, f_3^i, \dots) \tag{3.1}$$

As a representation of the set of all fixations  $f_k^i$ , a human gaze map  $H(\mathbf{x})$  was computed, under the assumption that this map is an integral of weighted point

spread functions  $h(\mathbf{x})$  located at the positions of the successive fixations. It is assumed that each fixation gives rise to a normally (gaussian) distributed activity. The width  $\sigma$  of the activity patch was chosen to approximate the size of the fovea. Formally,  $H(\mathbf{x})$  is computed according to Equation 3.2:

$$H(\mathbf{x}) = H(x, y) = \sum_{i=1}^{N_{subj}} \sum_{f_k \in T^i} \exp\left(\frac{(x_k - x)^2 + (y_k - y)^2}{\sigma^2}\right) \quad (3.2)$$

where  $(x_k, y_k)$  are the spatial coordinates of fixation  $f_k$ , in image coordinates. In Figure 3.10 gaze maps are presented as the heat maps where the colored blobs / human fixations are superimposed on the frame of a video to show the areas where observers gazed. The longer the gazing time, the warmer the color is.

As the stimuli used for the experiment is dynamic i.e. video sequences, it would have been incorrect to average all the fixations recorded during trial time (run length of video) to construct gaze maps as this could lead to biased analysis of the data. To meaningfully observe and analyze the gaze trend across one video sequence we have divided each video sequence in three mutually exclusive time periods. The first time period correspond to initial frames of the video sequence where the actor's face has no expression i.e. neutral face. The last time period encapsulates the frames where the actor is showing expression with full intensity (apex frames). The second time period is a encapsulation of the frames which has a transition of facial expression i.e. transition from the neutral face to the beginning of the desired expression (i.e neutral to onset of the expression). Then, the fixations recorded for a particular time period are averaged across 15 observers. Refer to Appendix B where gaze maps of five video sequences / expression are presented.

### 3.3.2 Observations from the gaze maps

Figure 3.10 gives the first intuition that gazes across all the observers are mostly attracted towards three facial regions i.e. eyes, nose and mouth for all the six universal facial expressions.

Secondly, gaze maps presented in the Figure 3.10 suggest the saliency of mouth region for the expressions of happiness and surprise. It can be observed from the figure that as the two said expressions become prominent (second and third time

periods) most of the gazes are attracted towards only one facial region and that is the mouth region. The same observation can be made for the facial expressions of sadness and fear but with some doubts. For the expressions of anger and disgust it seems from the gaze maps that no single facial region emerged as salient, as the gazes are attracted towards two to three facial regions even when the expression was shown at its peak.

### 3.3.3 Substantiating observations through statistical analysis

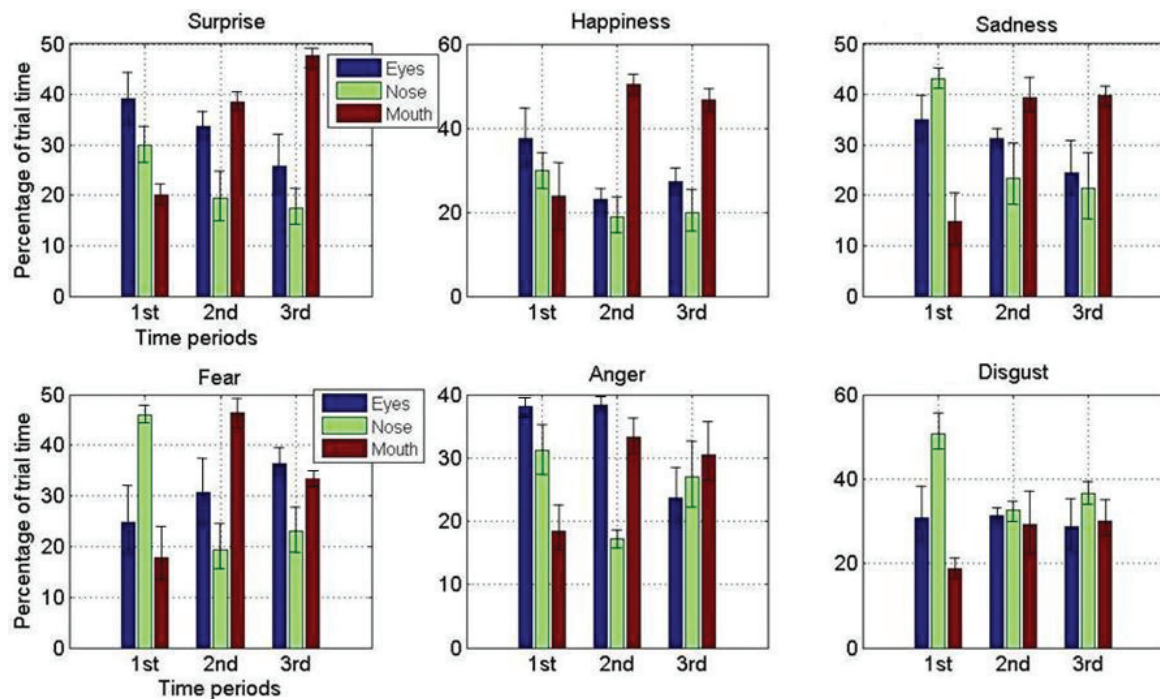


Figure 3.11: Time period wise average percentage of trial time observers have spent on gazing different facial regions. The error bars represent the standard error (SE) of the mean. First time period: initial frames of video sequence. Third time period: apex frames. Second time period: frames which has a transition from neutral face to particular expression.

In order to statistically confirm the intuition gained from the gaze maps about the saliency of different facial region(s) for the six universal facial expressions we



have calculated the average percentage of trial time observers have fixated their gazes at specific region(s) in a particular time period (definition of time period is same as described previously). The resulting data is plotted in Figure 3.11.

Figure 3.11 confirms the intuition that the region of mouth is the salient region for the facial expressions of happiness and surprise. Third time period in the figure corresponds to the time in the video when the expression was shown at its peak. It can be easily observed from the figure that as the expression of happiness and surprise becomes more prominent, the humans tend to fixate their gazes mostly on the facial region of mouth. The same can be observed from the Figure 3.12 and 3.13. This result is consistent with the results by Cunningham et al. [CKWB05], Nusseck et al. [NCWB08] and Boucher et al. [BE75].



Figure 3.12: Gaze maps for the facial expression of happiness. First, second and third columns show average gaze maps for the first, second and third time periods of stimuli respectively. Each row corresponds to different stimuli/video sequence for “sadness”.

Cunningham et al. [CKWB05] and Nusseck et al. [NCWB08] have reported that the recognition of facial expression of sadness requires a complicated interaction of mouth and eye region along with rigid head motion, but the data we have recorded from experiment and plotted in Figure 3.11 show that human visual system tends to divert its attention towards the region of mouth as the expression becomes prominent. The fact can be observed in the second and third



Figure 3.13: Gaze maps for the facial expression of surprise. First, second and third columns show average gaze maps for the first, second and third time periods of stimuli respectively. Each row corresponds to different stimuli/video sequence for “sadness”.

time periods. Nevertheless, the contribution of eye and nose regions cannot be considered negligible as in terms of percentage for the third time period observers have gazed around 40 percent of the trial time at the mouth region and around 25 percent each at the eye and nose regions. Figure 3.14 shows the average gaze maps from the 15 observers for the expression of sadness and it confirms the fact that the facial region of mouth get more attention than the facial regions of eye and nose.

Facial expression of disgust shows quite random behavior. Even when the stimuli was shown at its peak, observers have gazed all the three regions in approximately equal proportions. The only thing that can be point out from the Figure 3.11 is that there is more attraction towards the nose region and that could be due the fact that, wrinkles on the nose region becomes prominent and attracts more attention when the stimuli shows maximum disgust expression. Ironically, Cunningham et al.[CKWB05] and Nusseck et al.[NCWB08] while discussing the results for the expression of disgust have not considered the contribution of the nose region which has came out to be little bit more prominent than the other two facial regions in terms of saliency from the results

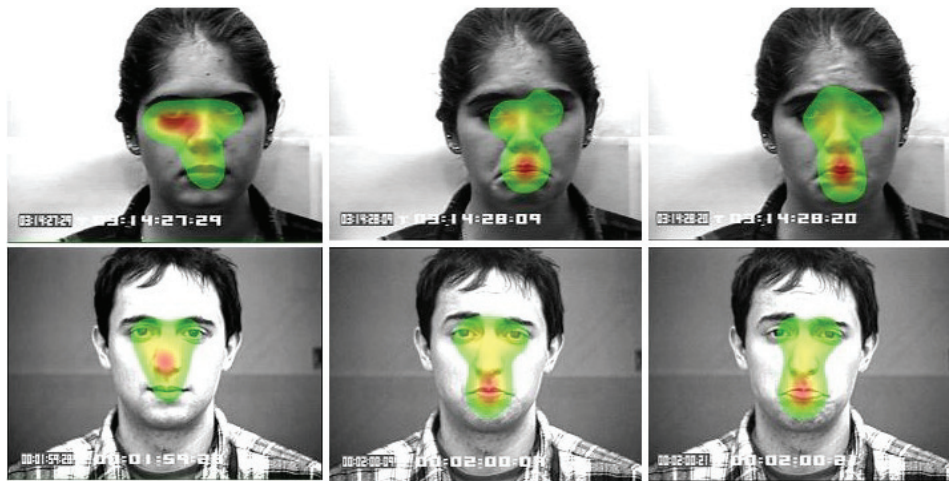


Figure 3.14: Gaze maps for the facial expression of sadness. First, second and third columns show average gaze maps for the first, second and third time periods of stimuli respectively. Each row corresponds to different stimuli/video sequence for “sadness”.



Figure 3.15: Gaze maps for the facial expression of disgust. First, second and third columns shows average gaze maps for the first, second and third time periods of stimuli respectively. Each row corresponds to different stimuli/video sequence for “disgust”.

of the current study. Figure 3.15 presents the average gaze maps from the 15 observers for the facial expression of disgust. From the gaze maps of two



presented video sequences it is evident that the wrinkles in the nose region gets bit more attention than the other two facial regions.

For the expression of fear, facial regions of the mouth and eyes attract most of the gazes. From Figure 3.11 it can be seen that in the second trial time period (period correspond to the time when observer experiences the change in face presented in stimuli toward the maximum expression) observers mostly gazed at the mouth region and in the final trial period eye and mouth regions attracts most of the attention. Hanawalt [Han44] reported that the expression of fear is mostly specified by the eye region but our study shows the interaction of facial regions of mouth and eyes for the fear. Figure 3.16 shows the average gaze maps for the expression of fear and these gaze maps confirm the argument that “fear” is accompanied with the interaction of mouth and eye regions.

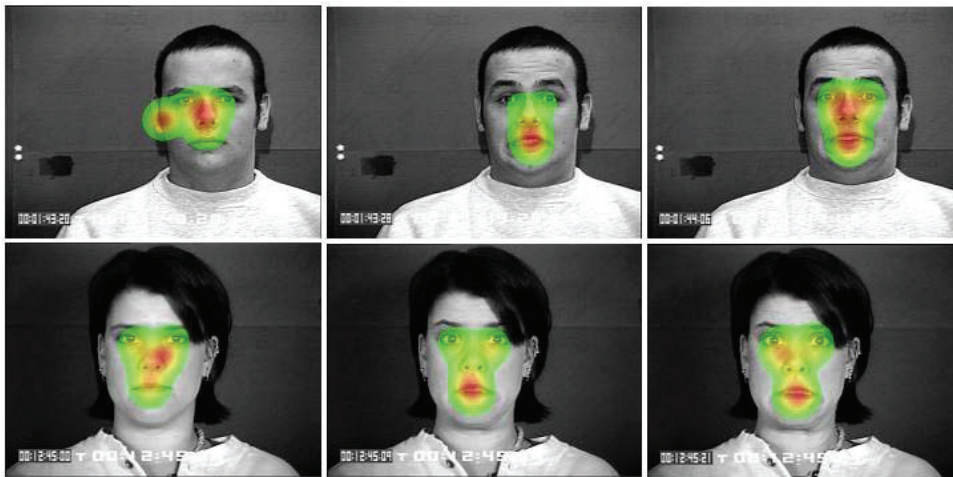


Figure 3.16: Gaze maps for the facial expression of fear. First, second and third columns show average gaze maps for the first, second and third time periods of stimuli respectively. Each row corresponds to different stimuli/video sequence for “fear”.

Boucher et al. [BE75] in 1975 wrote that “Anger differs from the other five facial expressions of emotion in being ambiguous” and this observation holds for the current study as well. “Anger” shows complex interaction of eye, mouth and nose regions without any specific trend. This fact is evident from the Figure 3.17 as observers have gazed at different regions of the face for the two stimuli showing “anger”. But one thing is common for all the stimuli in Figure 3.17 that for

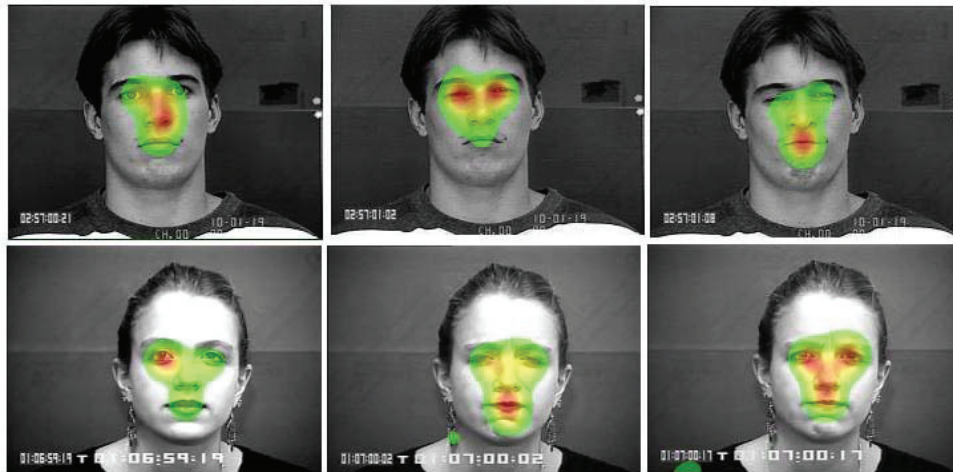


Figure 3.17: Gaze maps for the facial expression of anger. First, second and third columns show average gaze maps for the first, second and third time periods of stimuli respectively. Each row corresponds to different stimuli/video sequence for “anger”.

“anger” no facial region emerges as the salient but all the three regions are gazed interchangeably even when the expression was shown at its peak/apex. Figure 3.18 tabulates results from our psycho-visual experimental study.

### 3.4 Conclusion

The presented experimental study provides the insight into which facial region(s) emerges as the salient according to human visual attention for the six universal facial expressions. Eye movements of fifteen human observers were recorded using eye-tracker as they watch the stimuli which was taken from the widely used Cohn-Kanade facial expression database. Conclusions drawn from the experimental study are summarized in the Figure 3.18.

The study provided a evidence that the visual system is mostly attracted towards the mouth region for the expressions of happiness and surprise and it also shows almost the same trend for the expression of sadness. Expressions of disgust, fear and anger shows the interaction of two to three facial regions. Expression of fear shows the attractiveness of the eyes and the mouth regions. Expression of anger can be considered as complex expressions as it is

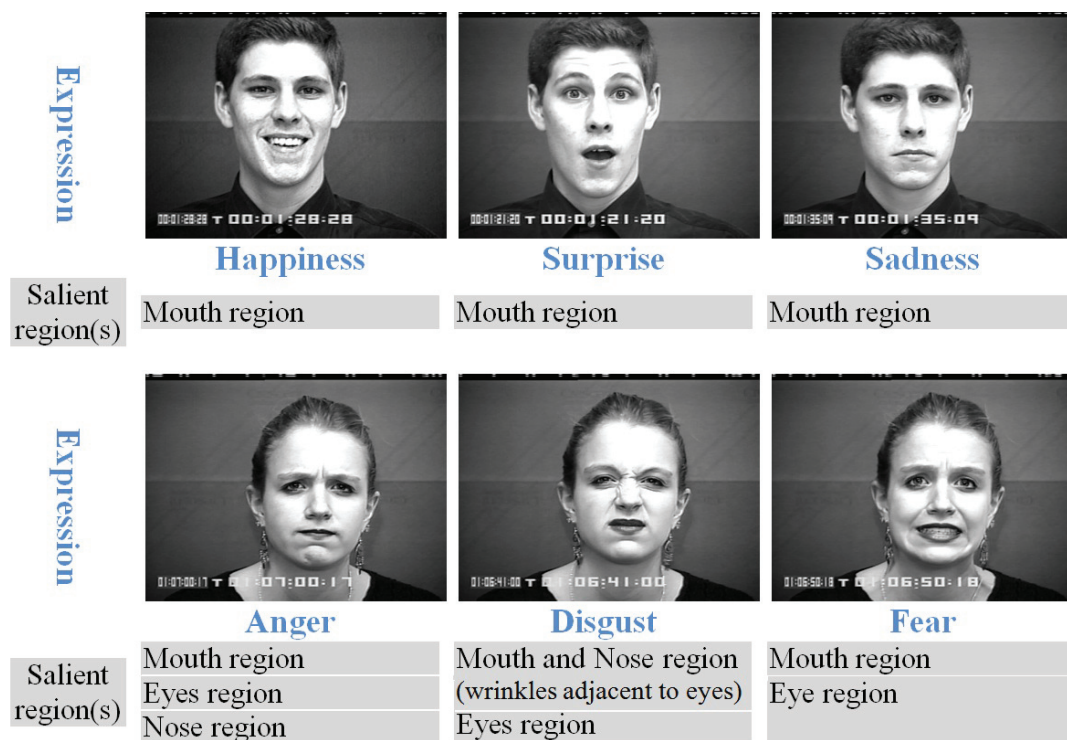


Figure 3.18: Summary of the facial regions that emerged as salient for six universal expressions. Salient regions are mentioned according to their importance (for example facial expression of “fear” has two salient regions but mouth is the most important region according to HVS).

accompanied with the interaction of three facial regions i.e. eye, nose and mouth and so does the expression of disgust.

Presented results can be used as the background knowledge by the computer vision community for deriving robust descriptor for the facial expression recognition (FER) as for FER, feature selection along with the regions from where these features are to be extracted is one of the most important step. Secondly, processing only salient regions could help in reducing computational complexity of the FER algorithms.

Work presented in this chapter is published in “IEEE International Conference on Computer Vision and Pattern Recognition Workshop” [KMKB12a].



# Chapter 4

## Facial expression recognition based on brightness and entropy features

### Contents

---

<b>4.1</b>	<b>Salient region detection . . . . .</b>	<b>73</b>
4.1.1	Biologically based . . . . .	74
4.1.2	Computational models . . . . .	75
4.1.3	Conclusion . . . . .	79
<b>4.2</b>	<b>Feature extraction . . . . .</b>	<b>79</b>
4.2.1	Brightness calculation . . . . .	81
4.2.2	Entropy calculation . . . . .	83
<b>4.3</b>	<b>Experiments . . . . .</b>	<b>84</b>
4.3.1	Experiment on the extended Cohn-Kanade (CK+) database . . . . .	85
4.3.2	Experiment on the FG-NET FEED database . . . . .	86
<b>4.4</b>	<b>Drawbacks of the proposed algorithm . . . . .</b>	<b>87</b>

---

Results of the visual experiment provided the evidence that human visual system gives importance mainly to two facial regions i.e. eye and mouth, while

decoding six universal facial expressions (for reference see Chapter 3). In the same manner, we argue that the task of expression analysis and recognition could be done in more conducive manner, if same regions are selected for further processing. We propose to extract two sets of features only from the salient regions of face. These two features are entropy and brightness.

Entropy is a statistical measure of uncertainty, randomness or absence of the information associated with the data [SW63, LFT10] while brightness as described by Wyszecki and Stiles [WS00] is an “*attribute of a visual sensation according to which a given visual stimulus appears to be more or less intense*”. Currently, there is no standard or reference formula for brightness calculation. We propose to use BCH (Brightness, Chroma, Hue) model [BB06] for brightness calculation.

Working of the proposed framework is summarized in algorithm 1 and the details related to each step is presented in subsequent subsections.

---

**Algorithm 1:** Proposed framework for facial expression recognition

---

**input** : video frame  
**output**: expression label

- 1 **for**  $i \leftarrow 1$  **to**  $numFrames$  **do**
- 2     automatically localize salient facial regions using viola-jones algorithm [VJ01]
- 3     calculate saliency map using “frequency-tuned salient region detection” algorithm [AHES09]
- 4     calculate entropy [SW63] from salient facial regions using:  
$$E = - \sum_{i=1}^n p(x_i) \log_2 p(x_i)$$
- 5     calculate brightness features from salient facial regions using BCH model [BB06]:  
$$B = \sqrt{D^2 + E^2 + F^2}$$
- 6     concatenate entropy and brightness feature to make feature vector, i.e.  $f = \{ E, B \}$
- 7     classify input stimuli to one of six universal expression using feature vector  $f$

---

The rationale behind extracting entropy and brightness features is that, as a second step framework calculates saliency map which show salient regions by highlighting them. By extracting brightness feature, framework calculates local

saliency value (brightness is proportional to saliency). While entropy values explains how well particular facial region is mapped as salient. Figure 4.1 show extracted values of entropy and brightness features from three facial regions. Figure illustrates discriminative abilities of these two features.






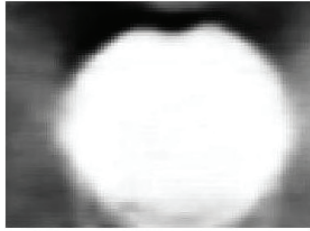
					
Entropy	Brightness	Entropy	Brightness	Entropy	Brightness
0.62	0.45	0.48	0.72	0.83	0.24
					
Entropy	Brightness	Entropy	Brightness	Entropy	Brightness
0.33	0.58	0.6	0.32	0.2	0.92

Figure 4.1: Brightness and entropy values from three different facial regions.

## 4.1 Salient region detection

First problem that is addressed, is to find salient region detection algorithm that produces saliency maps which detects similar salient facial regions as concluded by the psycho-visual experiment (see Chapter 3 for details). The idea is to use saliency map information to find appropriate weights (or value for brightness and entropy) for extracted features. In order to find appropriate saliency detection algorithm we examined four state-of-the-art methods.

Models of automatic saliency determination can be classified as either biologically based, purely computational, or a combination. We examined four state-of-the-art methods of automatic extraction of salient regions in order to



determine their suitability for our application. Four state-of-the-art methods for extracting salient regions are “*Itti’s model*” by Itti et al. [IKN98], “*frequency tuned salient region detection*” by Achanta et al. [AHES09], “*graph-based visual saliency*” by Harel et al. [JHP06] and “*spectral residual approach for saliency detection*” by Hou and Zhang [HZ07] referred here as IT, FT, GBVS and SR respectively. The choice of these algorithms is motivated by the following reasons:

1. **Citation in literature.** The classic approach of IT is widely cited.
2. **Recency.** GBVS, SR and FT are recent.
3. **Variety.** IT is biologically motivated, GBVS is a hybrid approach, FT and SR estimates saliency in the frequency domain, and FT outputs full-resolution saliency maps.

These models are briefly described below.

#### 4.1.1 Biologically based

Biological architecture developed by Koch and Ullman [KU85] is a basis of very famous model developed by Itti et al. [IKN98]. In this biologically-inspired system, an input image is decomposed into a nine spatial scales using dyadic Gaussian pyramid (successive Gaussian blurring and down sampling by 2 in each dimension). Each feature is computed by a set of linear “center-surround” operations on spatial discontinuities in the modalities of color, intensity and orientation. All feature maps are then combined into a unique scalar “saliency map” which encodes for the salience of a location in the scene irrespectively of the particular feature which detected this location as conspicuous. A winner-take-all neural network then detects the point of highest salience in the map at any given time, and draws the focus of attention towards this location. Figure 4.2 presents general architecture of the model under discussion.



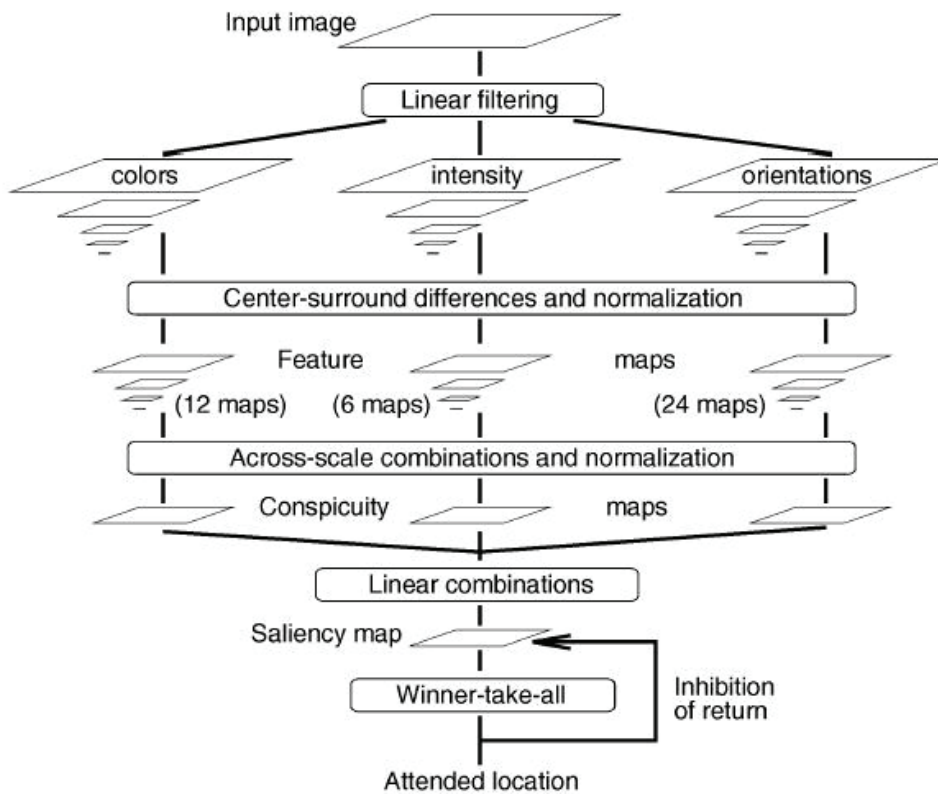


Figure 4.2: Itti's model architecture [IKN98].

## 4.1.2 Computational models

Some famous computational models [HXM<sup>+</sup>04, MZ03, HZ07, AHES09, JHP06] are not based on any biologically plausible vision architecture.

### 4.1.2.1 Frequency-tuned salient region detection (FT)

This algorithm [AHES09] finds low-level, pre-attentive, bottom-up saliency. Biological concept of center-surround contrast is the core of this algorithm, but is not based on any biological model. Frequency-tuned approach is used to estimate center-surround contrast using color and luminance features. According to Achanta et al. [AHES09] it offers three advantages over existing methods: uniformly highlighted salient regions with well defined boundaries, full resolution saliency maps, and computational efficiency.

This algorithms find the Euclidean distance between the CIELAB ( $L^*a^*b^*$  color space) [WS00] pixel vector in a Gaussian filtered image with the average CIELAB vector for the input image, this is illustrated in the Figure 4.3. See Appendix C for color space conversion formulas.

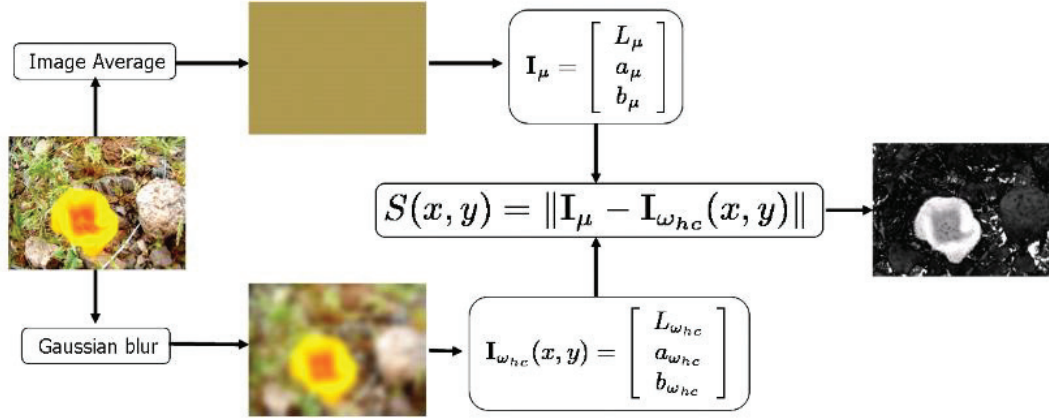


Figure 4.3: Frequency-tuned salient region detection algorithm [AHES09].

#### 4.1.2.2 Graph Based Visual Saliency (GBVS) method

Graph Based Visual Saliency (GBVS) method [JHP06] create feature maps using Itti's method but perform their normalization using a graph based approach. It consists of two steps: first forming activation maps on feature channels, and then normalizing them in a way which highlights conspicuity and admits combination with other maps. The activation maps are normalized using another Markovian algorithm which acts as a mass concentration algorithm, prior to additive combination of the activation maps. This algorithm exploits the computational power, topographical structure, and parallel nature of graph algorithms to achieve natural and efficient saliency computations. For both activation and normalization, this method constructs a directional graph with edge weights given from the input map, treat it as a Markov chain, and compute the equilibrium distribution. Figure 4.4 shows the architecture of the GBVS algorithm.

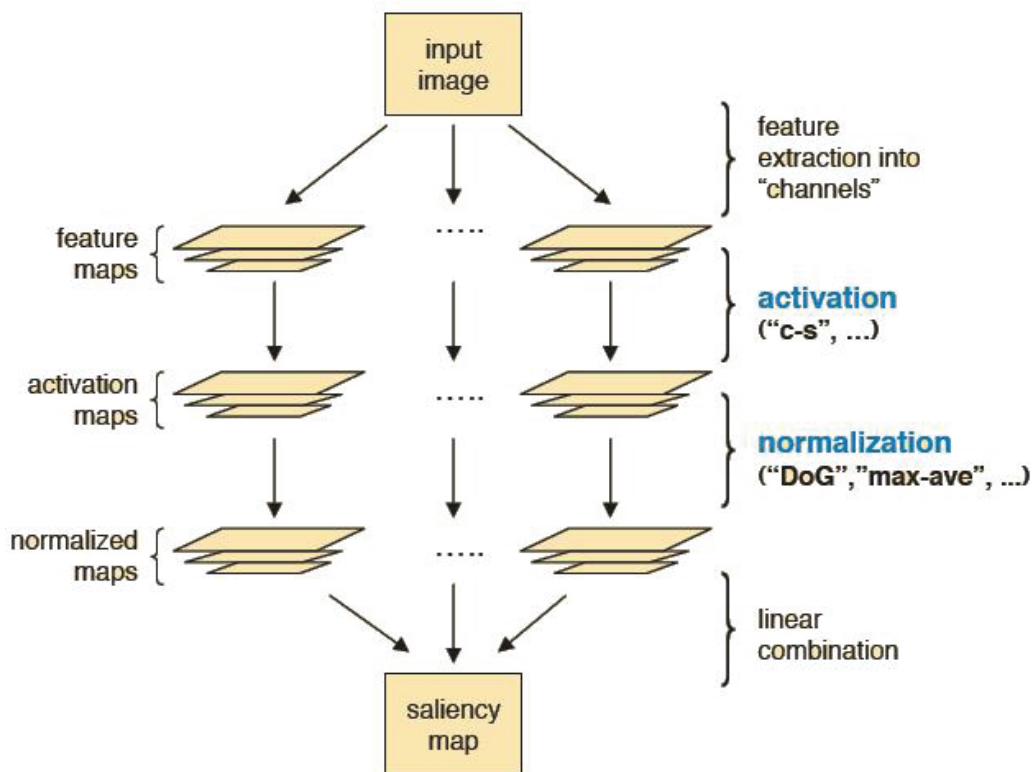


Figure 4.4: Graph Based Visual Saliency (GBVS) method's architecture (adopted from poster presentation [JHP06]).

#### 4.1.2.3 Spectral Residual(SR) approach

Spectral residual approach [HZ07] for detecting saliency in a given stimuli is a purely computational approach and is not based on any biological principle. The power of log spectrum is exploited by this approach in order to explore the properties of the background of a given stimuli. Similar trends are observed in log spectra of different images, though each containing statistical singularities. The similarities imply redundancies. If the similarity (trend of local linearity of natural images) is removed, the remaining singularity (spectral residual) should be the innovation of an image corresponding to its visual saliency. The main idea of Spectral Residual is to remove the redundant part of image's spectrum. It only needs Fourier Transformation of an image, so this algorithm is computationally efficient. This method outputs saliency map in 64 x 64 sized image regardless of the size of input stimuli and highlight the salient object

boundaries, but fail to uniformly map the entire salient region. These shortcomings result from the limited range of spatial frequencies retained from the original image in computing the final saliency map.

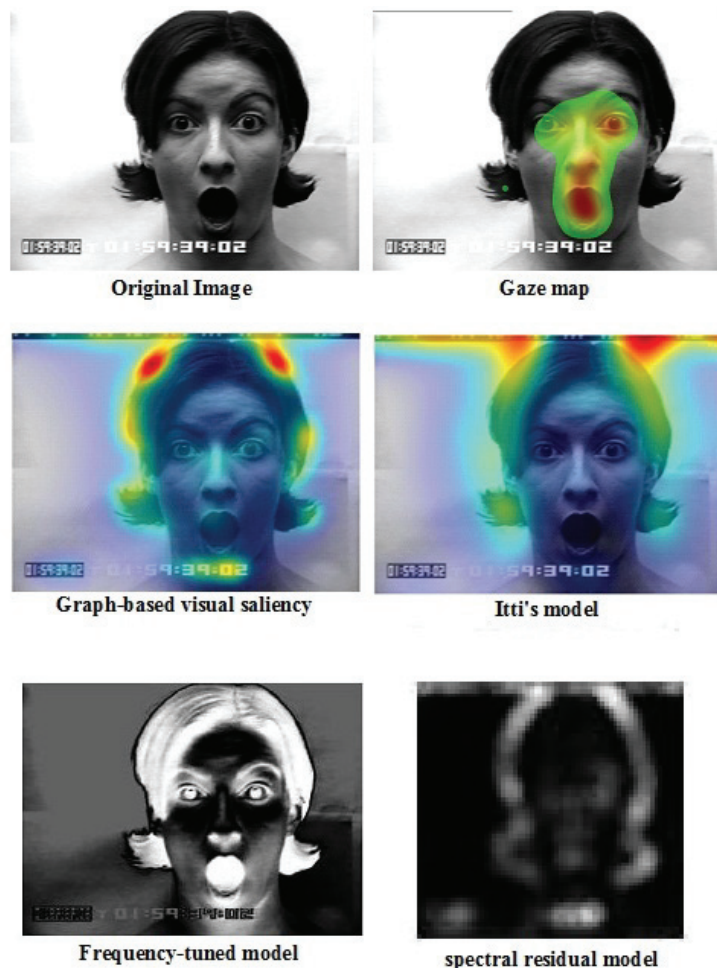


Figure 4.5: Comparison of automatic detected salient regions with gaze map obtained from psycho-Visual experiment (see Chapter 3 for reference). First row: original image and average gaze map of fifteen observers. Second row: saliency maps obtained from GBVS [JHP06] and Itti methods [IKN98] (shown as heat maps.). Third row: saliency maps obtained from FT [AHES09] and SR methods [HZ07].

### 4.1.3 Conclusion

We propose to use *frequency-tuned salient region detection* algorithm developed by Achanta et al. [AHES09] for detection of salient facial regions. We have chosen this model over other existing state-of-the-art models [IKN98, HZ07, JHP06] because it performs better in predicting human fixations (see Figure 4.6 and Figure 4.5).

Figure 4.5 shows that except FT model [AHES09], none of the other examined model correctly predicts human gazes. Itti method [IKN98] and GBVS method [JHP06] outputs quite similar saliency maps with wrong predictions, while SR method [HZ07] outputs saliency map that is only 64 x 64 pixels in size with no significant correct prediction.

Figure 4.6 shows salient regions for six expressions as detected by FT. It can be observed from the figure that most of the time it predicts three regions as salient facial region i.e. nose, mouth and eyes which is in accordance with visual experiment result (see Section 3.4 for reference). Secondly, a distinctive trend in detected salient regions and associated brightness can also be observed for different expressions. Another advantage of the FT model is its computational efficiency, which is very important for the system to run in real time. Lastly, this model outputs saliency maps in full resolution, which is not the case for SR model. Due to all of these benefits we concluded to use *frequency-tuned salient region detection* algorithm developed by Achanta et al. [AHES09] for detection of salient facial regions in our framework.

## 4.2 Feature extraction

We have chosen to extract the features of brightness and entropy for automatic recognition of expressions as these features have shown a discriminative trend, which can be observed from Figure 4.6 and 4.7. Figure 4.7 shows the average entropy values for the facial regions. Each video is divided in three equal time periods for the reasons discussed earlier. The entropy values for the facial regions corresponding to specific time periods (definition of time periods is same as discussed earlier) are averaged and plotted in Figure 4.7.



Figure 4.6: Salient region detection for different expressions using FT [AHES09]. Each row shows detected salient regions in a complete frame along with the zoom of three facial regions i.e. eyes, nose and mouth. Brightness of the salient regions is proportional to its saliency. First row shows expression of happiness, second row: surprise, third row: sadness, fourth row: anger, fifth row: fear and sixth row: disgust .

By using FT saliency model, we extracted salient regions and obtained saliency maps for every frame of the video. Then obtained saliency maps are further



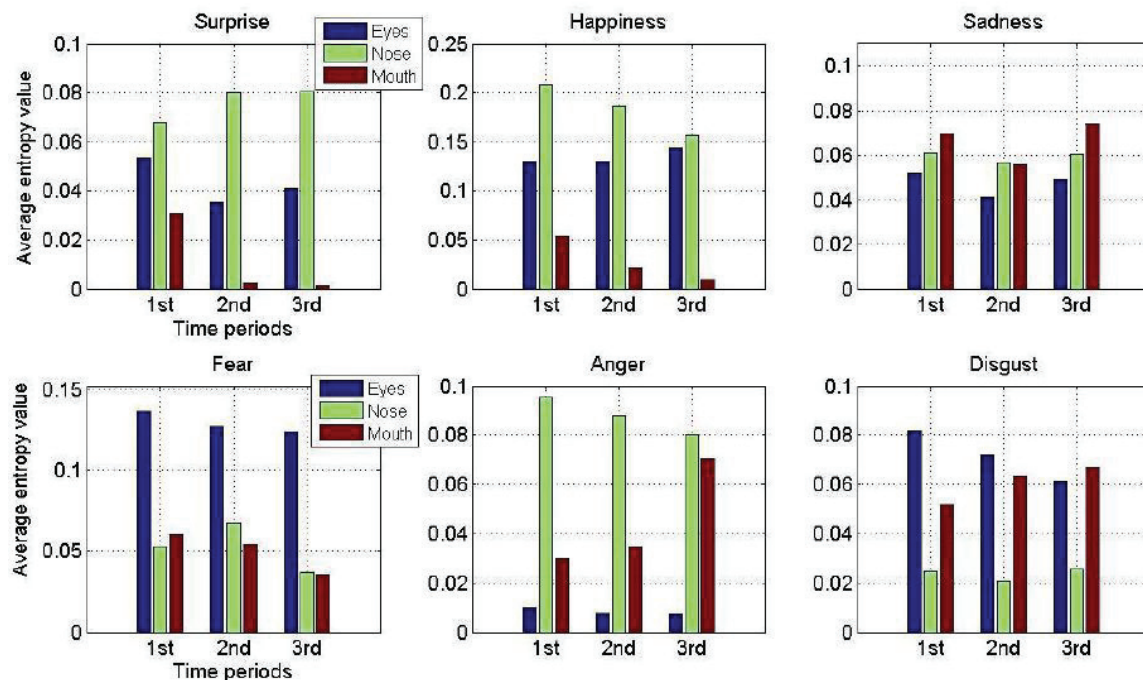


Figure 4.7: Average entropy value for different facial regions. First time period: initial frames of video sequence. Third time period: apex frames. Second time period: frames which has a transition from neutral face to particular expression.

processed for the calculation of brightness and entropy value for the three facial regions (eyes, nose and mouth).

#### 4.2.1 Brightness calculation

Brightness is one of the most significant pixel characteristics but currently, there is no standard formula for brightness calculation. The brightness values, as explained earlier, are calculated using BCH (Brightness, Chroma, Hue) model [BB06]. For B (Brightness) C (Chroma) H (Hue) color coordinate system (CCS), the following definitions for Brightness, Chroma and Hue are used:

1. B: a norm of a color vector S.
2. C: an angle between the color vector S and an axis D - color vector representing Day Light (for example D65, D55, EE etc.).

3. H: is the angle between the orthogonal projection of the color vector  $S$  on the plane orthogonal to the axis  $D$  and an axis  $E$  - the orthogonal projection of a color vector, corresponding to some fixed stimulus (for example, a monochromatic light with wavelength 700 nm), on the same plane.

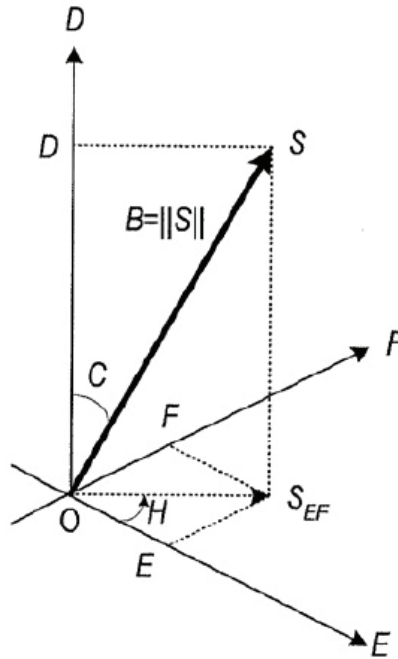


Figure 4.8: Color Coordinate Systems DEF and BCH [BB06].

Figure 4.8 illustrates the relationship between values  $D$ ,  $E$ , and  $F$  ( $E = F = 0$  for grey color in DEF color coordinate system), coordinates of the vector  $S$  in an orthogonal coordinate system DEF, and parameters  $B$ ,  $C$ , and  $H$ , which might be considered as spherical coordinates of the vector  $S$  in BCH coordinate system.

Use of stimulus length as a measure of Brightness introduced in BCH (Brightness, Chroma, Hue) model provides Brightness definition effective for different situations. Length is calculated according to Cohen metrics [Coh00].

$$B = \sqrt{D^2 + E^2 + F^2} \quad (4.1)$$



$$\begin{pmatrix} D \\ E \\ F \end{pmatrix} = \begin{pmatrix} 0.2053 & 0.7125 & 0.4670 \\ 1.8537 & -1.2797 & -0.4429 \\ -0.3655 & 1.0120 & -0.6104 \end{pmatrix} \cdot \begin{pmatrix} X \\ Y \\ Z \end{pmatrix} \quad (4.2)$$

where X, Y, and Z are tristimulus values [CIE31].

The main advantage of BCH model is that it performs only intended operation without unwilling concurrent modification/processing of other image parameters.

### 4.2.2 Entropy calculation

The entropy for different facial regions are calculated using equation 4.3:

$$E = - \sum_{i=1}^n p(x_i) \log_2 p(x_i) \quad (4.3)$$

where  $n$  is the total number of grey levels, and  $p = \{p(x_1), \dots, p(x_n)\}$  is the probability of occurrence of each level.

In the context of this work, we have used entropy as a measure to quantitatively determine whether a particular facial region is fully mapped as salient or not. Higher value of entropy for a particular facial region corresponds to higher uncertainty or points out the fact that the facial region is not fully mapped as salient.

From Figure 4.7 it can be observed that the average entropy values for the region of mouth, for the expressions of happiness and surprise are very low as compared to entropy values for the other regions. This finding shows that the region of mouth was fully mapped (can also be seen in Figure 4.6) as salient by saliency model, and the same we concluded from our visual experiment. It is also observable from the figure that the values of entropy for the region of mouth for these two expressions is lower than any other entropy values for the rest of facial expressions in the second and third time periods. This result shows that there is a discriminative trend in entropy values which will help in automatic recognition of facial expressions.

Entropy values for the expression of sadness show discriminative trend and suggests that nose and mouth regions are salient with more biasness towards mouth region. This results conforms very well with the results from visual experiment.

For the expression of disgust, entropy value for the facial region of nose is quite low pointing out the fact that the region of nose is mapped fully as salient which again is in accordance with our visual experiment result. This conclusion can also be exploited for the automatic facial expression recognition of disgust.

We obtained low entropy value for the facial region of eyes for the expression of anger. This points to the fact that according to the saliency model the region of eyes emerges as salient. But the results from the visual experiment show complex interaction of all three regions. Entropy values for the expression of fear also show different result from the visual experiment. The discrepancies found in the entropy values for the expressions of anger and fear are neither negligible nor significant and will be studied and addressed in future work.

### 4.3 Experiments

To measure the performance of proposed framework for facial expression recognition we conducted experiments on two databases: (a) extended Cohn-Kanade (CK+) database [LCK<sup>+</sup>10] (posed expressions) and (b) FG-NET FEED [Wal06] database (natural expressions). FG-NET FEED contains 399 video sequences across 18 different individuals showing seven facial expressions i.e. six universal expression [Ekm71] plus one neutral. In this database individuals were not asked to act rather expressions were captured while showing them video clips or still images to wake real expressions. CK+ database contains 593 sequences (posed / acted expressions) across 123 subjects which are FACS [EF78] coded at the peak frame. Details of CK+ and FG-NET FEED database are presented in Appendix Sections A.1 and A.3 respectively.

For both the experiments, the performance of the framework was evaluated using classical classifier i.e. “Support vector machine (SVM)” with  $\chi^2$  kernel and  $\gamma=1$  (for discussion on different classifiers refer Section 2.3.3). Average recognition accuracy / rate is calculated using 10-fold cross validation technique. In  $k$ -fold cross validation, features vector set is divided into  $k$  equal subsets.  $k-1$  subsets are

used for the training while a single set is retained for the testing. The process is repeated  $k$  times ( $k$ -folds), with each of the  $k$  subsets used exactly once for testing. Then, the  $k$  estimations from  $k$ -folds are averaged to produce final estimated value. The framework calculates brightness and entropy features explicitly from three facial regions i.e. eyes, nose and mouth. This is done to enhance discriminative ability of feature vector.

### 4.3.1 Experiment on the extended Cohn-Kanade (CK+) database

For the experiment we used all 309 sequences from the CK+ database which have FACS coded expression label [EF78]. The experiment was carried out on the frames which covers the status of onset to apex of the expression, as done by Yang et al. [YLM10]. Region of interest was obtained automatically by using Viola-Jones object detection algorithm [VJ01] and processed to obtain feature vector. The proposed framework achieved average recognition rate of 71.2% for six universal facial expressions using 10-fold cross validation.

#### 4.3.1.1 Comparison with state-of-the-art methods

Table 4.1 shows the comparison of the achieved average recognition rate of the proposed framework with the state-of-the-art methods using same database (i.e Cohn-Kanade database). Results from [YLM10] are presented for the two configurations. “[YLM10]a” shows the result when the method was evaluated for the last three frames from the sequence while “[YLM10]b” presents the reported result for the frames which encompasses the status from onset to apex of the expression. The method discussed in “[YLM10]b” is directly comparable to our method (frames which covers the status of onset to apex of the expression). Generally our framework achieved average recognition rate less than other state-of-the-art methods but this framework could be considered as the pioneer in the genre of frameworks that are based on human visual system. Secondly, framework can be improved by extracting and concatenating more features (from the salient facial regions) which have strong discriminative abilities. Lastly, feature vector dimensionality of the proposed framework is very low and even by

concatenating more features to it will not affect its appropriateness for real-time applications.

	Sequence Num	Class Num	Performance Measure	Recog. Rate (%)
[LBF <sup>+</sup> 06]	313	7	leave-one-out	93.3
[ZP07]	374	6	ten-fold	96.26
[KZP08]	374	6	five-fold	94.5
[Tia04]	375	6	-	93.8
[YLM10]a	352	6	66% split	92.3
[YLM10]b	352	6	66% split	80
Ours	309	6	ten-fold	71.2

Table 4.1: Comparison with the state-of-the-art methods

### 4.3.2 Experiment on the FG-NET FEED database

Second experiment was performed on the 288 videos of FG-NET FEED [Wal06] database. The expressions in this database are considered as realistic / natural as possible. All the experimental parameters were same as described in the Section 4.3.1. The proposed framework achieved average recognition rate of 65.7% for six universal facial expressions using 10-fold cross validation. Table 4.2 shows confusion matrix. Diagonal and off-diagonal entries of confusion matrix shows the percentages of correctly classified and misclassified samples respectively. Framework recognized expression of happiness better recognized than any other expression while expression of fear was most misclassified. Generally, proposed framework’s recognition rate is lower for expressions of anger, fear and disgust as compared to expressions of sadness, happiness and surprise.

As said previously, performance of the framework can be improved by extracting and concatenating more features (from the salient facial regions) which have strong discriminative abilities. We have not compared our results on FEED database with other state-of-the-art methods. The reason is that generally state-of-the-art methods do not show results for this database.

	Sadness	Happiness	Surprise	Anger	Disgust	Fear
Sadness	<b>68.1</b>	8.8	6.3	4.3	3.5	9
Happiness	10.8	<b>70.8</b>	16.4	0	2	0
Surprise	9	10.8	<b>70.1</b>	4	1.7	4.4
Anger	0	10.5	0	<b>62.1</b>	15.1	12.3
Disgust	10.3	15.5	8.4	0	<b>63.3</b>	2.5
Fear	3	2.6	3.3	10.1	20.7	<b>60.3</b>

Table 4.2: Confusion matrix for FG-NET FEED database.

## 4.4 Drawbacks of the proposed algorithm

Novel framework that is proposed in this chapter extracts features only from the perceptually salient facial regions as done in human visual system (HVS). The framework operates on the saliency maps obtained by the “frequency tuned salient region detection” (FT) to extract features. This model directly defines pixel saliency using the color differences from the average image color. We selected this method over other state-of-the art methods for saliency detection as it performs better (see Section 4.1), but it has some weaknesses that are also inherited in our proposed framework for expression recognition.

Secondly, *Frequency tuned salient region detection algorithm* only considers first order average color, which can be insufficient to analyze complicated variations in a given stimuli. Also this method ignore spatial relationships across image parts, which can be critical for reliable and coherent saliency detection [CZM<sup>+</sup>11]. All of these drawbacks of saliency detection algorithm contributes to the below average performance of the proposed framework.

Novel framework presented in this chapter is published in “IEEE International Conference on Intelligent Systems Design and Applications” [KMKB11].



# Chapter 5

## Facial region shape analysis for recognition of expressions

### Contents

---

<b>5.1</b>	<b>Proposed framework . . . . .</b>	<b>90</b>
<b>5.2</b>	<b>Feature extraction using PHOG . . . . .</b>	<b>92</b>
<b>5.3</b>	<b>Discriminative strength of PHOG features . . . . .</b>	<b>94</b>
<b>5.4</b>	<b>Expression recognition experiments . . . . .</b>	<b>94</b>
5.4.1	First experiment: CK+ database . . . . .	96
5.4.2	Second experiment: generalization on the new dataset . . . . .	99
5.4.3	Third experiment: low resolution image sequences . . . . .	101
<b>5.5</b>	<b>Conclusion . . . . .</b>	<b>102</b>

---

To overcome the drawbacks of proposed descriptor based on “Brightness” and “Entropy” Features (discussed in Section 4.4) we examined the “shape features” of facial region(s) for their descriptive abilities. By studying shape features directly from the stimuli, we overcome the dependency of our subsequently proposed framework for facial expression on saliency detection algorithm, which caused previously proposed framework to produce results below average (Chapter 4).

We hypothesized that shape features of different facial regions can have strong discriminative abilities, as from the different stimuli (see Figures 3.18 and 2.1 for example) it can be observed that different facial regions forms very discriminative and distinctive shapes when showing different expressions. To extract shape information from the stimuli we introduce *Pyramid Histogram of Oriented Gradients* (PHOG) descriptor. PHOG is an extension of *Histogram of Gradient Orientation* (HOG) by Dalal and Triggs [DT05] and it was initially proposed for human detection. As the proposed novel framework is based on Psycho-Visual experimental study (see Chapter 3), it extracts PHOG features only from the perceptual salient facial regions region(s). By processing only salient regions, proposed framework reduces computational complexity of feature extraction and thus, can be used for real-time applications. At the same time it overcomes the drawbacks of the previously proposed framework (refer Chapter 4) i.e. low discrimination ability of extracted features.

## 5.1 Proposed framework

Feature selection along with the region(s) from where these features are going to be extracted is one of the most important step to successfully analyze and recognize facial expressions automatically. As the proposed framework for automatic expression recognition draws its inspiration from the human visual system, it processes only perceptual salient facial region(s) for the feature extraction. The proposed framework creates a novel feature space by extracting Pyramid Histogram of Orientation Gradients (PHOG) [BZM07] features from the perceptually salient facial regions (See Figure 3.18 ). Schematic overview of the proposed framework is illustrated in Figure 5.1.

The steps of the proposed framework are as follows.

1. The framework first localizes salient facial regions using Viola-Jones object detection algorithm [VJ01] as it was done in the former proposed framework (refer Chapter 4). We selected this algorithm as it is the most cited and considered the fastest and most accurate pattern recognition method for face and facial region detection [KT04b].



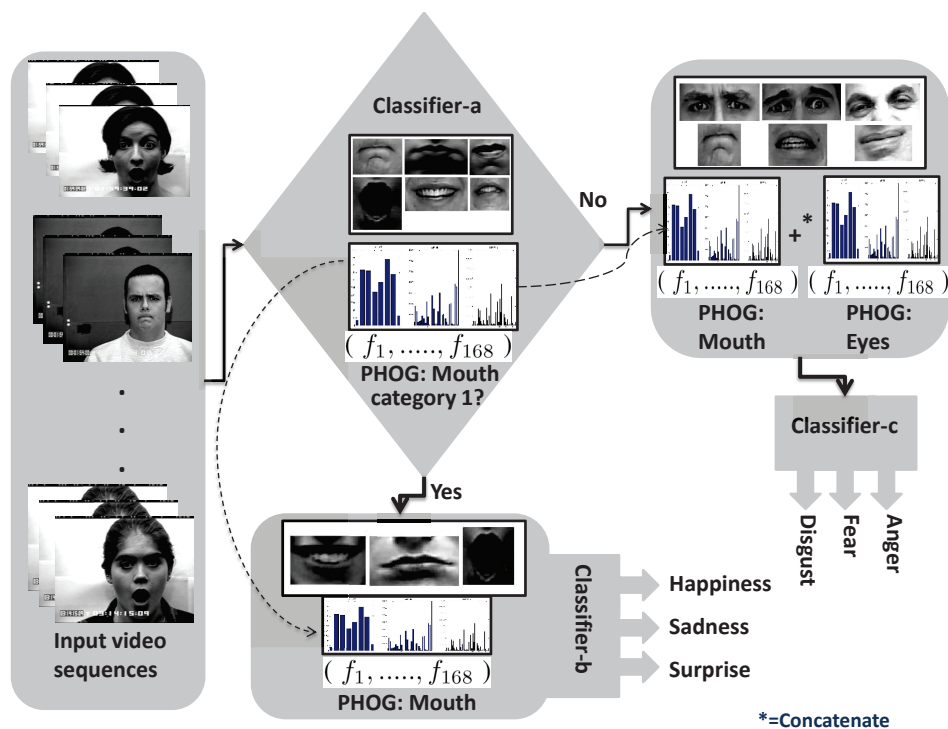


Figure 5.1: Schematic overview of the proposed framework

2. Then, the PHOG features (explained in the Section 5.2) are extracted from those localized mouth region. The classification (“Classifier-a” in the Figure 5.1) is carried out on the basis of extracted features in order to make two groups of facial expressions. First group comprises of those expressions that have one perceptual salient region while the second group is composed of those expressions that have two or more perceptual salient regions (see Section 3.4 or Figure 3.18 for the psycho-visual experiment results). Thus, the first group consists of the expressions of happiness, sadness and surprise while the expressions of anger, fear and disgust are categorized in the second group. The purpose of making two groups of expressions is to save feature extraction computational time.
3. If the input sequence is labeled as group one by the “Classifier-a”, then the next step is to classify expression either as happiness, sadness or surprise. Classification (“Classifier-b” in the Figure 5.1) is carried out on the already extracted PHOG features from the mouth region (results are presented in

the Section 5.4) as for these expressions it has been found that the facial region of “mouth” is the salient region (see Figure 3.18).

4. If the input sequence is classified in the second group, then the framework extracts PHOG features from the eyes region and concatenates them with the already extracted PHOG features from the mouth region. Features from the facial region of eyes are extracted as the results from the psycho-visual experiment suggests that the region of eye is also the salient region along with the region of mouth for the expressions of anger, fear or disgust (see Figure 3.18). Then, the concatenated features vector is fed to the classifier (“Classifier-c” in the Figure 5.1) for the final classification of the input sequence (see Section 5.4 for the classification results). It is worth mentioning here that for the expression of “disgust” nose region emerged as one of the salient regions but the framework do not explicitly extracts features from this region. This is due to the fact that, the region of nose that emerged as salient is the upper nose (wrinkles) area which is connected and already included in the localization of the eyes region.

## 5.2 Feature extraction using PHOG

PHOG is a spatial shape descriptor and got its inspiration from the works of Dalal et al. [DT05] on histograms of oriented gradients and Lazebnik et al. [LSP06] on spatial pyramid matching. It represents an image by its local shape and the spatial layout of the shape. Steps for the PHOG feature extraction are as follows:

1. Canny edge operator is applied to extract contours from the given stimuli. As illustrated in Figure 5.2 second row, edge contours represents the shape information.
2. Then, the image is divided into finer spatial grids by iteratively doubling the number of divisions in each dimension. It can be observed from Figure 5.2 that the grid at level  $l$  has  $2^l$  cells along each dimension.
3. Afterwards, a histogram of orientation gradients (HOG) are calculated on each edge point using 3 x 3 Sobel mask without Gaussian smoothing and

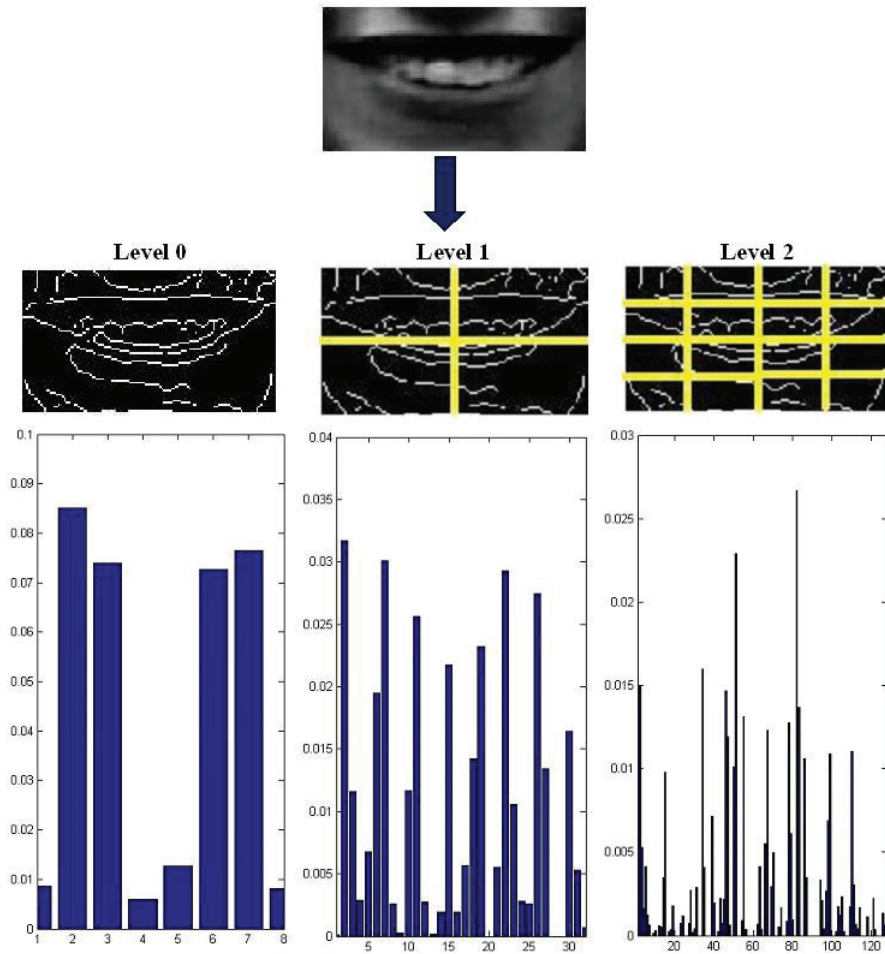


Figure 5.2: HOG feature extraction. First row: input stimuli, second row: edge contours at three different pyramid levels, third row: histograms of gradients (HOG) at three respective levels.

the contribution of each edge is weighted according to its magnitude. Within each cell, histogram is quantized into  $N$  bins. Each bin represents the accumulation of number of edge orientations within a certain angular range.

4. To obtain the final PHOG descriptor, histograms of gradients (HOG) at the same levels are concatenated. The final PHOG descriptor is a concatenation of HOG at different pyramid levels. Generally, the dimensionality of the PHOG descriptor can be calculated by:  $N \sum_l 4^l$ . In our experiment we

obtained 168 dimensional feature vector (  $f_1, \dots, f_{168}$  ) from one facial region, as we created two pyramid levels with 8 bins with the range of [0-360]. The same is shown in the Figure 5.2.

### 5.3 Discriminative strength of PHOG features

Figure 5.3 presents PHOG features (from the mouth region) which are extracted from the two categories of the expressions. It can be observed in the referred figure that PHOG features have a discriminative trend, specially at the *level 2* histograms have quite different shape. This discriminative ability is used in the proposed framework, initially to categorize expressions into two (“Classifier-a” in the Figure 5.1) and later for the final classification.

### 5.4 Expression recognition experiments

We conducted facial expression recognition experiments on two databases, the extended Cohn-Kanade (CK+) database [LCK<sup>+</sup>10] and the FG-NET facial expressions and emotion database(FEED) [Wal06]. Details related to CK+ database and FG-NET FEED are presented in the Appendix Sections A.1 and A.3 respectively.

The performance of the framework was evaluated using following four classical classifiers:

1. Support vector machine (SVM) with  $\chi^2$  kernel and  $\gamma=1$
2. C4.5 Decision Tree (DT) with reduced-error pruning
3. Random Forest (RF) of 10 trees
4. 2 Nearest Neighbor (2NN) based on Euclidean distance

The parameters of the classifiers were determined empirically. For discussion on different classifiers refer Section 2.3.3.

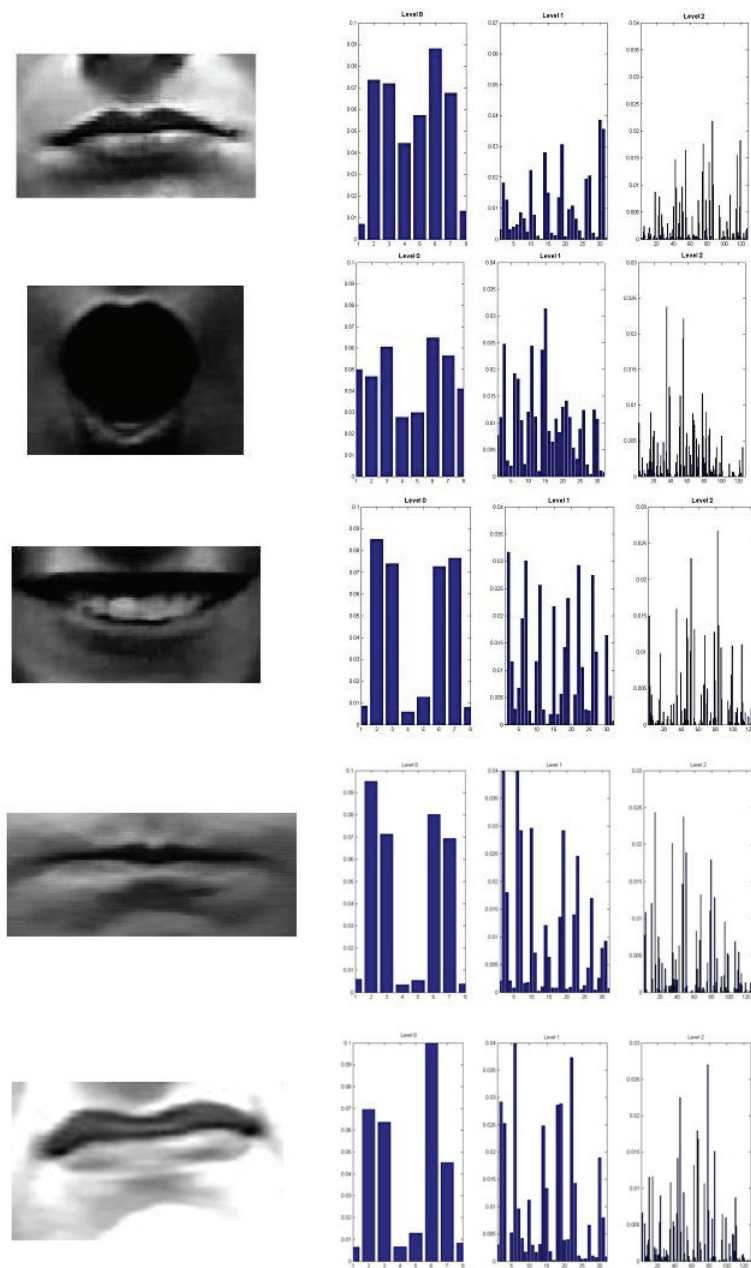


Figure 5.3: HOG features for different expressions. First row: sadness, second row: surprise, third row: happiness, fourth row: anger and fifth row: disgust. First column shows stimuli and second column shows respective HOG (only mouth facial region) at three levels.

### 5.4.1 First experiment: CK+ database

For the first study, we used all 309 sequences from the CK+ database which have FACS coded expression label. The experiment was carried out on the frames which covers the status of onset to apex, as done by Yang et al. [YLM10]. Region of interest was obtained automatically by using Viola-Jones object detection algorithm [VJ01] and processed to obtain PHOG feature vector <sup>1</sup>.

The proposed framework achieved average recognition rate of 95.3%, 95.1%, 96.5% and 96.7% for SVM, C4.5 decision tree, random forest and 2NN respectively. These values were calculated using 10-fold cross validation. One of the most interesting aspects of our approach is that it gives excellent results for a simple 2NN classifier which is a non-parametric method. This points to the fact that framework do not need computationally expensive methods such as SVM, Random forests or decision trees to obtain good results. In general, the proposed framework achieved high expression recognition accuracies irrespective of the classifiers, proves the descriptive strength of the features.

	Sa	Ha	Su	Fe	An	Di
Sa	<b>95.5</b>	0	0.5	0	4.0	0
Ha	0	<b>95.1</b>	0	4.1	0	0.8
Su	3.4	0	<b>96.6</b>	0	0	0
Fe	0	3.2	0	<b>94.6</b>	2.2	0
An	4.8	0	0	0	<b>95.2</b>	0
Di	0.8	0.9	0	0	3.4	<b>94.9</b>

Table 5.1: Confusion Matrix: SVM

For comparison and reporting results, we have used the classification results obtained by the SVM as it is the most cited method for classification in the literature. Table 5.1 shows the confusion matrix for SVM. Confusion matrices for the C4.5 decision tree, random forest and 2NN classifiers are not presented as the results are very similar. In the presented table expression of Happiness is referred by “Ha”, Sadness by “Sa”, Surprise by “Su”, Fear by “Fe”, Anger by “An” and

<sup>1</sup>video showing the result of the proposed framework on CK+ database is available at: <http://www.youtube.com/watch?v=wnF7Id9G6rM>

Disgust by “Di”. Diagonal and off-diagonal entries of confusion matrix shows the percentages of correctly classified and misclassified samples respectively.

We tested the proposed framework upto three pyramid levels (level 0 to level 2) (refer Figure 5.2). The framework was not tested for more pyramid levels as it produced results in the range of 95% which is better or equal than state-of-the-art methods (for reference see Table 5.2). By increasing pyramid levels it would increase the size of feature vector and thus increase the feature extraction time and likely would add few percents in the accuracy of framework which will be insignificant for a framework holistically.

	Pyramid Level		
	Level 0	Level 1	level 2
SVM	73.2	83.6	95.3
2NN	83.5	91	96.7
Decision tree	77.1	86.9	95.1
Random Forest	81.3	87.2	96.5

Table 5.2: Proposed framework recognition rate (%) for three pyramid levels.

#### 5.4.1.1 Behavior of the classifiers

Figure 5.4 shows the behavior of the four classifiers used in the experiment. For all the classifiers we have computed the average recognition accuracy using different number of folds ( $k$ 's) for the  $k$ -fold cross validation technique. In  $k$ -fold cross validation, features vector set is divided into  $k$  equal subsets.  $k-1$  subsets are used for the training while a single set is retained for the testing. The process is repeated  $k$  times ( $k$ -folds), with each of the  $k$  subsets used exactly once for testing. Then, the  $k$  estimations from  $k$ -folds are averaged to produce final estimated value. Generally, Figure 5.4 graphically presents the influence of the size of the training set on the performance of the classifiers. C4.5 decision tree classifier was influenced the most with less training data while 2NN classifier achieved highest recognition rate among the four classifiers with relatively small training set (i.e. 2-folds). This indicates how well our novel feature space was clustered.

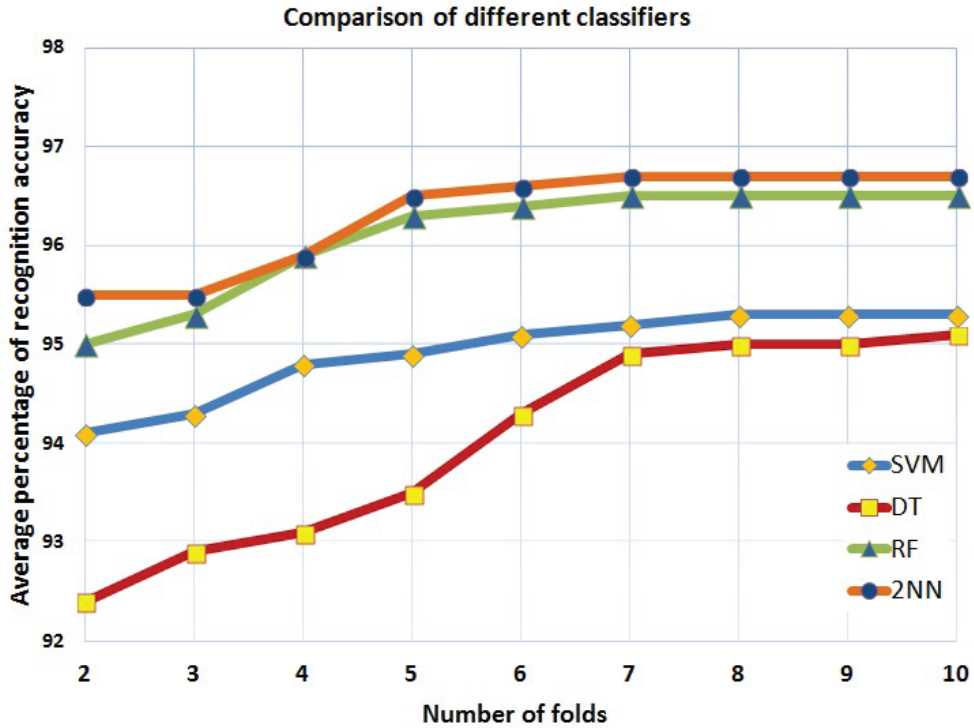


Figure 5.4: Evolution of the achieved average recognition accuracy for the six universal facial expressions with the increasing number of folds for the  $k$ -fold cross validation technique.

#### 5.4.1.2 Comparison with the state-of-the-art methods

Table 5.3 shows the comparison of the achieved average recognition rate of the proposed framework with the state-of-the-art methods [LBF<sup>+</sup>06, ZP07, KZP08, Tia04, YLM10, TTUP13, GL13] using the same database (i.e Cohn-Kanade database). The method proposed in [TTUP13] states results on 1632 images, which roughly corresponds to 55 video sequences as Cohn-Kanade database has average of 30 images per video sequence. Results from [YLM10] are presented for the two configurations. “[YLM10]a” shows the reported result when the method was evaluated for the last three frames (apex frames) from the sequence while “[YLM10]b” presents the reported result for the frames which encompasses the status from onset to apex of the expression. For comparison, we have used classification results obtained by SVM as it is the most cited method for classification in the literature.



	Sequence Num	Class Num	Performance Measure	Recog. Rate (%)
[LBF <sup>+</sup> 06]	313	7	leave-one-out	93.3
[ZP07]	374	6	ten-fold	96.26
[KZP08]	374	6	five-fold	94.5
[Tia04]	375	6	-	93.8
[YLM10]a	352	6	66% split	92.3
[YLM10]b	352	6	66% split	80
[TTUP13]	55	7	seven-fold	96.9
[GL13]	315	6	five-fold	97.3
<b>Ours</b>	<b>309</b>	<b>6</b>	<b>ten-fold</b>	<b>95.3</b>

Table 5.3: Comparison with the state-of-the-art methods

Although it is difficult to compare results directly from the different methods due to the variability in testing protocols or preprocessing, Table 5.3 still gives an indication of the discriminative ability of the different approaches. First observation that can be made from Table 5.3 is that the proposed framework is comparable to any other state-of-the-art method in terms of expression recognition accuracy. The method discussed in “[YLM10]b” where authors has used frames which encompasses the status from onset to apex of the expression is directly comparable to our method, as we also employed the same approach. In this configuration, our framework is better in terms of average recognition accuracy. It is also very interesting to mention that, in [YLM10] authors have shown facial regions of the top five compositional features (Haar-like features) which were selected after boosting learning. Facial regions of those features corresponds very well to the salient regions that we have determined for a particular expression after the psycho-visual experiment (see Figure 3.18).

#### 5.4.2 Second experiment: generalization on the new dataset

The aim of the second experiment was to study how well the proposed framework generalizes on the new dataset. According to our knowledge only Valstar et al. [VPP05] have reported such data earlier. Thus, this experiment

helps to understand how the framework will behave when it will be used to classify expressions in real life videos.

Experiment was performed in two different scenarios, with the same classifier parameters as the first experiment:

- a. In the first scenario samples from the CK+ database were used for the training of different classifiers and samples from FG-NET FEED [Wal06] were used for the testing. Obtained results are presented in Table 5.4.
- b. In the second scenario we used samples from the FG-NET FEED for the training and testing was carried out with the CK+ database samples. Results obtained are presented in Table 5.5.

Average recognition accuracies for training phase mentioned in Table 5.4 and 5.5 were calculated using 10-fold cross validation method.

	SVM	C4.5 DT	RF	2NN
Training samples	95.3%	95.1%	96.5%	96.7%
Test samples	80.5%	72.1%	71.1%	80%

Table 5.4: Average recognition accuracy: training classifier on CK+ database and testing it with FG-NET FEED

	SVM	C4.5 DT	RF	2NN
Training samples	90.3%	91.2%	89.5%	92.2%
Test samples	74.4%	72.2%	75.4%	81.9%

Table 5.5: Average recognition accuracy: training classifier on FG-NET FEED and testing it with CK+ database

Second experiment provided a good indication of how accurate the framework will perform in a challenging real life scenario. Results obtained from the second experiment shows that the performance of the framework does not deteriorate significantly even if it is used to classify samples which are different from training samples in terms of lighting conditions, resolution of the video and camera zoom.

### 5.4.3 Third experiment: low resolution image sequences

There exist many real world applications that require expression recognition system to work amicably on low resolution images. Smart meeting, video conferencing and visual surveillance are some examples of such applications. Ironically most of the existing state-of-the-art methods for expressions recognition report their results only on high resolution images without reporting results on low resolution images.



Figure 5.5: Example of stimuli with decreasing image resolution. First column shows stimuli in original resolution. Second to fifth column show stimuli in spatial resolution of: 144 x 192, 72 x 96, 36 x 48 and 18 x 24 respectively.

We have tested our proposed framework on low resolution images of four different facial resolutions (144 x 192, 72 x 96, 36 x 48, 18 x 24 ) based on Cohn-Kanade database as done by Tian [Tia04]. Example of the stimuli with different low resolutions are presented in Figure 5.5. Tian’s work can be considered as the pioneering work for low resolution image facial expression recognition. Low resolution image sequences were obtained by down sampling the original sequences. All the other experimental parameters are same as first two experiments.

Five different image resolutions (original + four down sampled) were used to evaluate the performance of the proposed framework. For all the classifiers we have computed the average recognition accuracy using 10-fold cross validation technique. The results are presented in Figure 5.6.

It can be observed from Figure 5.6 that the decrease in image spatial resolution is accompanied by a significant decrease in the performance of the proposed framework. Out of all the four tested classifiers, SVM’s performance is

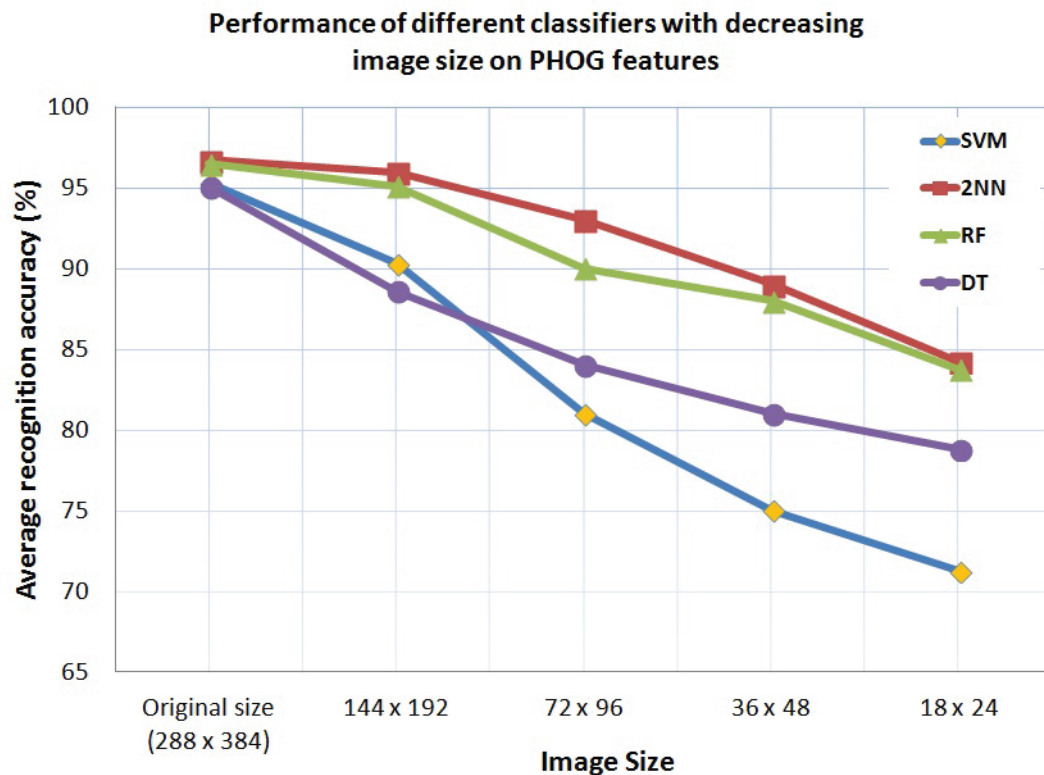


Figure 5.6: Robustness of different classifiers for facial expression recognition with decreasing image resolution.

deteriorated the most. The main reason for the drop of performance of the proposed framework is its reliance on the edge/contour based descriptor i.e. PHOG. The first step of the PHOG descriptor is to extract contour information from the given stimuli (for reference see Section 5.2) but as the stimuli spatial resolution gets decreased so does the sharpness of contours. The same can be observed in the Figure 5.5. Thus, PHOG fails to extract meaningful information from the low resolution images which explains the cause of bad performance of the framework on low resolution images.

## 5.5 Conclusion

It can be deduced from the presented results that the proposed framework is capable of producing results at par with the other state-of-the-art methods for the

stimuli recorded in controlled environment i.e. CK+ database (refer Table 5.3). The framework creates novel feature space by extracting features only from the perceptual salient facial regions. The novel feature space is conducive for facial expression recognition task as it achieved best result with “naïve” 2NN classifier (see Section 5.4.1.1). This indicates how well our novel feature space was clustered. By processing only salient regions, proposed framework reduces computational complexity of feature extraction and thus, can be used for real-time applications. Its current unoptimized Matlab implementation runs at 6 frames / second (on windows 7 machine, with i7-2760QM processor and 6 GB RAM) which is enough as facial expressions do not change abruptly.

The proposed framework showed its weakness on low resolution images (refer Section 5.4.3). The proposed framework is unable to cope with stimuli of low resolution or stimuli not having sharp contours. The reason for this weakness is its reliance on the edge/contour based descriptor i.e. PHOG.

Novel framework presented in this chapter is published in “IEEE International Conference on Image Processing” [KMKB12b].



# Chapter 6

## Recognizing expressions by analyzing texture

### Contents

---

<b>6.1</b>	<b>PLBP based framework . . . . .</b>	<b>106</b>
6.1.1	Novelty of the proposed descriptor . . . . .	109
<b>6.2</b>	<b>Expression recognition framework . . . . .</b>	<b>110</b>
<b>6.3</b>	<b>Results on universal expressions . . . . .</b>	<b>112</b>
6.3.1	First experiment: posed expressions . . . . .	113
6.3.2	Second experiment: low resolution image sequences . . .	118
6.3.3	Third experiment: generalization on the new dataset . .	121
6.3.4	Fourth experiment: spontaneous expressions . . . . .	122
<b>6.4</b>	<b>Pain recognition . . . . .</b>	<b>124</b>
6.4.1	Novelty of proposed approach . . . . .	125
6.4.2	Pain expression database . . . . .	126
6.4.3	Framework . . . . .	126
6.4.4	Experiment . . . . .	128
<b>6.5</b>	<b>Conclusion . . . . .</b>	<b>132</b>

---

To rectify the problems of the proposed framework based on edge / contour information (refer Chapter 5), we studied appearance features to recognize various facial expressions. We propose a novel descriptor for facial features analysis, “Pyramid of Local Binary Pattern (PLBP)”. PLBP is a spatial representation of local binary pattern (LBP) [OPH96] and it represents stimuli by its local texture (LBP) and the spatial layout of the texture. We chose to extend LBP descriptor as it is not based on edges (drawback of former descriptor) and has been proved to be effective for facial images analysis task [ZP07, SGM09, AHP04]. We combined pyramidal approach with LBP descriptor for facial feature analysis as this approach has already been proved to be very effective in a variety of image processing tasks [HGN04]. Thus, the proposed descriptor is a computationally efficient novel extension of LBP image representation, and it shows significantly improved performance for facial expression recognition tasks for low resolution images.

## 6.1 PLBP based framework

The proposed framework creates a novel feature space by extracting proposed PLBP (pyramid of local binary pattern) features only from the visually salient facial region (see Chapter 3 for details of psycho-visual experiment). PLBP is a *pyramidal-based spatial* representation of local binary pattern (LBP) descriptor. PLBP represents stimuli by their local texture (LBP) and the spatial layout of the texture. The spatial layout is acquired by tiling the image into regions at multiple resolutions. The idea is illustrated in Figure 6.1. If only the coarsest level is used, then the descriptor reduces to a global LBP histogram. Comparing to the multi-resolution LBP of Ojala et al.[OPM02] which is illustrated in Figure 6.2, our descriptor selects samples in a more uniformly distributed manner, whereas Ojala’s LBP takes samples centered around a point leading to missing some information in the case of face (which is different than a repetitive texture).

LBP features were initially proposed for texture analysis [OPH96], but recently they have been successfully used for facial expression analysis [ZP07, SGM09]. The most important property of LBP features is their tolerance against illumination



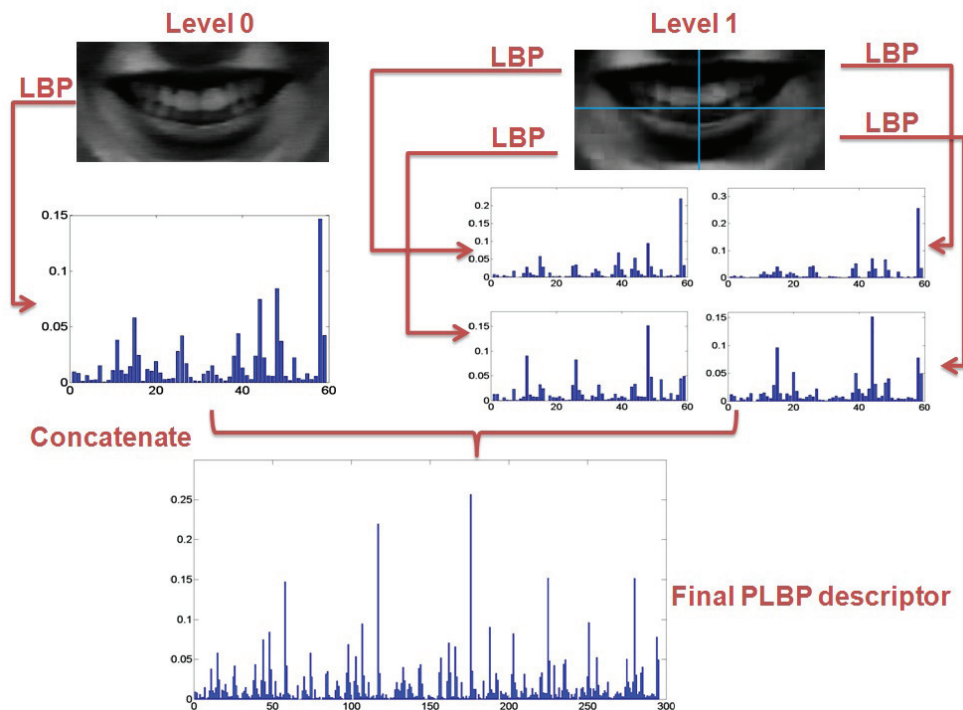


Figure 6.1: Pyramid of Local Binary Pattern. First row: stimuli at two different pyramid levels, second row: histograms of LBP at two respective levels, third row: final descriptor.

changes and their computational simplicity [OP99, OPH96, OPM02]. The operator labels the pixels of an image by thresholding the  $3 \times 3$  neighbourhood of each pixel with the center value and considering the result as a binary number. Then the histogram of the labels can be used as a texture descriptor. Formally, LBP operator takes the form:

$$LBP(x_c, y_c) = \sum_{n=0}^7 s(i_n - i_c) 2^n \quad (6.1)$$

where in this case  $n$  runs over the 8 neighbours of the central pixel  $c$ ,  $i_c$  and  $i_n$  are the grey level values at  $c$  and  $n$  and  $s(u)$  is 1 if  $u \geq 0$  or 0 otherwise.

The limitation of the basic LBP operator is its small  $3 \times 3$  neighborhood which can not capture dominant features with large scale structures. Hence the operator later was extended to use neighborhood of different sizes [OPM02]. Using circular neighborhoods and bilinearly interpolating the pixel values allow any radius and

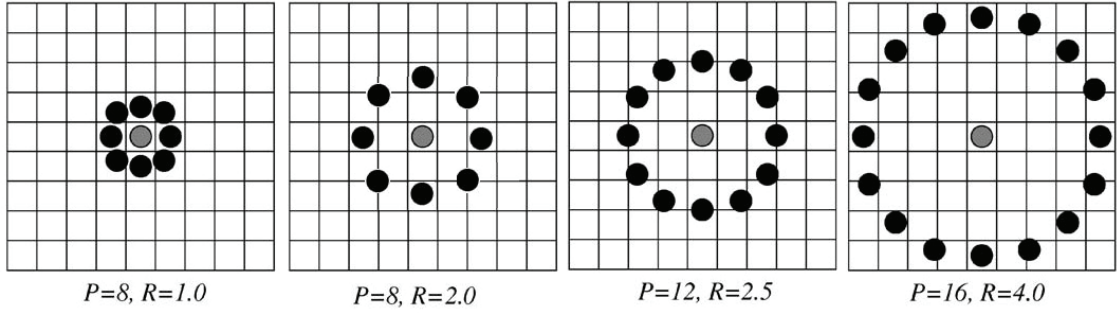


Figure 6.2: Examples of the extended LBP [OPM02]. The pixel values are bilinearly interpolated whenever the sampling point is not in the center of a pixel

number of pixels in the neighborhood. See Figure 6.2 for examples of the extended LBP operator, where the notation  $(P, R)$  denotes a neighborhood of  $P$  equally spaced sampling points on a circle of radius of  $R$  that form a circularly symmetric neighbor set.

The LBP operator with  $P$  sampling points on a circular neighborhood of radius  $R$  is given by:

$$LBP_{P,R} = \sum_{p=0}^{P-1} s(g_p - g_c) 2^p \quad (6.2)$$

where,  $g_c$  is the gray value of the central pixel,  $g_p$  is the value of its neighbors,  $P$  is the total number of involved neighbors and  $R$  is the radius of the neighborhood.

Another extension to the original operator is the definition of uniform patterns, which can be used to reduce the length of the feature vector and implement a simple rotation-invariant descriptor. This extension was inspired by the fact that some binary patterns occur more commonly in texture images than others. A local binary pattern is called uniform if the binary pattern contains at most two bitwise transitions from 0 to 1 or vice versa when the bit pattern is traversed circularly. For example, 00000000, 00011110 and 10000011 are uniform patterns. Accumulating the patterns which have more than 2 transitions into a single bin yields an LBP operator, denoted  $LBP_{P,R}^{u2}$  patterns. These binary patterns can be used to represent texture primitives such as spot, flat area, edge and corner.

We extend LBP operator so that the stimuli can be represented by its local texture and the spatial layout of the texture. We call this extended LBP operator

as pyramid of local binary pattern or PLBP. PLBP creates the spatial pyramid by dividing the stimuli into finer spatial sub-regions by iteratively doubling the number of divisions in each dimension. It can be observed from the Figure 6.1 that the pyramid at level  $l$  has  $2^l$  sub-regions along each dimension ( $R_0, \dots, R_{m-1}$ ). Histograms of LBP features at the same levels are concatenated. Then, their concatenation at different pyramid levels gives final PLBP descriptor (as shown in Figure 6.1). It can be defined as:

$$H_{i,j} = \sum_l \sum_{xy} I\{f_l(x,y) = i\} I\{(x,y) \in R_l\} \quad (6.3)$$

where  $l = 0 \dots m - 1$ ,  $i = 0 \dots n - 1$ .  $n$  is the number of different labels produced by the LBP operator and

$$I(A) = \begin{cases} 1 & \text{if A is true ,} \\ 0 & \text{otherwise} \end{cases} \quad (6.4)$$

While, the dimensionality of the descriptor can be calculated by:

$$N \sum_l 4^l \quad (6.5)$$

Where, in our experiment (see Section 6.3)  $l=1$  and  $N= 59$  as we created pyramid upto level 1 and extracted 59 LBP features using  $LBP_{8,2}^{u_2}$  operator, which denotes a uniform LBP operator with 8 sampling pixels in a local neighborhood region of radius 2. This pattern reduces the histogram from 256 to 59 bins. In our experiment we obtained 295 dimensional feature vector from one facial region i.e. mouth region (59 dimensions / sub-region), since we executed the experiment with the pyramid of level 1 (the same is shown in Figure 6.1). We create pyramid upto level 1 as the salient regions are not dimensionally large enough to be divided further.

### 6.1.1 Novelty of the proposed descriptor

There exists some methods in literature that uses Pyramid of LBP for different applications and they look similar to our proposed descriptor i.e.

[WCX11, GZZM10, MB11]. Our proposition is novel and there exist differences in the methodology that creates differences in the extracted information. Method for face recognition proposed in [WCX11] creates pyramids before applying LBP operator by down sampling original image i.e. scale-space representation, whereas we propose to create the spatial pyramid by dividing the stimuli into finer spatial sub-regions by iteratively doubling the number of divisions in each dimension. Thus, theoretically both the methods are extracting different data before applying LBP operator. Secondly, our approach reduces memory consumption (does not require to store same image in different resolutions) and is computationally more efficient. Guo et al. [GZZM10] proposed an approach for face and palmprint recognition based on multiscale LBP. Their proposed method seems similar to our method for expression recognition but how multiscale analysis is achieved deviates our approach. The approach proposed in [GZZM10] achieves multiscale analysis using different values of  $P$  and  $R$ , where  $LBP(P, R)$  denotes a neighborhood of  $P$  equally spaced sampling points on a circle of radius  $R$  (discussed earlier). Same approach has been applied by Moore et al. [MB11] for facial features analysis. Generally the drawback of using such approach is that it increases the size of the feature histogram and increases the computational cost. [MB11] reports dimensionality of feature vector as high as 30,208 for multiscale face expression analysis as compared to our proposition which creates 590 dimensional feature vector (see Section 6.2) for the same task. We achieve the task of multiscale analysis much more efficiently than any other earlier proposed methods. By the virtue of efficient multiscale analysis our framework can be used for real time applications (see Table 6.5 for the time and memory consumption comparison) which is not the case for other methods.

## 6.2 Expression recognition framework

Feature selection along with the region(s) from where these features are going to be extracted is one of the most important step to recognize expressions. As the proposed framework draws its inspiration from the human visual system (HVS), it extracts proposed features i.e. PLBP, only from the perceptual salient facial region(s) which were determined through Psycho-Visual experiment. Schematic

overview of the framework is presented in Figure 6.3. Steps of the proposed framework are as follows.

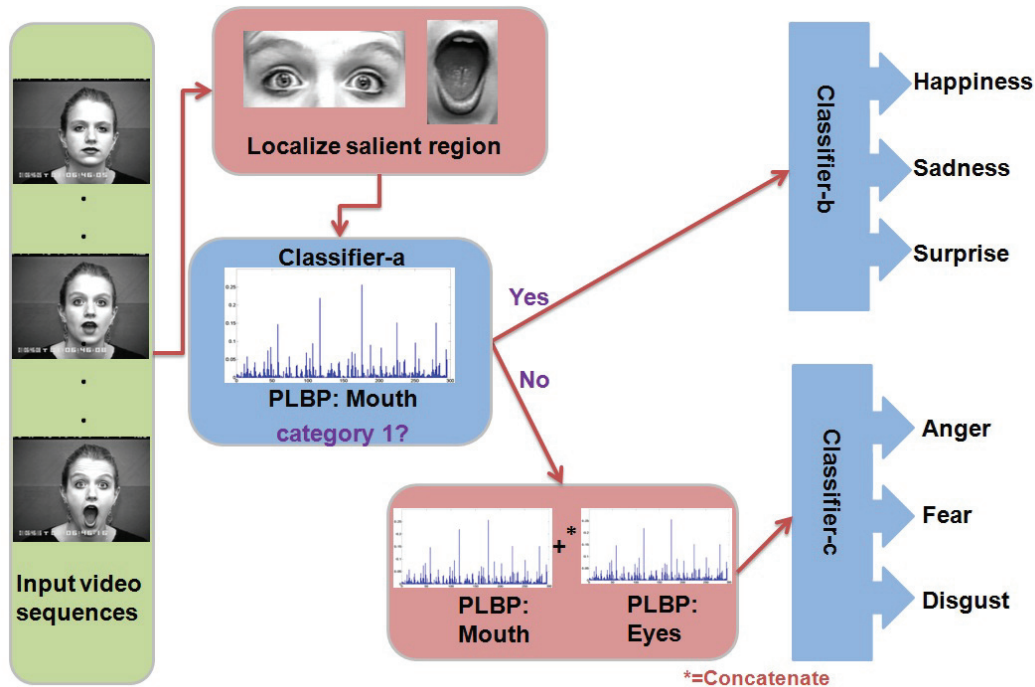


Figure 6.3: Schematic overview of the framework.

1. The framework first localizes salient facial regions using Viola-Jones object detection algorithm [VJ01] as it was done in the former proposed frameworks (Chapters 4 and 5).
2. Then, the framework extracts PLBP features from the mouth region, feature vector of 295 dimensions ( $f_1, \dots, f_{295}$ ). The classification (“Classifier-a” in the Figure 6.3) is carried out on the basis of extracted features in order to make two groups of facial expressions. First group comprises expressions that have one perceptual salient region i.e. happiness, sadness and surprise. The second group is composed of expressions that have two or more perceptual salient regions i.e. anger, fear and disgust (see Section 3.4). The purpose of making two groups of expressions is to reduce feature extraction computational time.

3. If the stimuli is classified in the first group, then it is classified either as happiness, sadness or surprise by the “Classifier-b” using already extracted PLBP features from the mouth region.
4. If the stimuli is classified in the second group, then the framework extracts PLBP features from the eyes region and concatenates them with the already extracted PLBP features from the mouth region, feature vector of 590 dimensions (  $f_1, \dots, f_{295} + f_1, \dots, f_{295}$  ). Then, the concatenated feature vector is fed to the classifier (“Classifier-c”) for the final classification. It is worth mentioning here that for the expression of “disgust”, the nose region emerged as one of the salient regions but the framework does not explicitly extracts features from this region. This is due to the fact that, the region of nose that emerged as salient is the upper nose (wrinkles) area which is connected and already included in the localization of the eyes region.

### 6.3 Results on universal expressions

We performed person-independent facial expression recognition using proposed PLBP features <sup>1</sup>. We have evaluated the performance of proposed novel framework on low resolution image sequences. There are many real world applications that require robust expression recognition system for low resolution images i.e. smart meeting, video conferencing and visual surveillance etc. Most of existing frameworks for expression recognition are not evaluated for the same. Thus, it is very important to develop such a system that works appropriately for both low and high resolution input stimuli. In total we have performed four experiments to evaluate proposed framework in different scenarios.

1. First experiment was performed on the extended Cohn-Kanade (CK+) database [LCK<sup>+</sup>10]. This database contains 593 sequences of posed universal expressions. Sequences were digitized into 640 x 490 pixel array

---

<sup>1</sup>video showing the result of the proposed framework on good quality image sequences is available at: [http://www.youtube.com/watch?v=RPeXBdS\\_pd8](http://www.youtube.com/watch?v=RPeXBdS_pd8)

with 8-bit precision for gray scale values, producing sequences with high resolution faces (see Appendix Section A.1 for reference).

2. Second experiment was performed to test the performance of the proposed framework on the low resolution image sequences. For this experiment low resolution sequences were created from the extended Cohn-Kanade (CK+) database by down sampling original sequences.
3. Third experiment tests the robustness of the proposed framework when generalizing on the new dataset.
4. Fourth experiment was performed on the MMI facial expression database (Part IV and V of the database) [VP10] which contains spontaneous/natural expressions (see Appendix Section A.2 for reference).

For the first two experiments we used all the 309 sequences from the CK+ database which have FACS coded expression label [EF78]. The experiment was carried out on the frames which covers the status of onset to apex of the expression, as done by Yang et al. [YLM10]. Region of interest was obtained automatically by using Viola-Jones object detection algorithm [VJ01] and processed to obtain PLBP feature vector. We extracted LBP features only from the salient region(s) using  $LBP_{8,2}^{u2}$  operator which denotes a uniform LBP operator with 8 sampling pixels in a local neighborhood region of radius 2<sup>1</sup>. In our framework we created image pyramid up to level 1, so in turn got five sub-regions from one facial region i.e. mouth region (see Figure. 6.1). In total we obtained 295 dimensional feature vector (59 dimensions / sub-region).

### 6.3.1 First experiment: posed expressions

This experiment measures the performance of the proposed framework on the classical database i.e. extended Cohn-Kanade (CK+) database [LCK<sup>+</sup>10]. Most of the methods in literature report their performance on this database, so this

---

<sup>1</sup>In the second experiment we adopted  $LBP_{4,1}^{u2}$  operator when the face resolution gets smaller than 36 x 48

experiment could be considered as the benchmark experiment for facial expression recognition framework.

The performance of the framework was evaluated for four different classifiers:

1. Support vector machine (SVM) with  $\chi^2$  kernel and  $\gamma=1$
2. C4.5 decision tree with reduced-error pruning
3. Random forest of 10 trees
4. 2 nearest neighbor (2NN) based on Euclidean distance.

### 6.3.1.1 Results

The framework achieved average recognition rate of 96.7%, 97.9%, 96.2% and 94.7 % for SVM, 2-nearest neighbor, Random forest and C4.5 decision tree respectively using 10-fold cross validation technique (refer Table 6.1). One of the most interesting aspects of our approach is that it gives excellent results for a simple 2NN classifier which is a non-parametric method. This points to the fact that our framework does not need computationally expensive methods such as SVM, random forests or decision trees to obtain good results. In general, the proposed framework achieved high expression recognition accuracies irrespective of the classifiers. This proves the descriptive strength of the extracted features (which minimizes within-class variations of expressions, while maximizes between class variation).

	Two-fold	Ten-fold
SVM	95.2	96.7
2-nearest neighbor	97.4	97.9
Random forest	92.4	96.2
C4.5 decision tree	90.5	94.7

Table 6.1: Average recognition performance(%)

For comparison and reporting results, we have used the classification results obtained by the SVM as it is the most cited method for classification in the literature. Table 6.2 shows the confusion matrix for SVM. In the presented table



	Sa	Ha	Su	Fe	An	Di
Sa	<b>96.5</b>	0	0.5	0	3.0	0
Ha	0	<b>97.1</b>	0	2.1	0	0.8
Su	2.9	0	<b>97.1</b>	0	0	0
Fe	0	3.3	0	<b>94.5</b>	2.2	0
An	3.5	0	0	0	<b>96.5</b>	0
Di	0.8	0.7	0	0	3.1	<b>96.4</b>

Table 6.2: Confusion Matrix: SVM

expression of Happiness is referred by “Ha”, Sadness by “Sa”, Surprise by “Su”, Fear by “Fe”, Anger by “An” and Disgust by “Di”. Diagonal and off-diagonal entries of confusion matrix shows the percentages of correctly classified and misclassified samples respectively.

Figure 6.4 shows the influence of the size of the training set on the performance of the four classifiers used in the experiment. For all the classifiers we have computed the average recognition accuracy using different number of folds ( $k$ 's) for the  $k$ -fold cross validation technique and plotted them in the Figure 6.4. It can be observed that C4.5 decision tree classifier was influenced the most with less training data while 2NN classifier achieved highest recognition rate among the four classifiers with relatively small training set (i.e. 2-folds). This indicates how well our novel feature space was clustered.

We recorded correct classification accuracy in the range of 95% for image pyramid level 1. We decided not to test the framework with further image pyramid levels as firstly, salient regions are not dimensionally large enough to be divided further. Secondly, creating more pyramid level would double the size of feature vector and thus increase the feature extraction time and likely would add few percents in the accuracy of framework which will be insignificant for a framework holistically. For reference see Tables 6.1 and 6.3.

### 6.3.1.2 Comparisons

We chose to compare average recognition performance of our framework with the framework proposed by Shan et.al [SGM09] with different SVM kernels. Our choice was based on the fact that both have common underlying descriptor i.e.

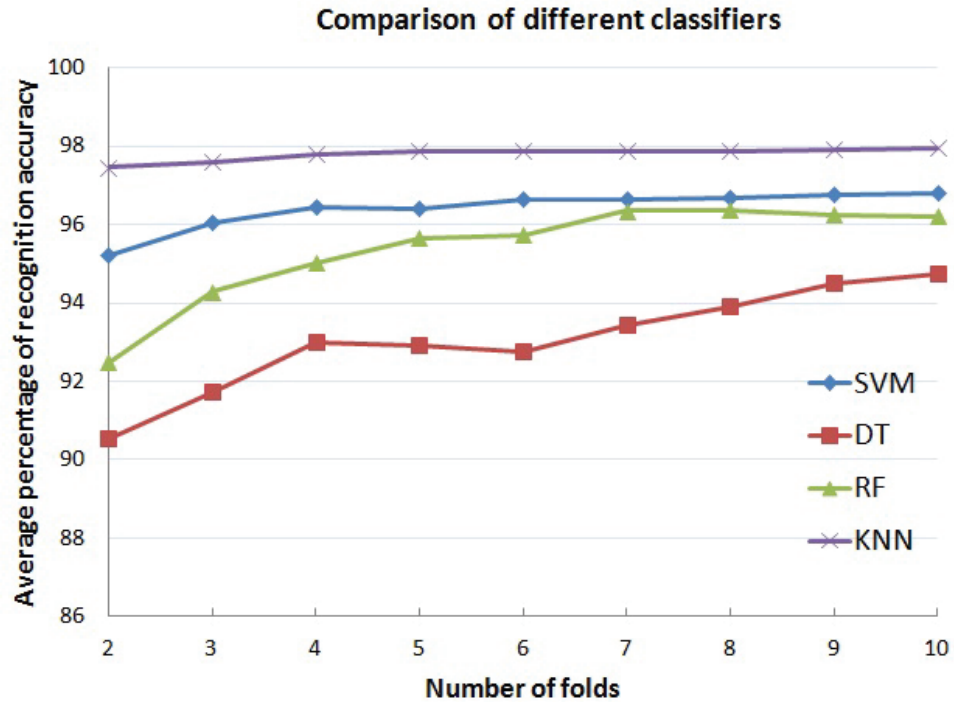


Figure 6.4: Evolution of the achieved average recognition accuracy for the six universal facial expressions with the increasing number of folds for the  $k$ -fold cross validation technique.

	Pyramid Level	
	Level 0	Level 1
SVM	86.3	96.7
2NN	91.6	97.9
Decision tree	89.1	94.7
Random Forest	90.3	96.2

Table 6.3: Proposed framework recognition rate (%) for two pyramid levels.

local binary pattern (LBP), secondly framework proposed by Shan et.al [SGM09] is highly cited in the literature. Table 6.4 shows the results and proves that the proposed framework works better than the compared framework for any SVM kernel. In terms of time and memory costs of feature extraction process, we have measured and compared our descriptor with the LBP and Gabor-wavelet features in Table 6.5. Table 6.5 shows the effectiveness of the proposed descriptor for facial feature analysis i.e. PLBP, for real-time applications as it is memory efficient

	LBP[SGM09]	<b>PLBP</b>
SVM(linear)	91.5	<b>93.5</b>
SVM(polynomial)	91.5	<b>94.7</b>
SVM(RBF)	92.6	<b>94.9</b>

Table 6.4: Average recognition percentages with different SVM kernels: comparison with [SGM09].

	LBP [SGM09]	Gabor [SGM09]	Gabor [BL+03]	<b>PLBP</b>
Memory (feature dimension)	2,478	42,650	92,160	<b>590</b>
Time (feature extraction time)	0.03s	30s	-	<b>0.01s</b>

Table 6.5: Comparison of time and memory consumption.

and its extraction time is much lower than other compared descriptor (see Section 6.2 for the dimensionality calculation). The proposed framework is compared with other state-of-the-art frameworks using same database (i.e Cohn-Kanade database) and the results are presented in Table 6.6.

Table 6.6 shows the comparison of the achieved average recognition rate of the proposed framework with the state-of-the-art methods using same database (i.e Cohn-Kanade database). The method proposed in [TTUP13] states results on 1632 images, which roughly corresponds to 55 video sequences as Cohn-Kanade database has average of 30 images per video sequence. Results from [YLM10] are presented for the two configurations. “[YLM10]a” shows the result when the method was evaluated for the last three frames from the sequence while “[YLM10]b” presents the reported result for the frames which encompasses the status from onset to apex of the expression. It can be observed from the Table 6.6 that the proposed framework is comparable to any other state-of-the-art method in terms of expression recognition accuracy. The method discussed in “[YLM10]b” is directly comparable to our method, as we also evaluated the framework on similar frames. In this configuration, our framework is better in terms of average recognition accuracy.

	Sequence Num	Class Num	Performance Measure	Recog. Rate (%)
[LBF <sup>+</sup> 06]	313	7	leave-one-out	93.3
[ZP07]	374	6	2-fold	95.19
[ZP07]	374	6	10-fold	96.26
[KZP08]	374	6	5-fold	94.5
[Tia04]	375	6	-	93.8
[YLM10]a	352	6	66% split	92.3
[YLM10]b	352	6	66% split	80
[TTUP13]	55	7	seven-fold	96.9
[GL13]	315	6	five-fold	97.3
<b>Ours:</b> framework proposed in Chapter 5	309	6	10-fold	95.3
<b>Ours</b>	<b>309</b>	<b>6</b>	<b>10-fold</b>	<b>96.7</b>
<b>Ours</b>	<b>309</b>	<b>6</b>	<b>2-fold</b>	<b>95.2</b>

Table 6.6: Comparison with the state-of-the-art methods for posed expressions.

In general, Tables 6.4, 6.5 and 6.6 shows that the framework is better than the state-of-the-art frameworks in terms of average expression recognition performance, time and memory costs of feature extraction processes. These results show that the system could be used for real-time applications with high degree of confidence.

### 6.3.2 Second experiment: low resolution image sequences

Most of the existing state-of-the-art systems for expressions recognition report their results on high resolution images with out reporting results on low resolution images. As mentioned earlier there are many real world applications that require expression recognition system to work amicably on low resolution images. Smart meeting, video conferencing and visual surveillance are some examples of such applications. To compare with Tian’s work [Tia04], we tested our proposed framework on low resolution images of four different facial resolutions (144 x 192, 72 x 96, 36 x 48, 18 x 24 ) based on Cohn-Kanade database. Tian’s work can be considered as the pioneering work for low resolution image facial expression recognition. Table 6.7 shows the images at different spatial resolution along with the average recognition accuracy achieved

by the different methods. Low resolution image sequences were obtained by down sampling the original sequences. All the other experimental parameters i.e. descriptor, number of sequences and region of interest, were same as mentioned earlier in the Section 6.3.






					
	288 x 384	144 x 192	72 x 96	36 x 48	18 x 24
PHOG [KMKB12b]	95.3	90.3	81	75	71.2
Gabor [Tia04]	91.7	92.2	91.6	77.6	68.2
Gabor [SGM09]	89.8	89.8	89.2	83	75.1
LBP [SGM09]	92.6	92.6	89.9	84.3	76.9
<b>PLBP</b>	<b>96.7</b>	<b>95.3</b>	<b>93.9</b>	<b>92.8</b>	<b>90.5</b>

Table 6.7: Average recognition accuracy (%) for six universal expressions on five different facial image resolutions. First column corresponds to original resolution.

Table 6.7 and Figure 6.5 report and compare the recognition results of the proposed framework with the state-of-the-art methods on four different low facial resolution images. Reported results of our proposed method are obtained using support vector machine (SVM) with  $\chi^2$  kernel and  $\gamma=1$ . In Figure 6.5 recognition curve for our proposed method is shown as PLBP-SVM, recognition curves of LBP [SGM09] and Gabor [SGM09] are shown as LBP[JIVC] and Gabor[JIVC] respectively, curve for Tian’s work [Tia04] is shown as Gabor[CVPRW] while Khan et al. [KMKB12b] proposed system’s curve is shown as PHOG[ICIP] (framework explained in Chapter 5 and specifically Section 5.4.3).

Results reports in LBP [SGM09] and Gabor [SGM09], the different facial image resolution are 110 x 150, 55 x 75, 27 x 37 and 14 x 19 which are comparable to the resolutions of 144 x 192, 72 x 96, 36 x 48, 18 x 24 pixels in our experiment. Referenced table and figure show the supremacy of the proposed framework for low resolution images. Specially for the smallest tested facial image resolution (18 x 24), our framework performs much better than any other compared state-of-the-art method. Figure 6.6 shows the spatial resolution of salient regions for the smallest

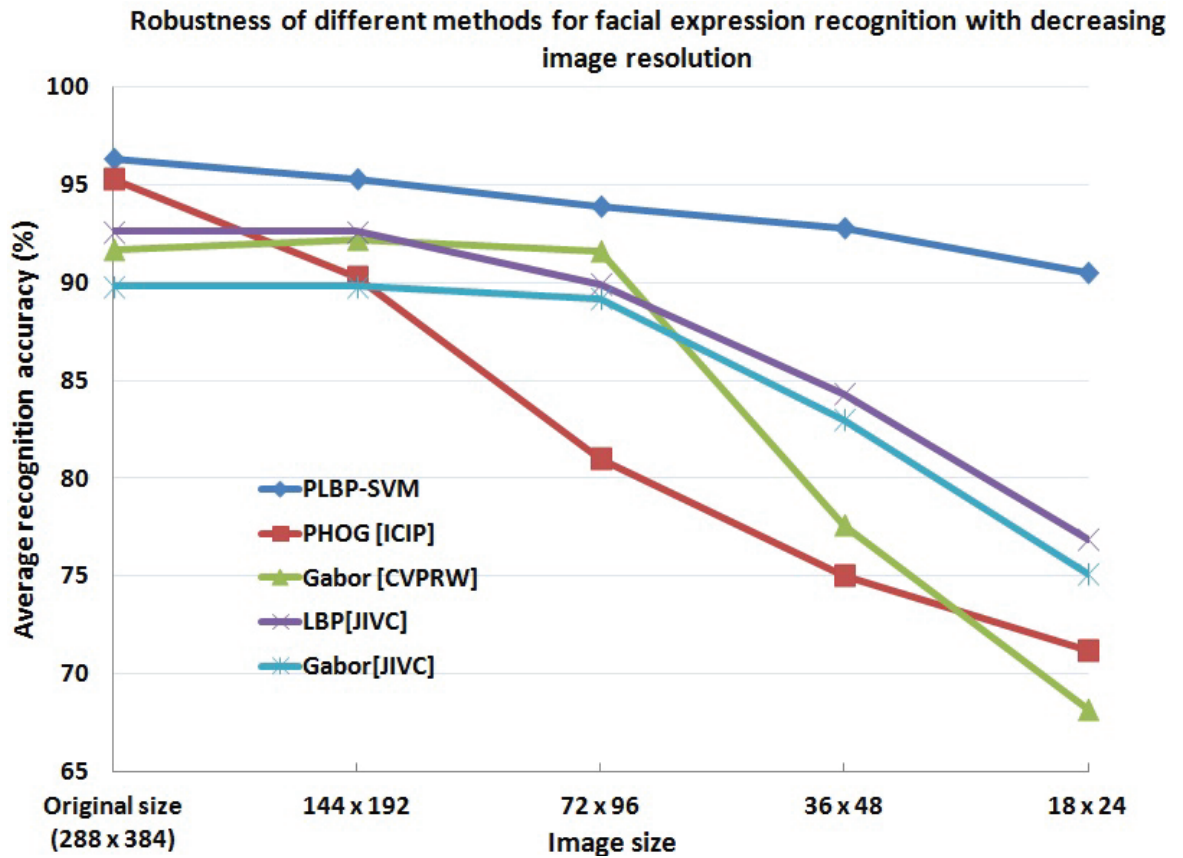


Figure 6.5: Robustness of different methods for facial expression recognition with decreasing image resolution (CK database). PHOG[ICIP] corresponds to framework proposed by Khan et. al [KMKB12b] (framework explained in Chapter 5 and specifically Section 5.4.3), Gabor [CVPRW] corresponds to Tian’s work [Tia04], LBP[JIVC] and Gabor[JIVC] corresponds to results reported by Shan et. al [SGM09]

tested facial image resolution. It is difficult to recognize expression with naked eye at this resolution but good results achieved by the proposed framework show the discriminative strength of the proposed descriptor i.e. PLBP. Results from the first and second experiments show that the proposed framework for facial expression recognition works amicably on classical dataset (CK dataset) and its performance is not affected significantly for low resolution images. Secondly, the framework has a very low memory requirement and thus it can be utilized for real-time applications.

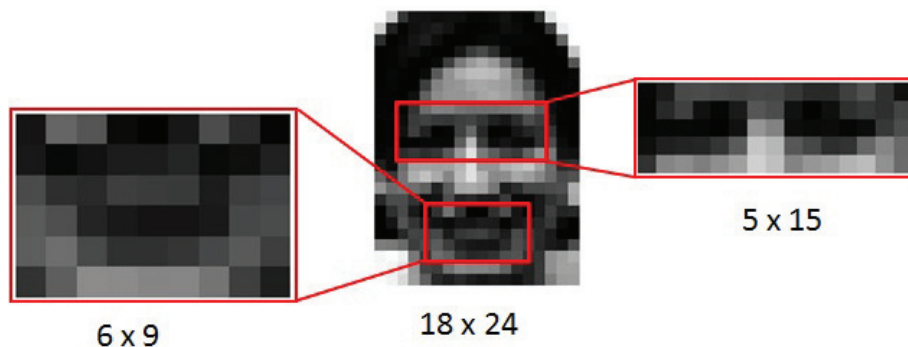


Figure 6.6: Example of lowest tested facial resolution

### 6.3.3 Third experiment: generalization on the new dataset

The aim of this experiment is to study how well the proposed framework generalizes on the new dataset. As mentioned previously, according to our knowledge only Valstar et al. [VPP05] have reported such data earlier. In this experiment we trained classifier(s) with one dataset and tested them with different dataset, as it was done for the former framework (refer Section 5.4.2). We used image sequences from CK+ dataset and FG-NET FEED (Facial Expressions and Emotion Database) [Wal06]. Refer Appendix Sections A.1 and A.3 for details related to the two databases.

The experiment was carried out on the frames which cover the status of onset to apex of the expression as done in the previous experiment. This experiment was performed in two different scenarios, with the same classifier parameters as the first experiment.

- a. In the first scenario, samples from the CK+ database were used for the training of different classifiers and samples from FG-NET FEED [Wal06] were used for the testing. Obtained results are presented in Table 6.8.
- b. In the second scenario, we used samples from the FG-NET FEED for the training and testing was carried out with the CK+ database samples. Results obtained are presented in Table 6.9.

This experiment simulates the real life situation when the framework would be employed to recognize facial expressions on unseen data. Obtained results are

presented in Tables 6.8 and 6.9. Reported average recognition percentages for the training phase were calculated using 10-fold cross validation method. Obtained results are encouraging and they can be further improved by training classifiers on more than one dataset before using in real life scenario.

	SVM	C4.5 DT	RF	2NN
Training samples	96.7	94.7	96.2	97.9
Test samples	81.9	74.8	79.5	83.1

Table 6.8: Average recognition accuracy (%): training classifier on CK+ database and testing it with FG-NET FEED

	SVM	C4.5 DT	RF	2NN
Training samples	92.3	91.2	90.5	93.3
Test samples	80.5	77.3	79	84.7

Table 6.9: Average recognition accuracy (%): training classifier on FG-NET FEED and testing it with CK+ database

### 6.3.4 Fourth experiment: spontaneous expressions

Spontaneous/natural facial expressions differ substantially from posed expressions [BLB<sup>+</sup>02]. The same has also been proved by psychophysical work [Ekm01, WBG87, EF82]. Ekman and Friesen [EF82] stated that the main difference between spontaneous and fake expression lies in some of the topographical and temporal aspect of these expressions. Weiss et al. [WBG87] investigated some of the temporal differences and found shorter onset times and more irregularities (pause and stepwise intensity changes) for posed/deliberate facial expressions. They also provided the evidence that spontaneous expressions are less irregular than posed expressions. Valstar et al. [VPAC06] experimentally showed that temporal dynamics of spontaneous and posed brow actions are different from each other. We also observed the same trend when working with posed (CK) and spontaneous expressions databases (MMI) [VP10] (refer Appendix Section A.2). In CK database actors show series of exaggerated expressions with stepwise intensity changes. While spontaneous expressions



displayed in MMI database are devoid of any exaggeration and very smooth in terms of intensity changes. Recently efforts are growing towards automatic analysis of spontaneous expressions but research needs to be done to recognize wide array of spontaneous expressions. Few existing spontaneous expression recognition algorithms are able to differentiate spontaneous from posed expressions i.e. identification of fake smile [CS04] and identification of fake pain expression [LBL07].

To test the performance of the proposed framework on spontaneous facial expressions we used 392 video segments from part IV and V of the MMI facial expression database [VP10]. Part IV and V of the database contains induced spontaneous expressions (deliberately evoked in subjects by outside perceived stimuli such as watching dramas or reading jokes) recorded from 25 participants aged between 20 and 32 years in two different settings (see Figure 6.7 for example). Due to ethical concerns the database contains only the video recording of the expressions of happiness, surprise and disgust [VP10]. Table 6.10 shows the obtained results for the the experiment.

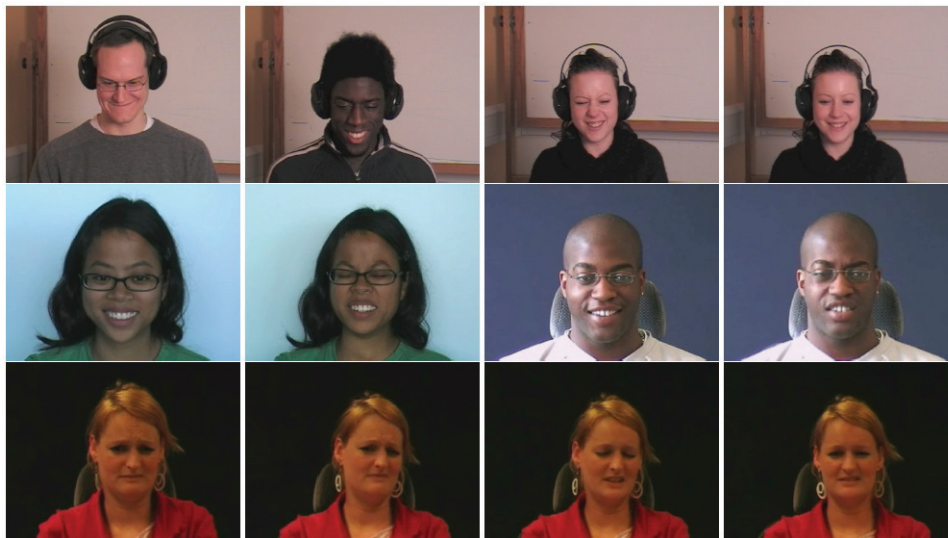


Figure 6.7: Examples frames from MMI-Facial Expression Database. The first row is taken from Part V of the database and shows expressions of happiness and disgust. The second row shows expressions of happiness and disgust taken from Part IV of the database. The third row shows four frames of a single sequence in which the participant showed an expression of disgust [VP10].

The experiment was again carried out on the frames which covers the status of onset to apex of the expression, as done in the first two experiments. Salient facial regions were obtained automatically by using Viola-Jones object detection algorithm [VJ01] and were processed to obtain proposed PLBP features. As done in other two experiments we created image pyramid up to level 1, so in turn got five sub-regions from one facial region i.e. mouth region.  $LBP_{8,2}^{u2}$  operator was employed to extract features from every sub-region making 295 dimensional feature vector (59 dimensions / sub-region, see Section 6.2 for the dimensionality calculation).

	Two-fold	Ten-fold
SVM	90.2	91
2-nearest neighbor	91	91.4
Random forest	88.3	90.3
C4.5 decision tree	81.7	88

Table 6.10: Average recognition performance(%) for spontaneous expressions

Algorithm of Park et al.[PK08] for spontaneous expression recognition achieved results for three expressions in the range of 56% to 88% for four different configurations which is less than recognition rate of our proposed algorithm, although results cannot be compared directly as they used different database.

## 6.4 Pain recognition

Most of the models for facial expressions recognition [LBF<sup>+</sup>06, ZP07, ZJ05, PP06, VPP05, KMKB12b] function only for six universal facial expressions. There exist very few computational models that can recognize very subtle facial expressions i.e. pain [LBL07, LCM<sup>+</sup>11, ALC<sup>+</sup>09] and fatigue [ZZ06, FYS07].

Pain monitoring of patients (in a clinical scenario) is a very complicated, subjective but as well as very important task. Usually pain is self reported and according to Hadjistavropoulos et al. [HCL04] it (self report) has many limitations. Thus, it is desirable to design such a system that can automate this task. Generally, manual monitoring of pain has following problems. First, pain

cannot be recorded continuously. Second, the problem of subjectivity i.e. different patients have different perception of pain and can under report or over report the pain. Lastly, the person recording the pain has to make judgment of pain level, which could vary from person to person (again subjectivity problem). An automatic computer vision system can solve all of the above mentioned problems.

### 6.4.1 Novelty of proposed approach

In this thesis we are proposing a framework that can recognize pain by analyzing face. This work can be considered as the first of its kind, as the previous algorithms that recognize pain [CB94, LCM<sup>+</sup>11, ALC<sup>+</sup>09] utilize facial action coding system (FACS) [EF78] or employ some kind of face registration, cropping or alignment [MR08, MR06, CLTA12] as a preprocessing. Our proposed framework is neither based on FACS nor it requires face alignment.

FACS describes the facial expressions in terms of 46 component movements or action units (AUs), which roughly correspond to the individual facial muscle movements. The problem with using FACS is the time required to code every frame of the video. FACS was envisioned for manual coding by FACS human experts. It takes over 100 hours of training to become proficient in FACS, and it takes approximately 2 hours for human experts to code each minute of video [LBL07]. Second limitation of existing algorithms for pain detection [LBL07, LCM<sup>+</sup>11, ALC<sup>+</sup>09] is the problem of face registration. The algorithms proposed in [LCM<sup>+</sup>11, ALC<sup>+</sup>09] are based on Active Appearance Models (AAMs) [CEJ98] and it is known that AAM fails to register face when either the initial shape estimate of face is too far off and /or the appearance model fails to direct search toward a good match. Another limitation of AAMs is the computational complexity associated with the training phase [LBHW07]. Our proposed algorithm rectifies these problems as it doesn't require FACS coding and face image to be registered.

We are proposing a model that can recognize pain by analyzing shape and appearance information of the face. We have used shape and appearance features for detecting pain as according to Lucey et al. [LCM<sup>+</sup>11] both shape (i.e. contour)

and appearance (i.e. texture) are important for pain detection. In our proposed model we have extracted shape information using pyramid histogram of orientation gradients (PHOG) [BZM07] (See Chapter 5) and appearance information using proposed descriptor called Pyramid local binary pattern (PLBP) (discussed earlier in Section 6.1).

### 6.4.2 Pain expression database

We have used UNBC-McMaster Shoulder Pain Expression Archive Database [LCP<sup>+</sup>11] to test the performance of the proposed model as done in [LCM<sup>+</sup>11, ALC<sup>+</sup>09]. For details on UNBC-McMaster Shoulder Pain Expression Archive Database see Appendix Section A.8.

All frames in the distribution are FACS coded and the PSPI (Prkachin and Solomon Pain Intensity Scale) pain score [Prk92, PS08] is also provided for every frame. PSPI defines pain with the help of FACS action units. According to PSPI pain is the sum of intensities of action units related to eye brow lowering, cheek raiser, nose wrinkles, lip raiser and eye closure. We used PSPI score to divide the database in two parts. First part contained frames with pain score of 0 (no pain), while the other part contained frames that show patients with pain (PSPI > 0). In this way 40,029 frames were categorized in first part (82.7%) and 8,369 frames were categorized in second part (17.3%).

### 6.4.3 Framework

As mentioned earlier, we extracted shape and appearance features from the face as according to Lucey et al. [LCM<sup>+</sup>11] both shape (i.e. contour) and appearance (i.e. texture) are important for detecting pain. In our proposed framework <sup>1</sup> for pain detection, we extracted shape information using pyramid histogram of orientation gradients (PHOG) [BZM07]. For extracting appearance information we are using proposed descriptor called Pyramid local binary pattern (PLBP) (discussed in Section 6.1).

---

<sup>1</sup>video showing the result of proposed framework is available at: [http://www.youtube.com/watch?v=0\\_AIde58ZEo](http://www.youtube.com/watch?v=0_AIde58ZEo)

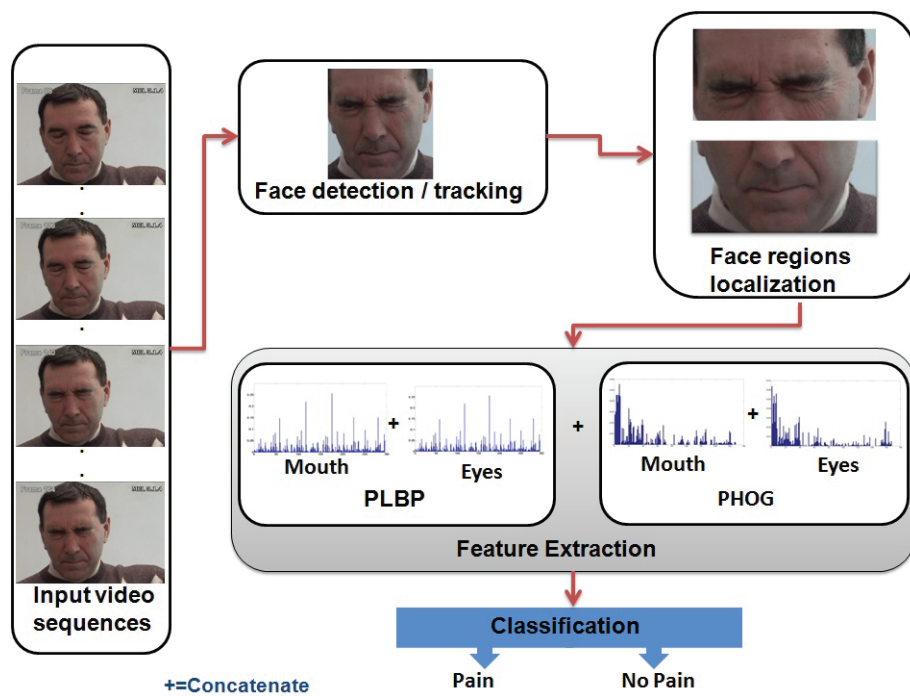


Figure 6.8: Overview of the framework.

The schematic overview of the proposed framework is illustrated in Figure 6.8 and its steps are discussed below.

1. The first step of the framework is to detect the face from the input image sequence. The framework uses Viola-Jones object detection algorithm [VJ01] to detect/track face in the video.
2. Then, the framework divides the detected face image into two equal parts. The upper face part contain regions of eyes and wrinkles on the upper portion of nose, while the lower part contains the regions of mouth and lower portion of the nose (see Figure 6.8 for illustration). This is done as according to Ashraf et al. [ALC<sup>+</sup>09], regions around the eyes, eyebrows, and lips contribute significantly towards pain vs. no pain detection and these regions can be roughly localized by dividing the face image into two parts. The purpose of dividing the face image into two is to give equal importance to the upper and lower portion of the face. Thus, the extracted features will contain localized as well as holistic information of the face as

the final feature vector is the concatenation of features from different regions and different pyramid levels.

3. Afterwards, the framework extracts PHOG and PLBP features from the upper and lower face portions and concatenates them to make the final feature vector. In Figure 6.8 the upper face portion is annotated as “eyes”, while the lower face portion is annotated as “mouth”.
4. Then, the concatenated feature vector is fed to the classifier for the final classification of the sequence.

#### 6.4.4 Experiment

The performance of the framework was evaluated for four different classifiers (mentioned below) and up to three pyramid levels (for PHOG and PLBP).

1. “Support Vector Machine (SVM)” with  $\chi^2$  kernel
2. C4.5 Decision Tree (DT) with reduced-error pruning
3. Random Forest (RF) of 10 trees
4. 2 Nearest Neighbor (2NN) based on Euclidean distance

The framework is evaluated on the complete database [LCP<sup>+</sup>11] (40,029 frames for no-pain examples and 8,369 frames for pain examples). The obtained results are presented in Figure 6.9 and Table 6.11. These values are calculated using 10-fold cross validation. The data presented in the figure not only shows the result for the proposed framework (last column in all four graphs, annotated as “combined”) but also shows the result if PLBP or PHOG descriptors are used separately (with the same framework as discussed in Section 6.4.3, the only difference will occur in step 3 of the framework, where instead of extracting both the features only one feature will be extracted). The result proves that the recognition accuracy of the proposed framework for pain detection (i.e pain vs no pain) increases by combining two features. The results of proposed framework are tabulated in Table 6.11.

One of the most interesting aspects of our approach is that it gives excellent results for a simple 2NN classifier which is a non-parametric method. This

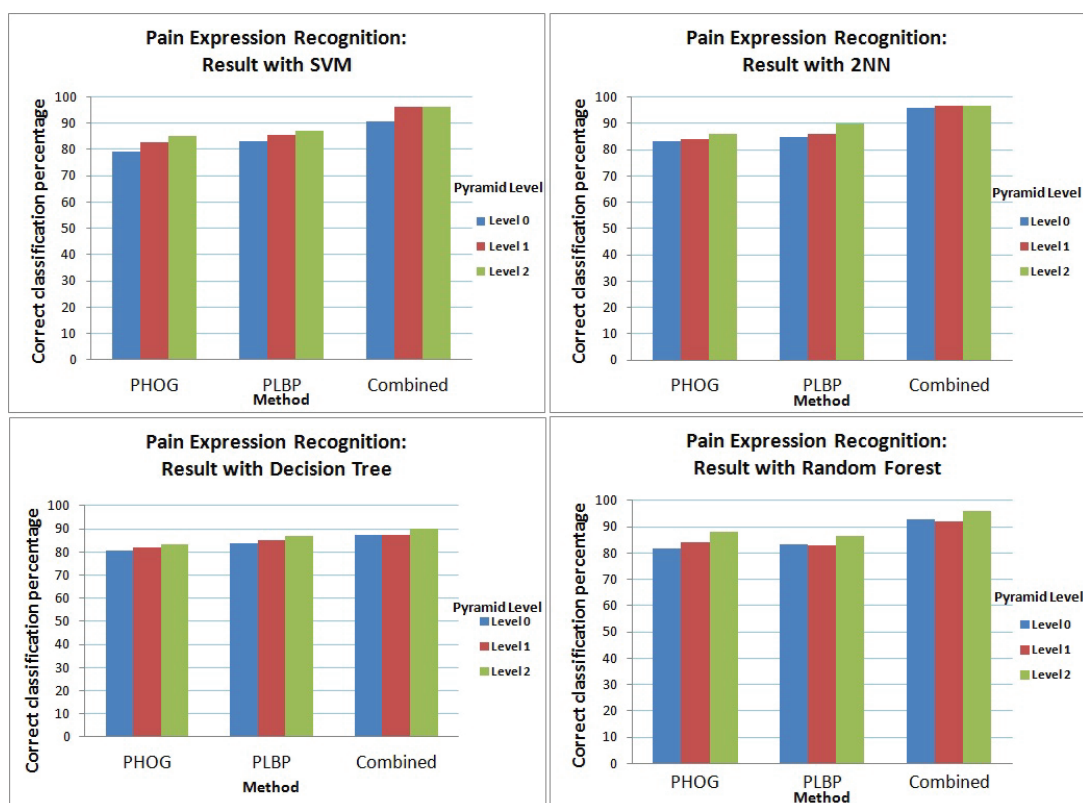


Figure 6.9: Results obtained with the proposed framework. Results are presented for four different classifiers, with the first row showing results for “SVM” and “2NN” while the second row showing results for “decision tree” and “random forest”.

points to the fact that framework do not need computationally expensive methods such as SVM, Random forests or decision trees to obtain good results. In general, the proposed framework achieved high expression recognition accuracies irrespective of the classifiers, proves the descriptive strength of the features. For comparison and reporting results (reference Table 6.12), we have used the classification results obtained by the SVM as it is the most cited method for classification in the literature.

Figure 6.10 shows the influence of the size of the training set on the performance of the four classifiers used in the experiment. For all the classifiers we have computed the average recognition accuracy using different number of folds ( $k$ 's) for the  $k$ -fold cross validation technique and plotted them in the



	Pyramid Level		
	Level 0	Level 1	Level 2
SVM	90.7	96.1	96.4
2NN	96.1	96.9	96.9
Decision tree	87.3	87.5	90.2
Random Forest	92.7	92	95.9

Table 6.11: Proposed framework recognition rate (%) for three pyramid levels.

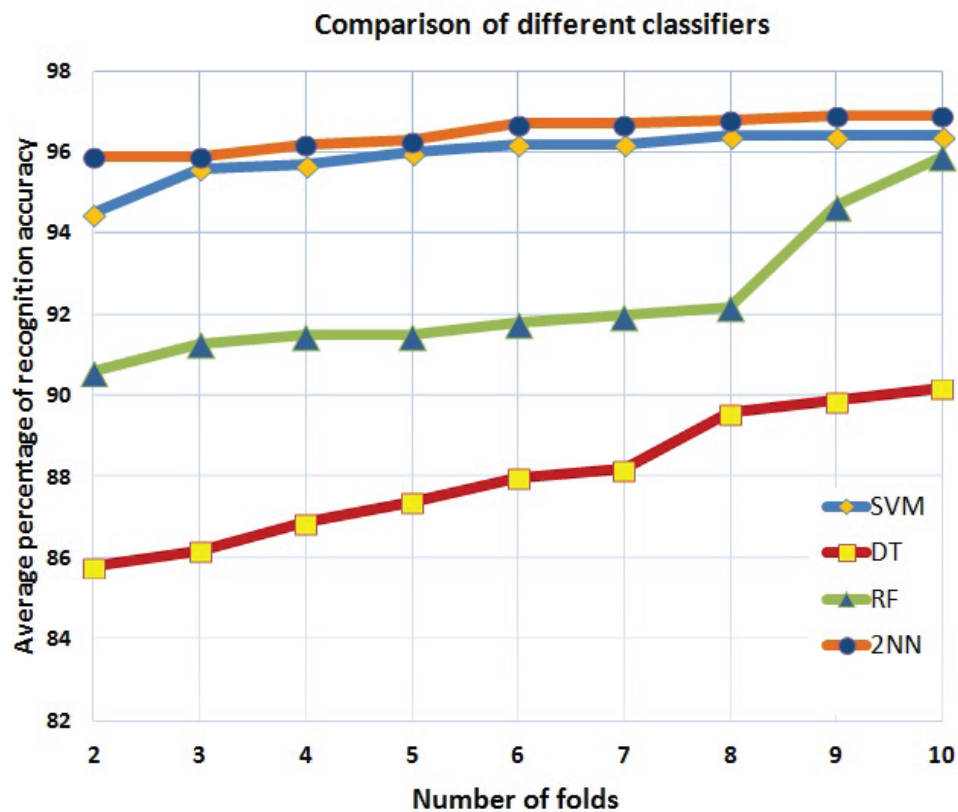


Figure 6.10: Evolution of the achieved average recognition accuracy for the expression of pain with the increasing number of folds for the  $k$ -fold cross validation technique.

Figure 6.10. Figure 6.10 also shows the supremacy of 2NN classifier in terms of achieved recognition rate. It is also observable from the figure that 2NN classifier achieved highest recognition rate among the four classifiers even with relatively



small training set (i.e. 2-folds). This indicates how well our novel feature space was clustered.

Method	Database used	Recognition rate (%)
[LCM <sup>+</sup> 11]	UNBC-McMaster [LCP <sup>+</sup> 11]	84.7
[ALC <sup>+</sup> 09]	UNBC-McMaster [LCP <sup>+</sup> 11]	81.2
[MR08]	UnKnown	93
[MR06]	UnKnown	92.08
[CLTA12]	UNBC-McMaster [LCP <sup>+</sup> 11]	89.1
<b>Ours</b>	UNBC-McMaster [LCP <sup>+</sup> 11]	<b>96.4</b>

Table 6.12: Result comparison with the state-of-the-art methods for pain recognition

Another significant contribution of the proposed framework is the computational simplicity. State-of-the-art algorithms [LCM<sup>+</sup>11, ALC<sup>+</sup>09] achieves hit rate of 84.7% and 81.2 % respectively by using  $\sim 27,000$  dimensional feature vector. While the proposed framework is able to produce results better than state-of-the-art algorithms (see Table 6.12) and it utilizes relatively significantly smaller feature vector (in terms of dimensions). Feature vector dimensionality for different pyramid levels are presented in Table 6.13. Table 6.12 shows the comparison of the achieved average recognition rate of the proposed framework with the state-of-the-art methods for pain recognition.

	PHOG [BZM07]	PLBP	Combined (proposed descriptor)
Level 0	16	118	134
Level 1	80	590	670
Level 2	336	2468	2814

Table 6.13: Feature vector dimensionality for different descriptors. Values presented here are obtained after concatenation of histograms for upper and lower face images.

With the proposed framework high recognition accuracy, reduction in feature vector dimensionality and reduction in computational time for feature extraction is achieved. Our proposed framework for pain recognition can be used for real-time applications since its unoptimized Matlab implementation run at 8 frames /

second (on windows 7 machine, with i7-2760QM processor and 6 GB RAM) which is enough as facial expression does not change abruptly.

## 6.5 Conclusion

In this chapter we presented novel descriptor (PLBP) and framework for automatic and reliable facial expression recognition. Framework is based on initial study of human vision (see Chapter 3) and works adequately on posed as well as on spontaneous expressions (Novel framework published in “Pattern Recognition Letters” [KMKB13a]). Key conclusions drawn from the study are:

1. Facial expressions can be analyzed automatically by adopting human visual system phenomenon i.e. extracting features only from the salient facial regions.
2. Features extracted using proposed pyramidal local binary pattern (PLBP) operator have strong discriminative ability as the recognition result for six basic expressions is not effected by the choice of classifier.
3. Proposed framework is robust for low resolution images, spontaneous expressions and generalizes well on unseen data.
4. Proposed framework can be used for real-time applications since its unoptimized Matlab implementation runs at 30 frames/second on Windows 64 bit machine with i7 processor running at 2.4 GHz having 6GB of RAM.

In the last part of chapter, we presented framework for automatic recognition of “pain” (Framework for pain detection published in “IEEE International Conference on Multimedia and Expo” [KMKB13b]). We extended and tweaked previously proposed two frameworks (i.e. first based on PHOG and second based on PLBP features) for facial expression recognition in order to recognize very subtle expression of pain. This work can be considered as the first of its kind, as the previous algorithms that recognize pain utilize facial action coding system (FACS) or employ some kind of face registration, cropping or alignment as a preprocessing. Our proposed framework is neither based on FACS nor it requires face alignment.

# Chapter 7

## Conclusion and perspectives

### Contents

---

<b>7.1 Contributions . . . . .</b>	<b>133</b>
7.1.1 Exploring human visual system . . . . .	134
7.1.2 Descriptor for low resolution stimuli . . . . .	136
7.1.3 Novel framework for pain recognition . . . . .	137
<b>7.2 Perspectives . . . . .</b>	<b>137</b>

---

### 7.1 Contributions

In the beginning of this report, challenges faced by computer vision community for recognizing facial expressions automatically are mentioned (refer Section 1.2.1). These challenges include computational complexity, inadequacy for uncontrolled environment i.e. low resolution images, recognition of subtle and micro expressions.

In this research work we have proposed different frameworks for facial expression recognition to overcome some of the mentioned challenges. All of proposed frameworks are inspired from human visual system, thus extracts features only from perceptual salient regions (refer Section 7.1.1). To understand human visual system, we have conducted psycho-visual experimental study with the help of an eye-tracking system. Results deduced from the experiment serves as the basis to determine salient facial regions which are algorithmically

processed to extract features for automatic analysis of expressions. Summary of results obtained by proposed frameworks on different databases is presented in Table 7.1 and are also summarized in this conclusion.

Reference Chapter	Features	Database	Recognition Rate (%)
Chapter 4	Brightness and entropy	CK+, universal expressions (Refer Appendix A.1)	71.2
Chapter 4	Brightness and entropy	FEED, universal expressions (Refer Appendix A.3)	65.7
Chapter 5	PHOG	CK+, universal expressions	95.3
Chapter 5	PHOG	FEED, universal expressions	90.3
Chapter 6	PLBP	CK+, universal expressions	96.7
Chapter 6	PLBP	FEED, universal expressions	92.3
Chapter 6	PLBP	MMI, spontaneous Expressions (Refer Appendix A.2)	91
Chapter 6	PHOG and PLBP	Pain Expression Database (Refer Appendix A.8)	96.4

Table 7.1: Summary of results obtained by different novel frameworks proposed in this research work.

### 7.1.1 Exploring human visual system

In the literature survey (for reference see Chapter 2) different methods for automatic facial expression recognition are mentioned. To analyze face in order to get discriminative information, most of these methods extract features based on some mathematical or geometrical heuristic. It is demonstrated in this research work that the task of expression analysis and recognition could be done in more conducive manner by understanding human visual system.

One of the most acceptable theory for answering the question of how human visual system analyzes stimuli in real time is by considering “salient regions” [Zha06]. According to oxford dictionary “salient” means most noticeable or most important. Then, saliency in stimuli refers to the most noticeable part or region of a scene. By focusing only on salient regions, allow only a small part of incoming sensory information to reach short term memory thus understanding a

complex scene is a series of computationally less demanding, local visual analysis problem.

Thus, we begin this research work by conducting a psycho-visual experimental study to find out which facial regions are perceptually salient. We have considered six universal facial expressions for psycho-visual experimental study as these expressions are proved to be consistent across cultures. These six expressions are anger, disgust, fear, happiness, sadness and surprise [Ekm71]. To find out which facial region is salient for different expressions eye movements of 15 subjects were recorded with an eye-tracker (Eyelink II system from SR Research, Canada) in free viewing conditions as they watch a collection of 54 videos selected from Cohn-Kanade (CK) facial expression database (Refer Appendix Section A.1). Experimental study helped in understanding visual attention and provided insight into which facial region(s) emerges as the salient according for the six universal facial expressions (See Chapter 3 for details). Results deduced from the study were then as the basis for the frameworks proposed during the course of this research work. Following are the main advantages gained by understanding and utilizing human visual attention.

1. We have validated the classical results (on visual attention) from the domain of human psychology, cognition and perception by a novel approach which incorporates eye-tracker in the experimental methodology protocol. At the same time results have been extended to include all the six universal facial expressions which was not the case in the classical studies.
2. It is demonstrated that highly discriminative feature space is created by extracting features only from the perceptually salient facial regions. Thus, human visual system inspired frameworks achieved high facial expression recognition (FER) accuracy (see result section of Chapter 5 and 6).
3. As the algorithms are based on human vision they extract features only from the salient facial region. Thus reducing feature vector dimensions and feature extraction computation time. This makes proposed algorithms suitable for real-time applications.

## 7.1.2 Descriptor for low resolution stimuli

We have proposed novel descriptor for facial features analysis, “Pyramid of Local Binary Pattern” (PLBP) that works adequately on high as well as low resolution stimuli. PLBP is a spatial representation of local binary pattern (LBP) and it represents stimuli by its local texture (LBP) and the spatial layout of the texture. The spatial layout is acquired by tiling the image into regions at multiple resolutions. If only the coarsest level is used, then the descriptor reduces to a global LBP histogram. Comparing to the multi-resolution LBP of Ojala et al. [OPM02] our descriptor selects samples in a more uniformly distributed manner, whereas Ojalas LBP takes samples centered around a point leading to missing some information in the case of face (which is different than a repetitive texture). Based on PLBP descriptor we have proposed framework for facial expression recognition. Framework achieved results similar or better than state-of-the-art methods for high as well as low resolution stimuli (for reference see Chapter 6).

Table 7.2 reports and compares the recognition results of our proposed framework (refer Chapter 5 and Chapter 6) with the state-of-the-art methods on four different low facial resolution images. Reported results of our proposed methods are obtained using support vector machine.






					
	288 x 384	144 x 192	72 x 96	36 x 48	18 x 24
PHOG [KMKB12b]	95.3	90.3	81	75	71.2
Gabor [Tia04]	91.7	92.2	91.6	77.6	68.2
Gabor [SGM09]	89.8	89.8	89.2	83	75.1
LBP [SGM09]	92.6	92.6	89.9	84.3	76.9
<b>PHOG: Chapter 5</b>	<b>95.3</b>	<b>90.3</b>	<b>81</b>	<b>75</b>	<b>71.2</b>
<b>PLBP: Chapter 6</b>	<b>96.7</b>	<b>95.3</b>	<b>93.9</b>	<b>92.8</b>	<b>90.5</b>

Table 7.2: Average recognition accuracy (%) for six universal expressions on five different facial image resolutions. First column corresponds to original resolution.

### 7.1.3 Novel framework for pain recognition

Most of the models for facial expressions recognition work only for six universal facial expressions. There exist very few computational models that can recognize very subtle facial expressions i.e. fatigue or pain. Pain monitoring of patients (in a clinical scenario) is a very complicated but as well as very important task. Usually pain is self reported, thus carry lot of subjectivity. It could be very beneficial for medical practitioners to have a system that can assist them in pain monitoring of patients. Thus, it is desirable to design such a system that can recognize pain automatically.

We have proposed model that can recognize pain by analyzing shape and appearance information of the face. We have used shape and appearance features for detecting pain as according to Lucey et al. [LCM<sup>+</sup>11] both shape (i.e. contour) and appearance (i.e. texture) are important for pain detection. In our proposed model we have extracted shape information using pyramid histogram of orientation gradients (PHOG) and appearance information using proposed descriptor called Pyramid local binary pattern (PLBP). This work can be considered as the first of its kind, as the previous algorithms that recognize pain utilize facial action coding system (FACS) [EF78] or employ some kind of face registration, cropping or alignment as a preprocessing. Our proposed framework is neither based on FACS nor it requires face alignment. We have tested our proposed model on UNBC-McMaster Shoulder Pain Expression Archive Database and achieved encouraging results (for reference see Section 6.4.4 and Table 7.1).

## 7.2 Perspectives

In future, we plan to investigate the effect of occlusion as this parameter could significantly impact the performance of the framework for real world applications. Secondly, the notion of movement could improve the performance of the proposed framework for real world applications as the experimental study conducted by Bassili [Bas79] suggested that dynamic information is important for facial expression recognition. Another parameter that needs to be

investigated is the variations of camera angle as for many applications frontal facial pose is difficult to record. Lastly, in future we would also like to evaluate the proposed framework on streaming media artifacts i.e. ringing, contouring, posterization, etc.

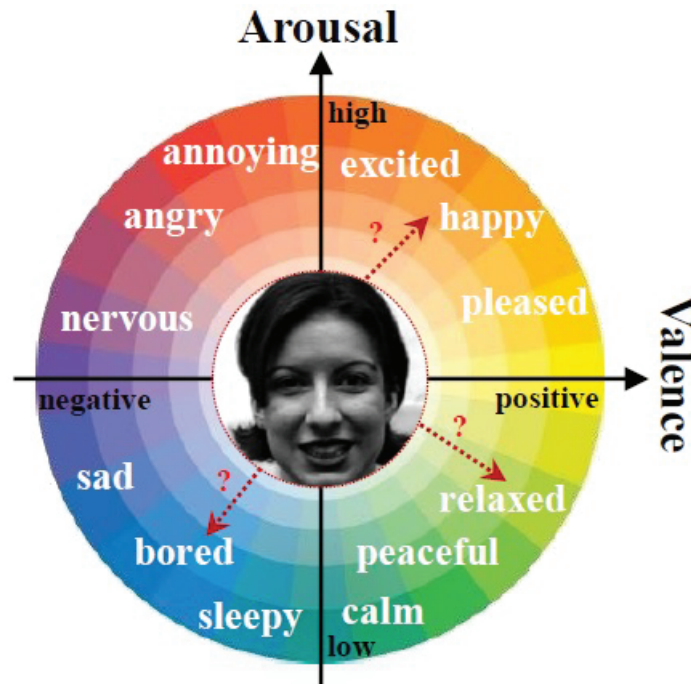


Figure 7.1: The valence-arousal (V-A) space for emotion analysis. Illustration from [HTKW13].

In a larger context, computer vision community is moving from categorical (fix or predefined number of expressions) to continuous/dimensional approach in recognizing facial expressions i.e. continuous affect analysis. Continuous affect analysis refers to continuous analysis as well as analysis that uses affect phenomenon represented in dimensional space (e.g. valence-arousal space). In continuous affect analysis expressions are considered as regions falling in a 2D space e.g. valence and arousal (i.e., V-A space) [GS13, HTKW13], as illustrated in Figure 7.1. Arousal refers to the overall level of physiological arousal and valence refers to the state of pleasure, ranging from negative to positive. For more discussion, refer to Section 2.1.4 which presents Russell’s circumplex model that advocates affective states are not discrete rather maps them to continuous



space having dimensions of valence and arousal. To develop a system that can perform continuous affect analysis, number of challenges are required to be tackled [GS13].

1. How to process continuous input. In continuous input no information about starting and ending time of affective events, expressions and affective states is available. In non-continuous input data is usually flagged with the onset, offset and apex of expression.
2. Modalities and cues. Humans express affect and emotions through different modalities i.e. vocal signals, visual signals and bio signals. It is difficult to quantify the importance of different modalities and cues, which is essential for the continuous, fast and efficient affect analysis.
3. Database. It is difficult to create affective database for continuous analysis as it is hard to engage human subjects for a longer duration of time. Secondly, responsiveness of subjects decreases with time.
4. Performance evaluation. Categorical affect recognition methods use different metrics to evaluate their performance e.g. F1 measure, average recognition accuracy (also used in this research work), area under the ROC curve etc. Finding an optimal evaluation metrics for dimensional and continuous affect prediction remains an open research issue [GP10].
5. Miscellaneous. Other problems include feature extraction, finding an optimal set of features, creating prediction methods that can handle continuous input, and training automatic predictors that can generalize well.

Another interesting problem that is catching the attention of computer vision community is to recognize facial micro expressions. Facial micro-expressions are rapid involuntary facial expressions which reveal suppressed affect. These are very rapid (1/3 to 1/25 second) involuntary facial expressions which give a brief glimpse to feelings that people undergo but try not to express [PLZP11]. The major challenges in recognising micro expressions involve their very short duration, involuntariness and lack of training and benchmarking database.



# Appendix A

## Facial expression databases

### Contents

---

A.1 Cohn-Kanade facial expression database . . . . .	142
A.2 MMI facial expression database . . . . .	143
A.3 FG-NET Facial Expressions and Emotion Database . .	147
A.4 Japanese Female Facial Expression Database . . . . .	147
A.5 AR database . . . . .	149
A.6 CAS-PEAL Database . . . . .	150
A.7 Radboud Faces Databases (RaFD) . . . . .	152
A.8 Pain Expression Database . . . . .	153
A.9 Drawbacks of the current databases . . . . .	155

---

One of the most important aspects of developing any new facial expression recognition or detection system is the choice of the database that will be used for testing the new system. If a common database is used by all the researchers, then testing the new system, comparing it with the other state of the art systems and benchmarking the performance becomes a very easy and straightforward job.

However, building such a common database that can satisfy the various requirements of the problem domain and become a standard for future research is a difficult and challenging task.

Let us now look at some of the popular expression databases that are publicly and freely available. There are many databases available and covering all of them will not be possible. Thus, I will be covering only those databases that have mostly been used in the past few years.

## A.1 Cohn-Kanade facial expression database

Cohn-Kanade(CK) database also known as the CMU-Pittsburg AU coded database [KCT00]. This is a fairly extensive database and has been widely used by the face expression recognition community.

*Subjects:* The database contains 97 university students enrolled in introductory psychology classes. They ranged in age from 18 to 30 years. 65% were female, 15% were African-American, and 3% were Asian or Latino.

*Samples:* The observation room was equipped with a chair for the subject and two Panasonic WV3230 cameras, each connected to a Panasonic S-VHS AG-7500 video recorder with a Horita synchronized time-code generator. One of the cameras was located directly in front of the subject, and the other was positioned  $30^\circ$  to the right of the subject. Only image data from the frontal camera was available in this database. Subjects were instructed by an experimenter to perform a series of 23 facial displays that included single action units (e.g., AU 12, or lip corners pulled obliquely) and combinations of action units (e.g., AU1+2, or inner and outer brows raised). Before performing each display, an experimenter described and modelled the desired display. Six of the displays were based on descriptions of prototypic basic emotions (i.e., joy, surprise, anger, fear, disgust, and sadness). See Figure A.1 for the sample face expression images from the CohnKanade database.

Later, CK database was extended to extended Cohn-Kanade (CK+) database [LCK<sup>+</sup>10]. CK+ database contains 593 sequences across 123 subjects which are FACS [EF78] coded at the peak frame. Out of 593 sequences only 327 sequences have emotion labels. This is because these are the only ones that fit the prototypic

definition. Database consists of subjects aged from 18 to 50 years old, of which 69% were female, 81% Euro-American, 13% Afro-American and 6% others. Each video (without sound) showed a neutral face at the beginning and then gradually developed into one of the six facial expression



Figure A.1: Example of Cohn- Kanade Facial Expression Database.

*Salient features:*

- a. Image sequences considered instead of mug shots.
- b. Evaluation performed based on Action Unit recognition.

## A.2 MMI facial expression database

The developers of MMI facial expression database are from the Man-Machine Interaction group of Delft University of Technology, Netherlands. This was the first web-based facial expression database [PVRM05]. The basic criteria defined for this database include easy accessibility, extensibility, manageability, user-friendliness, with online help files and various search criteria. The database contains both still

as well as video streams depicting the six basic expressions: happiness, anger, sadness, disgust, fear and surprise (see Figure A.2). It contains more than 3000 samples of both static images and image sequences of faces in frontal and in profile view displaying various facial expressions of emotion, single AU activation, and multiple AU activation.

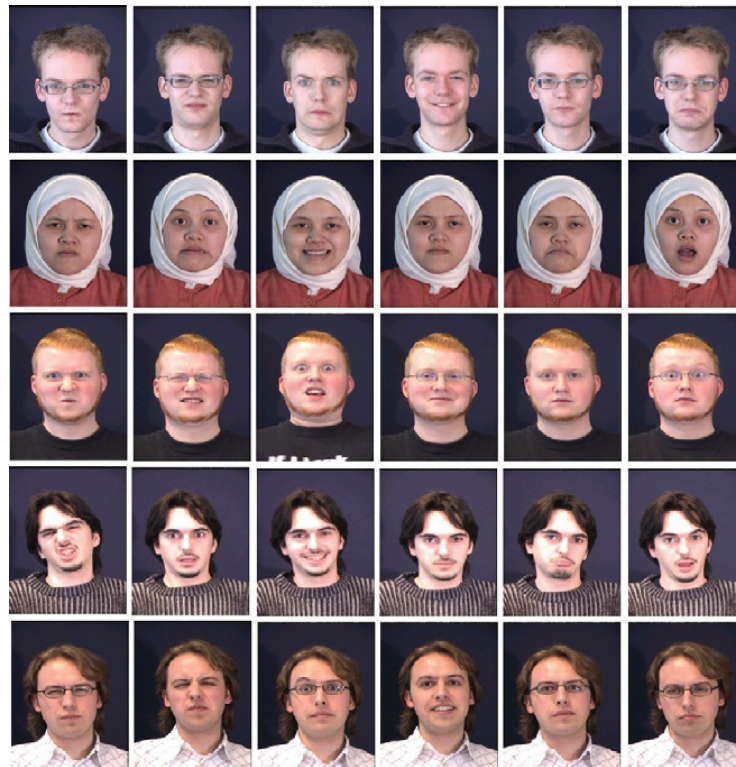


Figure A.2: Example of MMI Facial Expression Database.

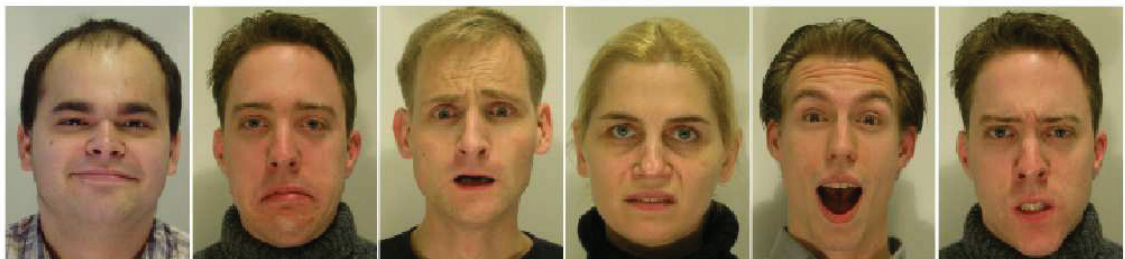


Figure A.3: Examples of static frontal-view images of facial expressions in the MMI Facial Expression Database.





Figure A.4: Examples of apex frames of dual-view image sequences in MMI Facial Expression Database.

The properties of the database can be summarised in the following way:

*Sensing:* The static facial-expression images are all true colour (24-bit) images which, when digitised, measure 720 x 576 pixels. There are approximately 600 frontal and 140 dual-view static facial-expression images (see Figure A.3). Dual-view images combine frontal and profile view of the face, recorded using a mirror. All video sequences have been recorded at a rate of 25 frames per second using a standard PAL camera. There are approximately 335 frontal-view, 30 profile-view, and 2000 dual-view facialexpression video sequences (see Figure A.4). The sequences are of variable length, lasting between 40 and 520 frames, picturing neutral-expressive-neutral facial behaviour patterns.

*Subjects:* Database includes 69 different faces of students and research staff members of both sexes (44% female), ranging in age from 19 to 62, having either a European, African, Asian, Carribean or South American ethnic background.

*Samples:* The database consists of four major parts: one part of posed expression still images, one part of posed expression videos and two parts of spontaneous expression videos. For the posed expressions the subjects were asked to display 79 series of expressions that included either a single AU (e.g., AU2) or a combination of a minimal number of AUs (e.g., AU8 cannot be displayed without AU25) or a prototypic combination of AUs (such as in expressions of emotion). The subjects were instructed by an expert (a FACS coder) on how to display the required facial expressions.

For the posed videos, the subjects were asked to include a short neutral state at the beginning and at the end of each expression. They were asked to display the required expressions while minimising out-of-plane head motions. The posed

expression videos were recorded using a mirror placed on a table next to the subject at a 45 degrees angle so that the subjects profile face was recorded together with the frontal view. The still images were recorded using natural lighting and variable backgrounds (e.g., Figure A.3). The posed expression videos were recorded with a blue screen background and two high-intensity lamps with reflective umbrellas (e.g., Figure A.4).

The first part of the spontaneous expression videos was recorded in a living room environment with no professional lighting added. The subjects were shown both funny and disgusting clips on a PC. Their reaction to the clips was recorded and cut into separate neutral-expressive-neutral videos. The expressions recorded were mainly happiness and disgust, with a fair number of surprise expressions captured as well. The second part of the spontaneous data consists of 11 primary school children who were recorded by a television crew of the Dutch tv program Klokhuis. They were asked to laugh on command. There was also a comedian present who made jokes during the recording, which made the children laugh. These spontaneous expressions were again cut into videos that contain neutral-expressive-neutral sequences. This set of data contains severe head pose variations, as the children were free to move and thought they weren't being recorded at the time.

During this research work we have used part IV and V of MMI facial expression database [VP10] to test the performance of our proposed framework. Part IV and V of the database contains spontaneous/naturalistic expressions recorded from 25 participants aged between 20 and 32 years. Of these, 12 were female and 13 male. Of the female participants, three were European, one was South American, and eight were Asian. Of the men, seven were European, two were South American and four were of Asian background. Part IV of the database has been annotated for the six basic emotions and facial muscle actions. Part V of the database has been annotated for voiced and unvoiced laughters.

*Salient features:*

- a. First web-based facial expression database.
- b. Includes both still images and image sequences.



## **A.3 FG-NET Facial Expressions and Emotion Database**

The FG-NET Facial Expressions and Emotion Database (FG-NET FEED) from the Technical University Munich is an image database containing face images showing a number of subjects performing the six different basic emotions (see Figure A.5) defined by Ekman et al. [Ekm71]. The database has been developed in an attempt to assist researchers who investigate the effects of different facial expressions [Wal06]. The database has been generated as part of the European Union project FG-NET (Face and Gesture Recognition Research Network).

*Subjects:* The database contains material gathered from 18 different individuals so far. It is intended to expand this gallery in the future. Each individual performed all six desired actions three times. Additionally three sequences doing no expressions at all are recorded. Altogether this gives an amount of 399 sequences. Depending on the kind of emotion, a single recorded sequence can take up to several seconds.

*Samples:* The images were acquired using a Sony XC-999P camera equipped with a 8mm COSMICAR 1:1.4 television lens. A BTTV 878 framegrabber card was used to grab the images with a size of 640x480 pixels, a colour depth of 24 bits and a framerate of 25 frames per second. Due to capacity reasons, the images were converted into 8 Bit JPEG-compressed images with a size of 320x240.

*Salient features:*

- a. The expressions on the faces are considered as natural as possible.

## **A.4 Japanese Female Facial Expression Database**

*Subjects:* Ten female subjects posed for the six basic expressions: happiness, sadness, anger, disgust, fear and surprise, and the neutral face (see Figure A.6).

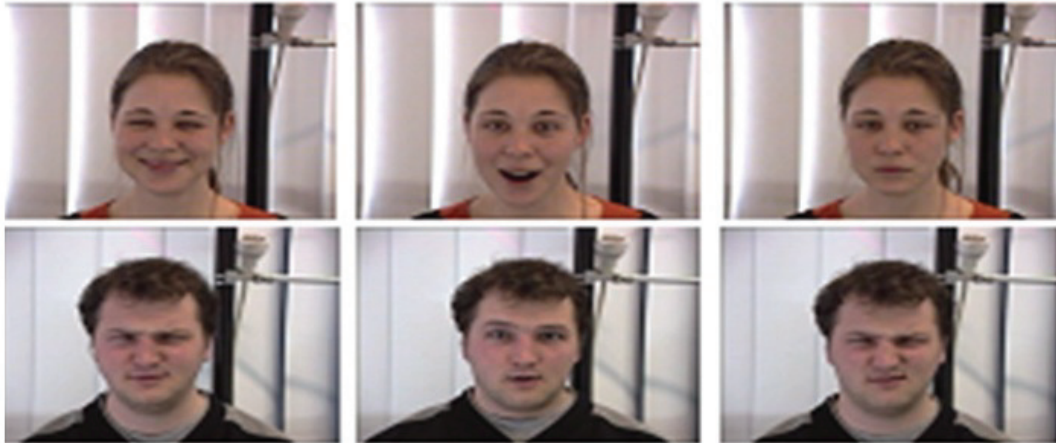


Figure A.5: Image captures from the video sequences of the six universal expressions from the FG-NET FEED.

Each of the subjects posed with three to four examples per expression to make a total of 219 images [LSKG98].

*Samples:* The still images were captured in a controlled environment. The semantic ratings of the expressions were performed from psychological experiments averaged over 60 Japanese female subjects as ground truth. According to Michael J Lyons, any expression is never a pure expression but a mixture of different emotions. So, a 5 level scale was used for each of the expression images (5 for high and 1 for low). Two such ratings were given, one with fear expression images and the other without fear expression images. The expression images are labeled as per the predominant expression in that image. Considerably low resolution images used 256 x 256 with the number of subjects just equal to ten (smallest in comparison with other databases).

*Salient features:*

- a. It is the only facial expression database that uses the minimum number of subjects.
- b. Manual rating used to identify facial expressions.

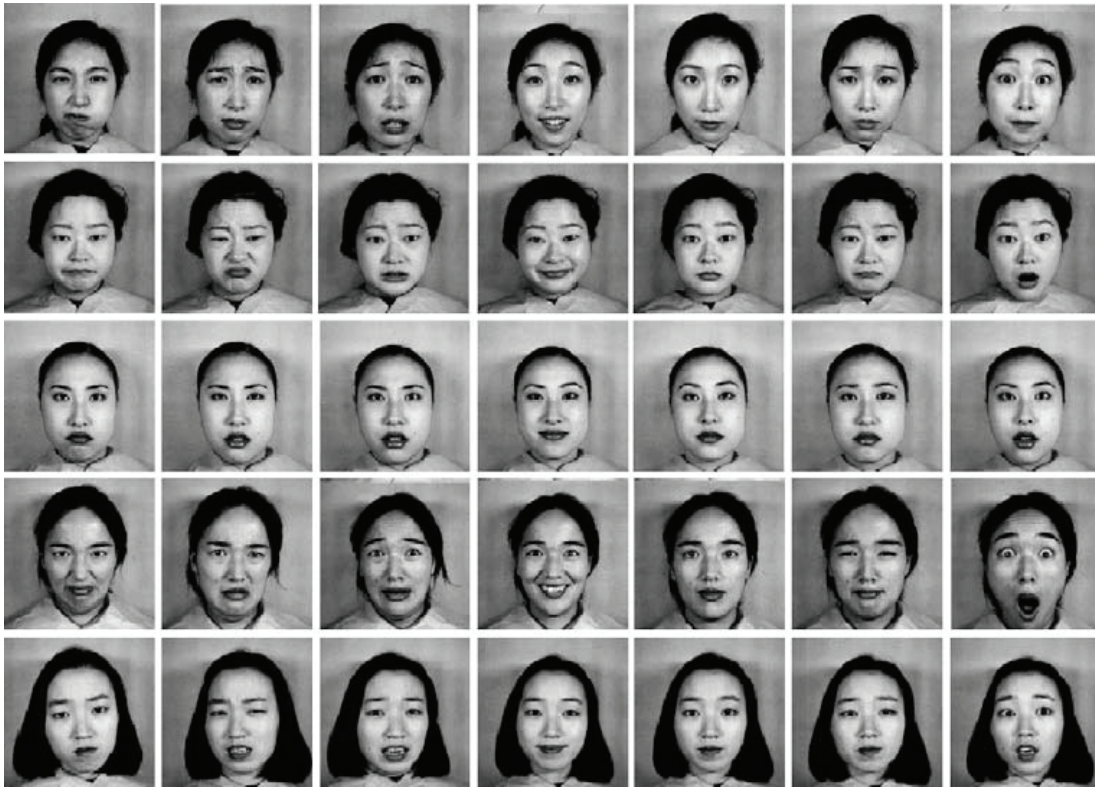


Figure A.6: Example images from the Japanese Female Facial Expression(JAFFE) database.

## A.5 AR database

The AR database was collected at the Computer Vision Centre in Barcelona, Spain in 1998 [MB98].

*Subjects:* It contains images of 116 individuals (63 men and 53 women).

*Samples:* The imaging and recording conditions (camera parameters, illumination setting, and camera distance) were carefully controlled and constantly recalibrated to ensure that settings are identical across subjects. The resulting RGB colour images are 768 576 pixels in size. The subjects were recorded twice at a 2-week interval. During each session 13 conditions with varying facial expressions, illumination and occlusion were captured. Figure A.7 shows an example for AR database. So far, more than 200 research groups have accessed the database.

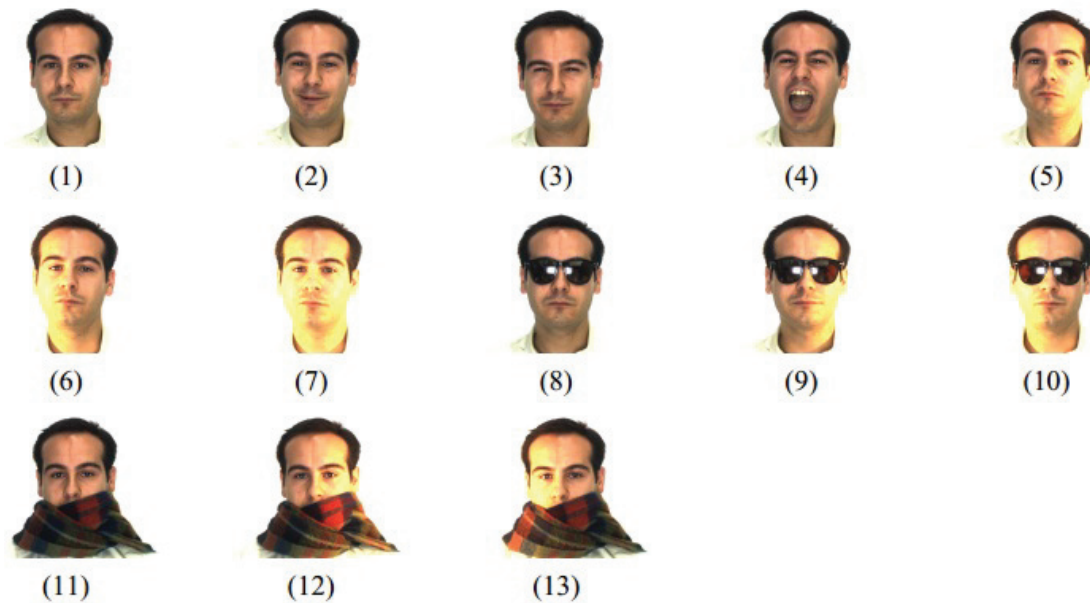


Figure A.7: AR database. The conditions are (1) neutral, (2) smile, (3) anger, (4) scream, (5) left light on, (6) right light on, (7) both lights on, (8) sun glasses, (9) sun glasses/left light (10) sun glasses/right light, (11) scarf, (12) scarf/left light, (13) scarf/right light.

*Salient features:*

- a. First ever facial expression database to consider occlusions in face images.
- b. Inclusion of scream, a non-prototypic gesture, in the database.
- c. To enable testing and modelling using this database, 22 facial feature points are manually labelled on each face.

## A.6 CAS-PEAL Database

The CAS-PEAL (pose, expression, accessory, lighting) Chinese face database was collected at the Chinese Academy of Sciences (CAS) between August 2002 and April 2003 [GCS<sup>+</sup>04].

*Subjects:* It contains images of 66 to 1040 subjects (595 men, 445 women) in seven categories: pose, expression, accessory, lighting, background, distance, and

time. Of the 99,594 images in the database, 30,900 images are available in the current release.

*Samples:* For the pose subset, nine cameras distributed in a semicircle around the subject were used. Images were recorded sequentially within a short time period (2 seconds). In addition, subjects were asked to look up and down (each time by roughly  $30^\circ$ ) for additional recordings resulting in 27 pose images. The current database release includes 21 of the 27 different poses. See Figure A.8 for example images.

To record faces under varying yet natural looking lighting conditions, constant ambient illumination together with 15 manually operated fluorescent lamps were used. The lamps were placed at  $(-90, -45, 0, 45, 90)$  azimuth and  $(-45, 0, 45)$  elevation. Recording of the illumination images typically took around two minutes; therefore small changes between the images might be present. Example images for all illumination conditions are shown in Figure A.9. For the expression subset of the database, subjects were asked to smile, to frown, to look surprised, to close their eyes, and to open the mouth. Images were captured using all nine cameras as described above. In the current database release only the frontal facial expression images are included. A smaller number of subjects were recorded wearing three types of glasses and three types of hats.



Figure A.8: Pose variation in the CAS-PEAL database. The images were recorded using separate cameras triggered in close succession. The cameras are each about  $22.5^\circ$  apart. Subjects were asked to look up, to look straight ahead, and to look down. Shown here are seven of the nine poses currently being distributed.

*Salient features:*





Figure A.9: Illumination variation in the CAS-PEAL database. The images were recorded with constant ambient illumination and manually triggered fluorescent lamps.

- a. Time/age consideration during image collection.
- b. Inclusion of multiple accessories in database.
- c. Consideration of surprise and open mouth categories in the database.

## A.7 Radboud Faces Databases (RaFD)

RaFD is a set of pictures of 67 models (including Caucasian males and females, Caucasian children, both girls and boys, and Moroccan Dutch males) displaying eight different emotions [LDB<sup>+</sup>10]. The RaFD is an initiative of the Behavioural Science Institute of the Radboud University Nijmegen, which is located in Nijmegen (the Netherlands), and can be used freely for non-commercial scientific research by researchers who work for an officially accredited university.

*Subjects:* 67 models were trained accordingly to the Facial Action Coding System, each model was trained to show the following expressions: Anger, disgust, fear, happiness, sadness, surprise, contempt, and neutral (Figure A.10 (a)). Each

emotion was shown with three different gaze directions and all pictures were taken from five camera angles simultaneously (Figure A.10(b) and (c) respectively).

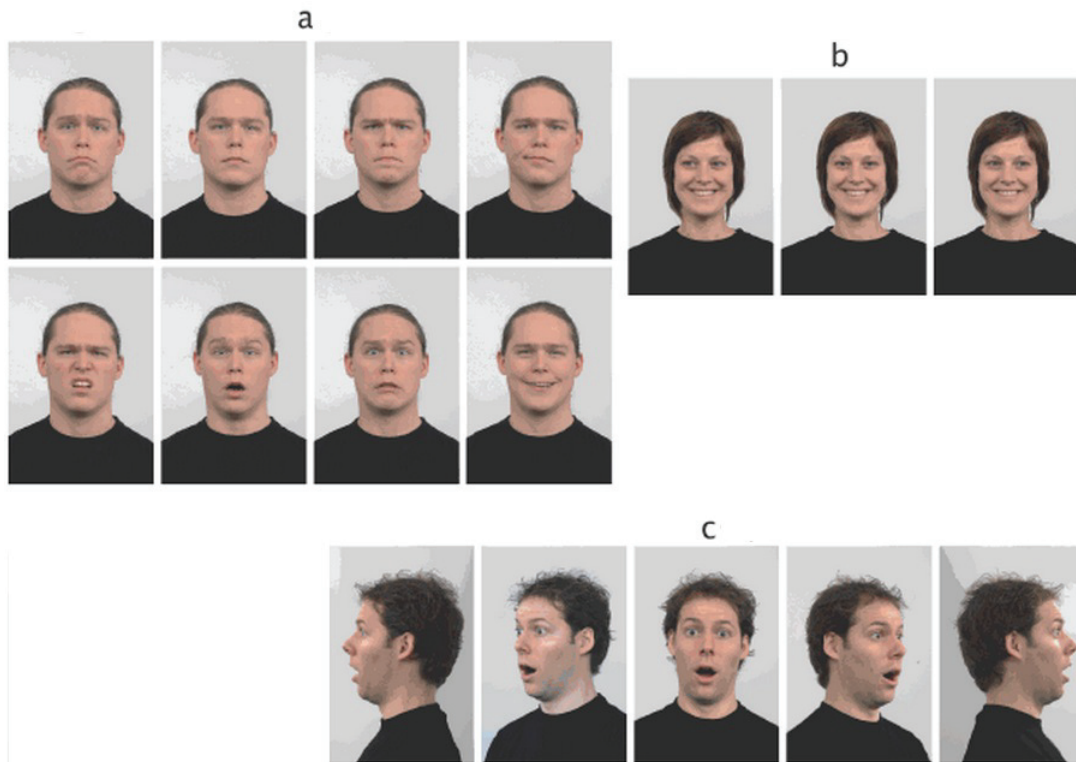


Figure A.10: (a) Eight emotional expressions from top left: sad, neutral, anger, contemptuous, disgust, surprise, fear and happiness, (b) Three gaze directions: left, straight and right, (c) Five camera angles at  $180^\circ$ ,  $135^\circ$ ,  $90^\circ$ ,  $45^\circ$  and  $0^\circ$ .

*Salient features:*

- a. Contempt, a non-prototypic expression considered.
- b. Different gaze directions considered.
- c. It is latest facial expression database.

## A.8 Pain Expression Database

In this research work we have used “UNBC-McMaster Shoulder Pain Expression Archive Database” [LCP<sup>+</sup>11] to test our proposed algorithm that recognizes

expression of pain. Researchers at the McMaster University and University of Northern British Columbia (UNBC) captured video of patient's faces (who were suffering from shoulder pain) while they were performing a series of range-of-motion tests (abduction, flexion, and internal and external rotation of each arm separately) to their affected and unaffected limbs on two separate occasions [LCP<sup>+</sup>11]. Frames in the distribution have a spatial resolution of 320 x 240 pixels. In the distributed database archive there are 200 sequences across 25 subjects, which totals 48,398 images. Spontaneous expression of pain from patients is recorded using digital cameras. Figure A.11 shows an example frames from the database. It is observable from the figure that there is a considerable head movement that occurs during sequences as the patient experiences pain.



Figure A.11: Examples of some of the sequences from the UNBC-McMaster Pain Shoulder Archive

All frames in the distribution are FACS coded and the PSPI (Prkachin and Solomon Pain Intensity Scale) pain score [Prk92, PS08] is also provided for every frame. PSPI defines pain with the help of FACS action units. According to PSPI pain is the sum of intensities of action units related to eye brow lowering, cheek raiser, nose wrinkles, lip raiser and eye closure.

*Salient features:*

1. Temporal Spontaneous Expressions: 200 video sequences containing spontaneous facial expressions relating to genuine pain.



2. Manual FACS codes: 48,398 FACS coded frames,
3. Self-Report and Observer Ratings: associated pain self-report and observer ratings at the sequence level
4. Tracked Landmarks: 66 point AAM landmarks.

## A.9 Drawbacks of the current databases

Some of the problems faced by researchers with respect to the use of available databases are:

1. Temporal patterns of the videos: Cohen et al. reported that they could not make use of the Cohn-Kanade database to train and test a Multi-Level HMM classifier because each video sequence ends in the peak of the facial expression, i.e. each sequence was incomplete in terms of its temporal pattern [CSG<sup>+</sup>03].
2. Topographic modeling: Wang and Yin reported that they note that topographic modeling is a pixel based approach and is therefore not robust against illumination changes. But in order to conduct illumination related studies, they were unable to find a database that had expressive faces against various illuminations [WY07].
3. Low resolution stimuli: As mentioned earlier there are many real world applications that require expression recognition system to work amicably on low resolution images. Smart meeting, video conferencing and visual surveillance are some examples of such applications. There is no standard database that provides low resolution stimuli. Thus in this research work we spatially downgraded stimuli from Cohn-Kanade database to test our proposed method.



# Appendix B

## Gaze Maps

As mentioned in the Section 3.3.1, the most intuitively revealing output that can be obtained from the recorded fixations data is to obtain gaze maps. During the psycho-Visual experiment, for every frame of the video and each subject  $i$ , the eye movement recordings yielded an eye trajectory  $T^i$  composed of the coordinates of the successive fixations  $f_k$ , expressed as image coordinates  $(x_k, y_k)$ :

$$T^i = (f_1^i, f_2^i, f_3^i, \dots) \quad (\text{B.1})$$

As a representation of the set of all fixations  $f_k^i$ , a human gaze map  $H(\mathbf{x})$  was computed, under the assumption that this map is an integral of weighted point spread functions  $h(\mathbf{x})$  located at the positions of the successive fixations. It is assumed that each fixation gives rise to a normally (gaussian) distributed activity. The width  $\sigma$  of the activity patch was chosen to approximate the size of the fovea. Formally,  $H(\mathbf{x})$  is computed according to Equation B.2:

$$H(\mathbf{x}) = H(x, y) = \sum_{i=1}^{N_{subj}} \sum_{f_k \in T^i} \exp\left(\frac{(x_k - x)^2 + (y_k - y)^2}{\sigma^2}\right) \quad (\text{B.2})$$

where  $(x_k, y_k)$  are the spatial coordinates of fixation  $f_k$ , in image coordinates. In all of the figures in this appendix gaze maps are presented as the heat maps where the colored blobs / human fixations are superimposed on the frame of a

video to show the areas where observers gazed. The longer the gazing time, the warmer the color is. Video showing gaze pattern of one subject for six universal expressions is available at: <http://www.youtube.com/watch?v=3pH31Xf8Ik4>.

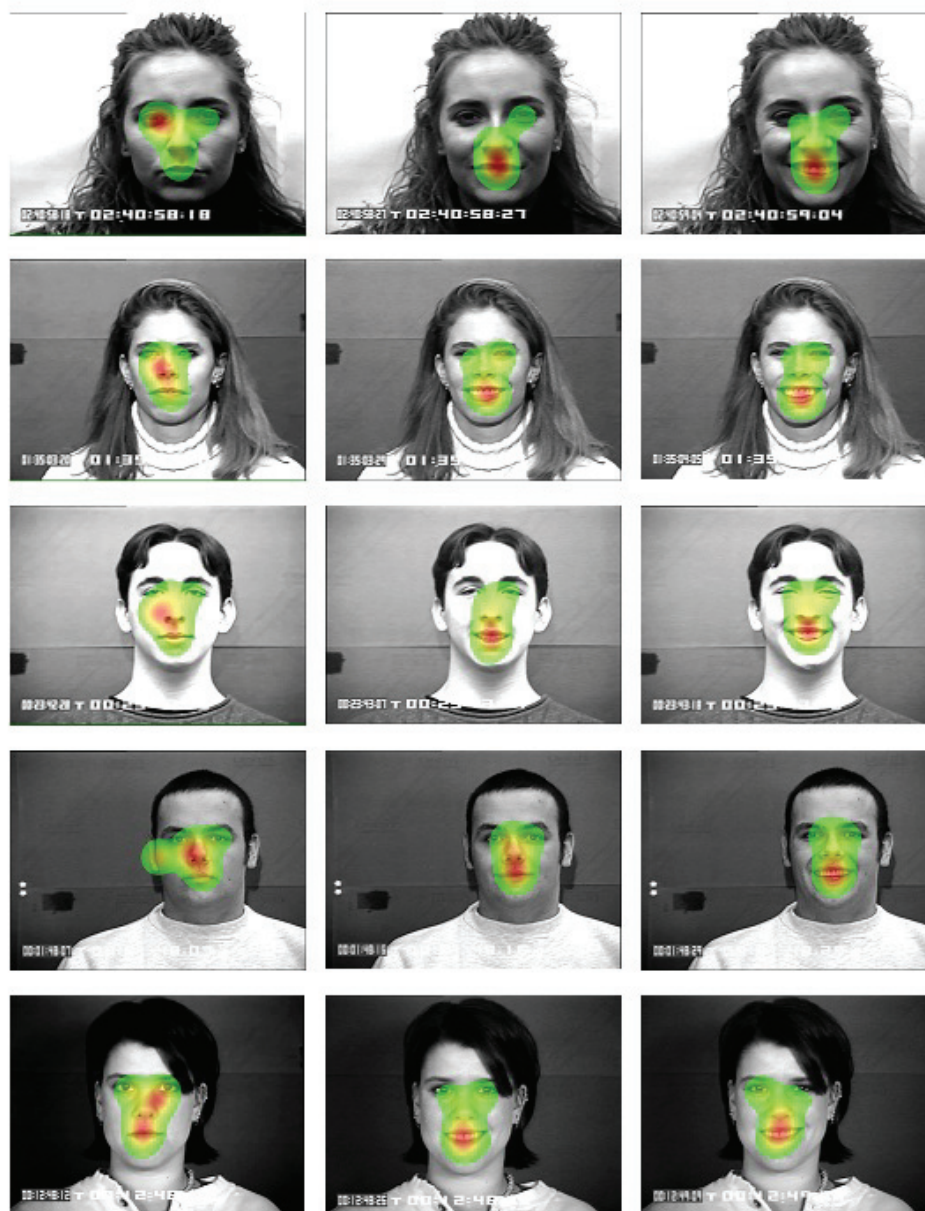


Figure B.1: Gaze maps for the expression of **happiness**.

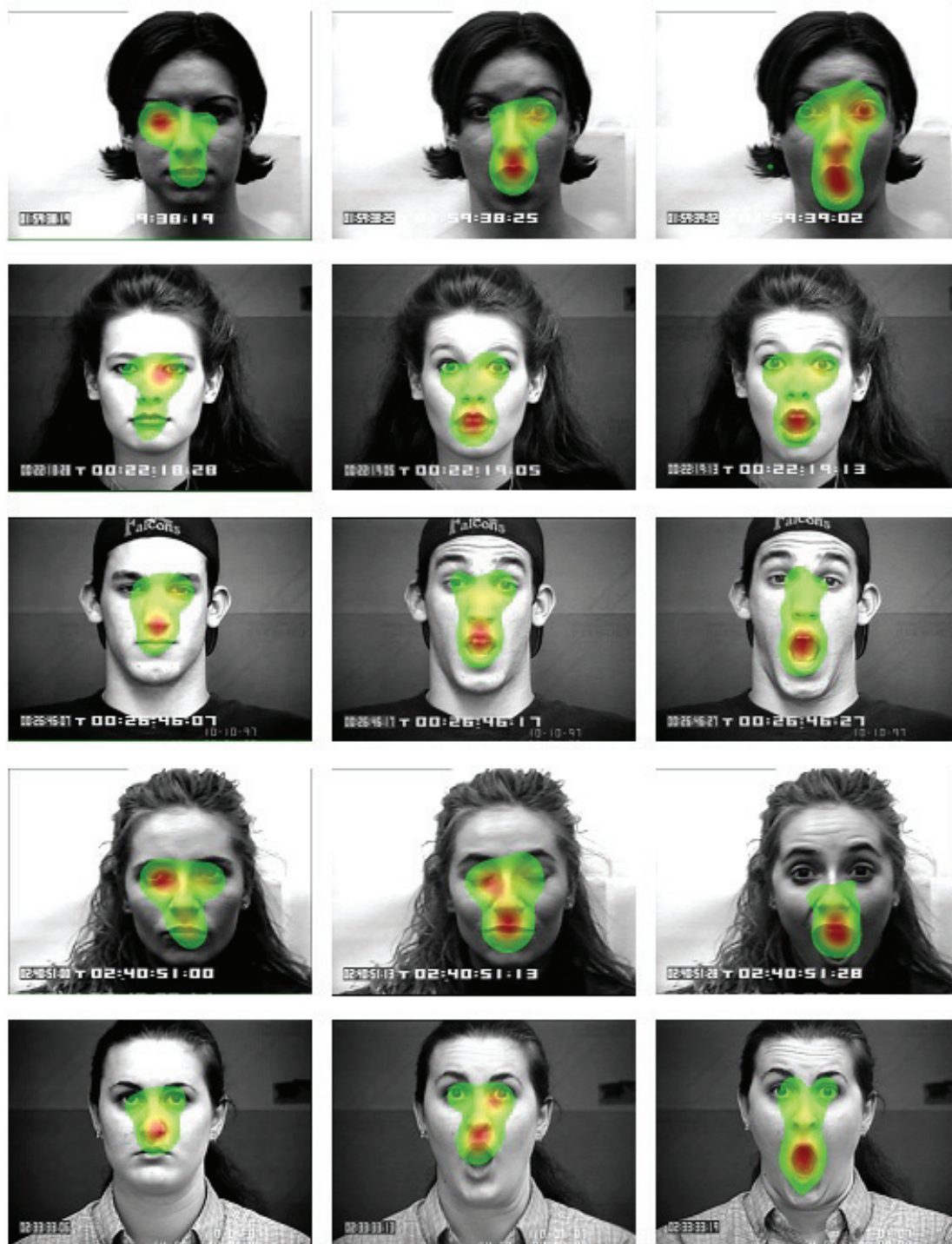


Figure B.2: Gaze maps for the expression of **surprise**.



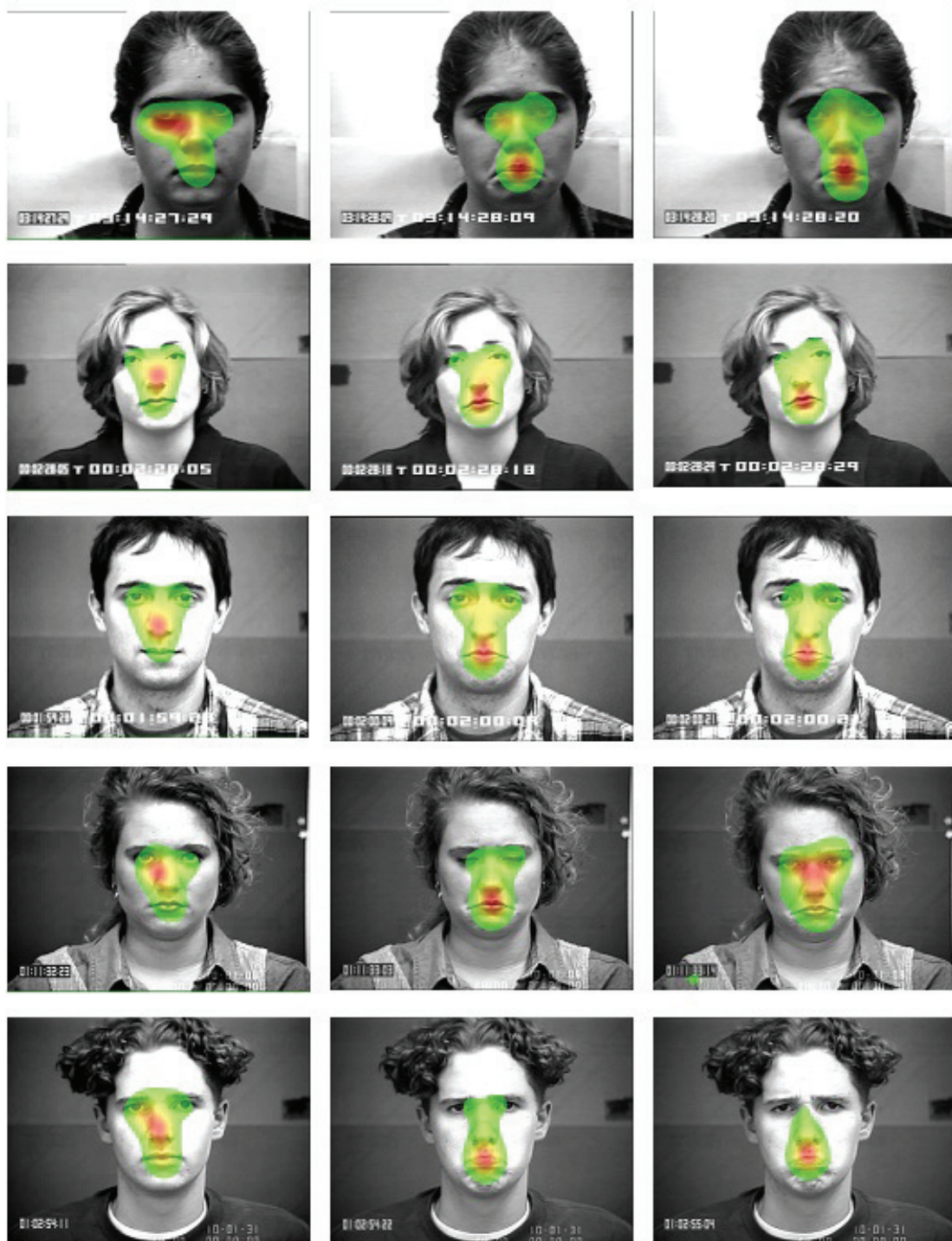


Figure B.3: Gaze maps for the expression of **sadness**.

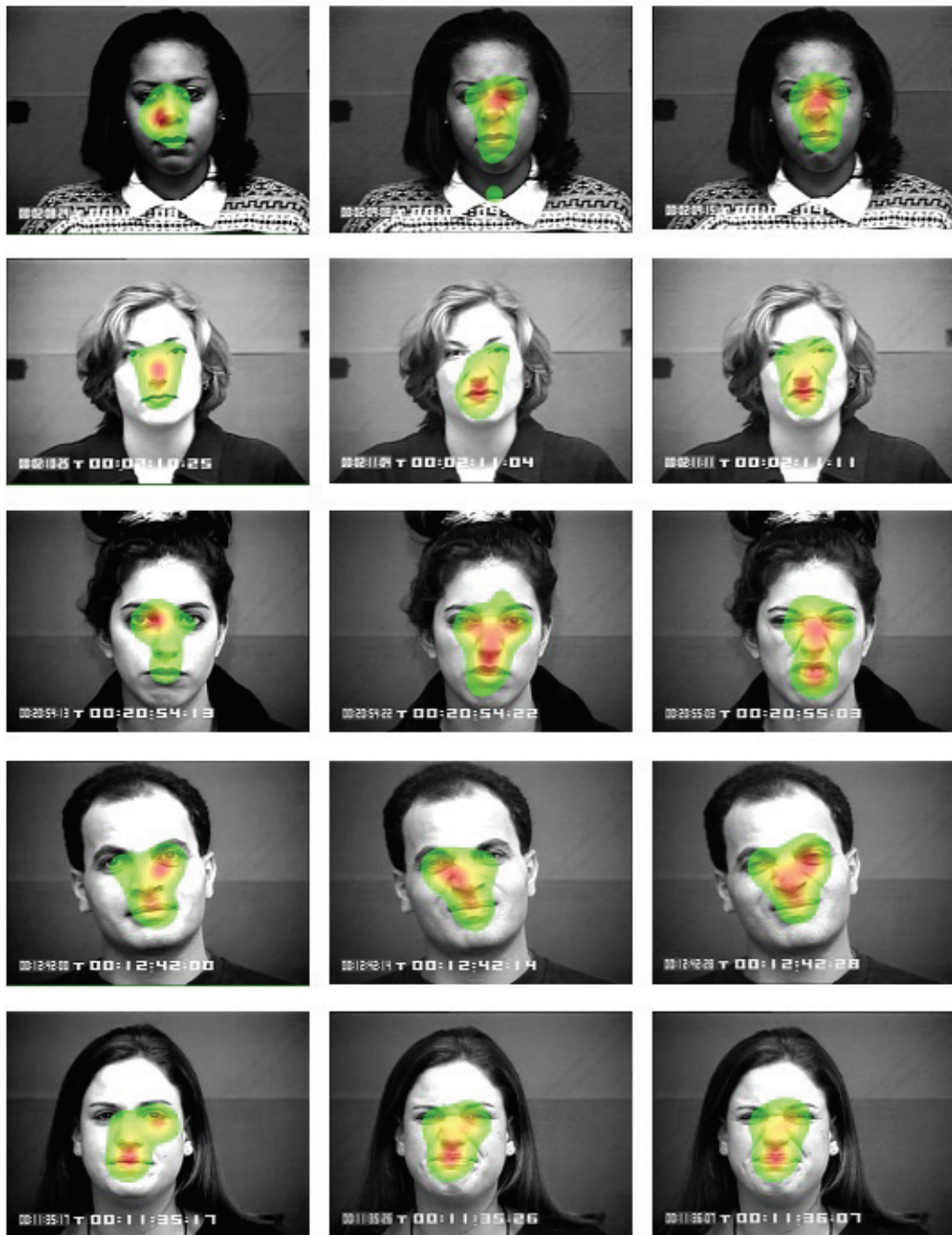


Figure B.4: Gaze maps for the expression of **disgust**.



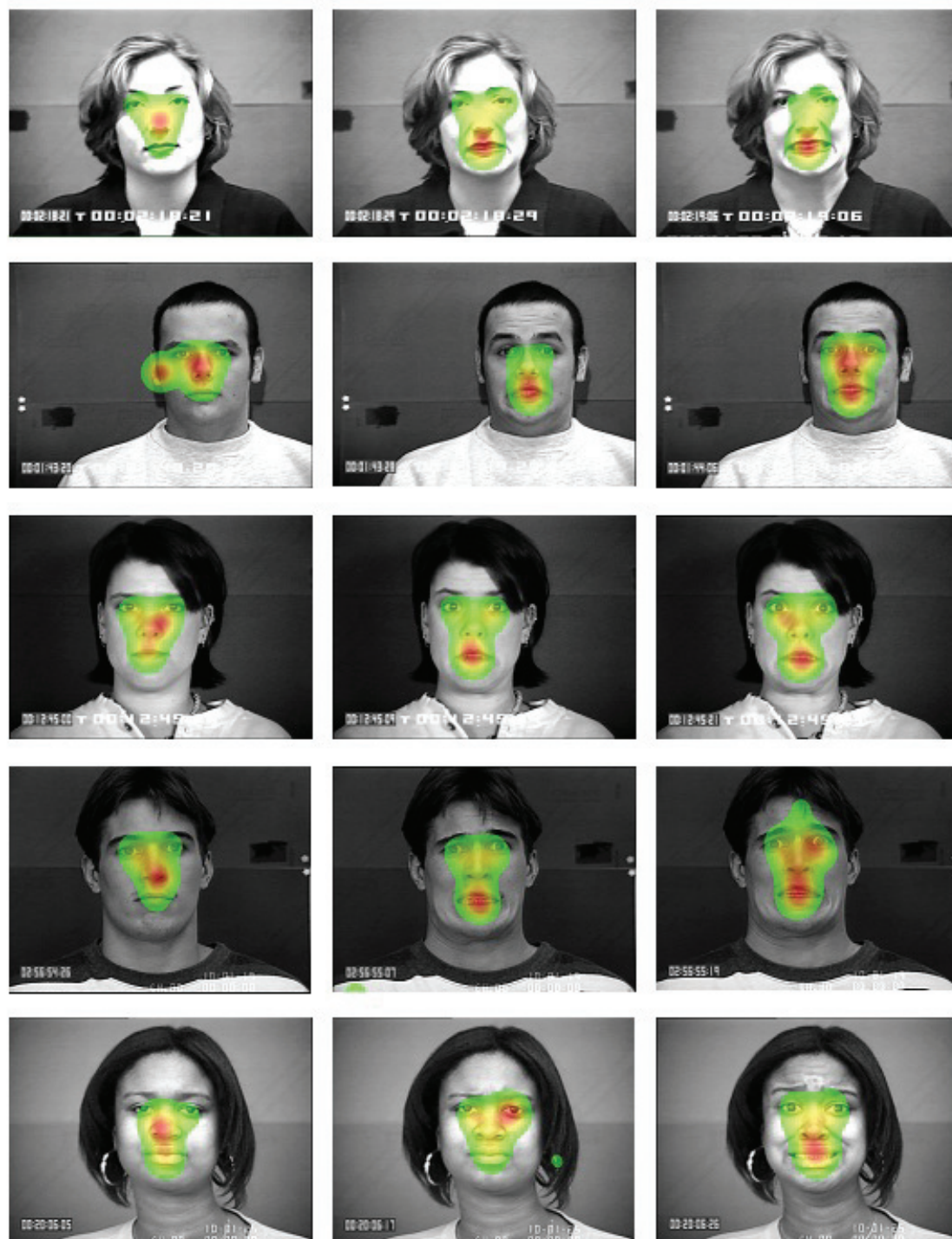


Figure B.5: Gaze maps for the expression of fear.





Figure B.6: Gaze maps for the expression of **anger**.



# Appendix C

## Color space conversion

Following are the equations to convert  $XYZ$  to  $L^*a^*b^*$  color space:

$$L^* = 116f(Y/Y_n) - 16 \quad (\text{C.1})$$

$$a^* = 500 [f(X/X_n) - f(Y/Y_n)] \quad (\text{C.2})$$

$$b^* = 200 [f(Y/Y_n) - f(Z/Z_n)] \quad (\text{C.3})$$

where

$$f(t) = \begin{cases} t^{1/3} & \text{if } t > (\frac{6}{29})^3 \\ \frac{1}{3} (\frac{29}{6})^2 t + \frac{4}{29} & \text{otherwise} \end{cases} \quad (\text{C.4})$$

Here  $X$ ,  $Y$  and  $Z$  are the CIE XYZ tristimulus values, while  $X_n$ ,  $Y_n$  and  $Z_n$  are the CIE XYZ tristimulus values of the reference *white point* (the subscript  $n$  suggests "normalized").

Following is the equations to convert RGB to XYZ color space:

$$\begin{bmatrix} X \\ Y \\ Z \end{bmatrix} = \begin{bmatrix} 2.7690 & 1.7518 & 1.1300 \\ 1.0000 & 4.5907 & 0.0601 \\ 0.0000 & 0.0565 & 5.5943 \end{bmatrix} \cdot \begin{bmatrix} R \\ G \\ B \end{bmatrix} \quad (\text{C.5})$$



# References

- [AHES09] R. Achanta, S. Hemami, F. Estrada, and S. Susstrunk. Frequency-tuned salient region detection. In *IEEE International Conference on Computer Vision and Pattern Recognition*, 2009. [xx](#), [xxi](#), [72](#), [74](#), [75](#), [76](#), [78](#), [79](#), [80](#)
- [AHP04] T. Ahonen, A. Hadid, and M. Pietikäinen. Face recognition with local binary patterns. In *European Conference on Computer Vision*, 2004. [41](#), [106](#)
- [ALC<sup>+</sup>09] A.B. Ashraf, S. Lucey, J. F. Cohn, T. Chen, Z. Ambadar, K. M. Prkachin, and P. E. Solomon. The painful face - pain expression recognition using active appearance models. *Image and Vision Computing*, 27(12):1788 – 1796, 2009. [124](#), [125](#), [126](#), [127](#), [131](#)
- [AM04] K. Anderson and P. W. McOwan. Robust real-time face tracker for use in cluttered environments. *Computer Vision and Image Understanding*, 95:184–200, 2004. [28](#)
- [AM06] K. Anderson and P. W. McOwan. A real-time automated system for the recognition of human facial expressions. *Trans. Sys. Man Cyber. Part B*, 36:96–105, 2006. [8](#)
- [AR92] N. Ambady and R. Rosenthal. Thin slices of expressive behavior as predictors of interpersonal consequences: A metaanalysis. *Psychological Bulletin*, 11(2):256–274, 1992. [2](#), [14](#)

- [AS93] M.F. Augusteijn and T.L. Skufca. Identification of human faces through texture-based feature recognition and neural network technology. In *IEEE International Conference on Neural Networks*, 1993. 28
- [AS07] S. Avidan and A. Shamir. Seam carving for content-aware image resizing. In *ACM Transactions on Graphics*, volume 26, page Article No.10, 2007. 50
- [Bas79] J. N. Bassili. Emotion recognition: The role of facial movement and the relative importance of upper and lower areas of the face. *Journal of Personality and Social Psychology*, 37:2049–2058, 1979. 137
- [BB06] S. Bezryadin and P. Bourov. Color coordinate system for accurate color image editing software. In *International Conference Printing Technology*, pages 145–148, 2006. xxi, 72, 81, 82
- [BE75] J. D. Boucher and P. Ekman. Facial areas and emotional information. *Journal of communication*, 25:21–29, 1975. 64, 67
- [BGJH09] Y. Bai, L. Guo, L. Jin, and Q. Huang. A novel feature extraction method using pyramid histogram of orientation gradients for smile recognition. In *International Conference on Image Processing*, 2009. 38, 39
- [BL<sup>+</sup>03] M. S. Bartlett, G. Littlewort, , I. Fasel, and J. R. Movellan. Real time face detection and facial expression recognition: Development and applications to human computer interaction. In *Conference on Computer Vision and Pattern Recognition Workshop, 2003.*, june 2003. 117
- [BLB<sup>+</sup>02] M. S. Bartlett, G. Littlewort, B. Braathen, T. J. Sejnowski, and J. R. Movellan. A prototype for automatic recognition of spontaneous facial actions. In *Advances in Neural Information Processing Systems*, 2002. 23, 122

- [BLF<sup>+</sup>06] M. S. Bartlett, G. C. Littlewort, M. G. Frank, C. Lainscsek, I. R. Fasel, and J. R. Movellan. Automatic recognition of facial actions in spontaneous expressions. *Journal of Multimedia*, pages 1–14, 2006. 23
- [Bul01] P. Bull. State of the art: Nonverbal communication. *Psychologist*, 14:644–647, 2001. 2, 14
- [Bus35] G.T. Buswell. *How people look at pictures*. The University of Chicago Press, 1935. 49
- [BZM07] A. Bosch, A. Zisserman, and X. Munoz. Representing shape with a spatial pyramid kernel. In *6th ACM International Conference on Image and Video Retrieval*, pages 401–408, 2007. 90, 126, 131
- [CB94] J. Cacioppo and G. Berntson. Relationship between attitudes and evaluative space: A critical review, with emphasis on the separability of positive and negative substrates. *Psychological Bulletin*, 115:401–423, 1994. 21, 125
- [CE05] J. F. Cohn and P. Ekman. Measuring facial action by manual coding, facial emg, and automatic facial image analysis. In J. A. Harrigan, R. Rosenthal, and K. Scherer, editors, *Handbook of nonverbal behavior research methods in the affective sciences*, pages 9 – 64. Oxford University Press, NY., 2005. 15
- [CEJ98] T. F. Cootes, G. J. Edwards, and Taylor C. J. Active appearance models. In *European Conference on Computer Vision*, 1998. 125
- [CET98] T. F. Cootes, G. J. Edwards, and C. J. Taylor. Active appearance models. In *European Conference on Computer Vision*, 1998. 29, 38
- [CHTH94] T. F. Cootes, A. Hill, C. Taylor, and J. Haslam. The use of active shape models for locating structures in medical images. *Image and Vision Computing*, 12:355–366, 1994. 29, 38
- [CIE31] CIE1931. *Commission internationale de l’Eclairage proceedings (CIE)*. Cambridge University Press, Cambridge., 1931. 83



- [CKWB05] D. W. Cunningham, M. Kleiner, C. Wallraven, and H. H. Bühlhoff. Manipulating video sequences to determine the components of conversational facial expressions. *ACM Transactions on Applied Perception*, 2:251–269, 2005. 64, 65
- [CLFD94] P. Carrera-Levillain and J. Fernandez-Dols. Neutral faces in context: Their emotional meaning and their function. *Journal of Nonverbal Behavior*, 18:281–299, 1994. 2, 14
- [CLTA12] J. Chen, X. Liu, P. Tu, and A. Aragonés. Person-specific expression recognition with transfer learning. In *IEEE International Conference on Image Processing (ICIP)*, 2012. 125, 131
- [Coh00] J. B. Cohen. *Visual Color and Color Mixture: The Fundamental Color Space*. University of Illinois Press, 2000. 82
- [CS04] J. F. Cohn and K. L. Schmidt. The timing of facial motion in posed and spontaneous smiles. *International Journal of Wavelets, Multiresolution and Information Processing*, 2:1–12, 2004. 123
- [CSE+92] H. Collewijn, M. R. Steinman, J. C. Erkelens, Z. Pizlo, and J. Steen. *The Head-Neck Sensory Motor System*. Oxford University Press, 1992. 60
- [CSG+03] I. Cohen, N. Sebe, A. Garg, L. S. Chen, , and T. S. Huang. Facial expression recognition from video sequences: Temporal and static modeling. *Computer Vision and Image Understanding*, 91:160–187, 2003. 155
- [CZM+11] M Cheng, G. Zhang, N. J. Mitra, X. Huang, and S. Hu. Global contrast based salient region detection. In *Computer Vision and Pattern Recognition*, 2011. 87
- [DAGG11] A. Dhall, A. Asthana, R. Goecke, and T. Gedeon. Emotion recognition using PHOG and LPQ features. In *IEEE Automatic Face and Gesture Recognition Conference FG2011, Workshop on Facial Expression Recognition and Analysis Challenge FERA*, 2011. 40, 42

- [Dar72] C. Darwin. *The Expression of the Emotions in Man and Animals*. 1872. 16
- [DBH<sup>+</sup>99] G. Donato, M. S. Bartlett, J. C. Hager, P. Ekman, and T. J. Sejnowski. Classifying facial actions. *IEEE Transaction on Pattern Analysis and Machine Intelligence*, 21:974–989, 1999. 34, 35
- [dCW02] A. C. de C. Williams. Facial expression of pain: An evolutionary account. *Behavioral and Brain Sciences*, 25:439–488, 2002. 9
- [DN96] Y. Dai and Y. Nakano. Face-texture model based on SGLD and its application in face detection in a color scene. *Pattern Recognition*, 29:1007–1017, 1996. 28
- [DT05] N. Dalal, , and B. Triggs. Histograms of oriented gradients for human detection. In *IEEE Conference on Computer Vision and Pattern Recognition*, 2005. 90, 92
- [EA02] H. A. Elfenbein and N. Ambady. On the universality and cultural specificity of emotion recognition: A meta-analysis. *Psychological Bulletin*, 28:203–235, 2002. 51
- [EF75] P. Ekman and W. V. Friesen. *Unmasking the Face: A Guide to Recognizing Emotions from Facial Clues*. Prentice Hall, Englewood Cliffs, New Jersey, 1975. 2, 14
- [EF78] P. Ekman and W. Friesen. The facial action coding system: A technique for the measurement of facial movements. *Consulting Psychologist*, 1978. 4, 9, 15, 17, 39, 40, 60, 84, 85, 113, 125, 137, 142
- [EF82] P. Ekman and W. Friesen. Felt, false, and miserable smiles. *Journal of Nonverbal Behavior*, 6(4):238–252, 1982. 122
- [EFE72] P. Ekman, W. V. Friesen, and P. Ellsworth. *Emotion in the Human Face: Guidelines for Research and an Integration of Findings*. Pergamon Press, New York, 1972. 2, 14

- [Ekm71] P. Ekman. Universals and cultural differences in facial expressions of emotion. In *Nebraska Symposium on Motivation*, pages 207–283. Lincoln University of Nebraska Press, 1971. 2, 15, 50, 84, 135, 147
- [Ekm93] P. Ekman. Facial expression of emotion. *Psychologist*, 48:384–392, 1993. 2, 14, 15
- [Ekm01] P. Ekman. *Telling Lies: Clues to Deceit in the Marketplace, Politics, and Marriage*. W. W. Norton & Company, New York, 3rd edition, 2001. 2, 14, 122
- [Ekm06] P. Ekman, editor. *Darwin and Facial Expression: A Century of Research in Review*. Malor Books, 2006. 16
- [EP95] I. Essa and A. Pentland. Facial expression recognition using a dynamic model and motion energy. In *International Conference on Computer Vision*, 1995. 41
- [ER05] P. Ekman and E. L. Rosenberg. *What the face reveals: Basic and applied studies of spontaneous expression using the Facial Action Coding System*. Oxford University Press. NY., 2005. 9, 23
- [FDWS91] J. Fernandez-Dols, H. Wallbott, and F. Sanchez. Emotion category accessibility and the decoding of emotion from facial expression and context. *Journal of Nonverbal Behavior*, 15:107–123, 1991. 2, 14
- [FMGP04] B. Fasel, F. Monay, and D. Gatica-Perez. Latent semantic analysis of facial action codes for automatic facial expression recognition. In *Proceedings of the 6th ACM SIGMM international workshop on Multimedia information retrieval*, pages 181–188, 2004. 19
- [FS95] Y. Freund and R. E. Schapire. A decision-theoretic generalization of on-line learning and an application to boosting. In *European Conference on Computational Learning Theory*, pages 23–37. Springer-Verlag, 1995. 30, 31, 43

- [FYS07] X. Fan, B. Yin, and Y. Sun. Yawning detection for monitoring driver fatigue. In *International Conference on Machine Learning and Cybernetics*, volume 2, pages 664–668, aug. 2007. 124
- [GCS<sup>+</sup>04] W. Gao, B. Cao, S. Shan, and X. Zhang D. Zhou, and D. Zhao. CAS-PEAL large-scale chinese face database and evaluation protocols. Technical report, JDL-TR-04-FR-001, Joint Research & Development Laboratory, 2004, 2004. 24, 150
- [GL13] D. Ghimire and J. Lee. Geometric feature-based facial expression recognition in image sequences using multi-class adaboost and support vector machines. *Sensors*, 13:7714–7734, 2013. 5, 98, 99, 118
- [GMK02] M.A Golner, W.B. Mikhael, and V. Krishnang. Modified jpeg image compression with region-dependent quantization. *Circuits, Systems and Signal Processing*, 21(2):163–180, 2002. 50
- [GP10] H. Gunes and M. Pantic. Automatic, dimensional and continuous emotion recognition. *International Journal of Synthetic Emotions*, 1:68–99, 2010. 139
- [GS13] H. Gunes and B. Schuller. Categorical and dimensional affect analysis in continuous input: Current trends and future directions. *Image and Vision Computing*, 31(2):120–136, 2013. 138, 139
- [GZZM10] Z. Guo, L. Zhang, D. Zhang, and X. Mou. Hierarchical multiscale lbp for face and palmprint recognition. In *IEEE International Conference on Image Processing*, pages 4521–4524, sept. 2010. 110
- [HAL09] Y. Huang, X. Ao, and Y. Li. Real time face detection based on skin tone detector. *International Journal of Computer Science and Network Security*, 9:71–77, 2009. 27
- [Han44] N. Hanawalt. The role of the upper and lower parts of the face as the basis for judging facial expressions: Ii. in posed expressions and

- "candid camera" pictures. *Journal of General Psychology*, 31:23–36, 1944. 67
- [Har06] Jonathon Stephen Hare. *Saliency for Image Description and Retrieval*. PhD thesis, University of Southampton, 2006. 6, 50
- [HBK00] U. Hess, S. Blairy, and R. E. Kleck. The influence of facial emotion displays, gender, and ethnicity on judgments of dominance and affiliation. *Nonverbal Behavior*, 24:265–283, 2000. 51
- [HCL04] T. Hadjistavropoulos, K. D. Craig, and S.K. Lacelle. *Pain: Psychological Perspectives*, chapter Social influences and the communication of pain, pages 87–112. 2004. 124
- [HFH<sup>+</sup>09] M. Hall, E. Frank, G. Holmes, B. Pfahringer, P. Reutemann, and I. Witten. The WEKA data mining software. *SIGKDD Explorations*, 11, 2009. 42
- [HGN04] E. Hadjidemetriou, M.D. Grossberg, and S.K. Nayar. Multiresolution histograms and their use for recognition. *IEEE Transactions on Pattern Analysis and Machine Intelligence*, 26(7):831–847, july 2004. 106
- [HMHY<sup>+</sup>97] C. Han, L. Mark, Hong-Yuan, G. Yu, and L. Chen. Fast face detection via morphology-based pre-processing. In *Image Analysis and Processing*, pages 469–476. Springer Berlin Heidelberg, 1997. 27
- [HTKW13] L. Hsu, W. Tseng, L. Kang, and Y. Wang. Seeing through the expression: Bridging the gap between expression and emotion recognition. In *IEEE International Conference on Multimedia and Expo*, 2013. xxiii, 138
- [HXM<sup>+</sup>04] Y. Hu, X. Xie, W.-Y. Ma, L.-T. Chia, and D. Rajan. Salient region detection using weighted feature maps based on the human visual attention model. In *Pacific Rim Conference on Multimedia*, 2004. 75

- [HZ07] X. Hou and L. Zhang. Saliency detection: A spectral residual approach. In *IEEE Conference on Computer Vision and Pattern Recognition*, 2007. [xxi](#), [74](#), [75](#), [77](#), [78](#), [79](#)
- [IKN98] L. Itti, C. Koch, and E. Niebur. A model of saliency-based visual attention for rapid scene analysis. In *IEEE Transactions on Pattern Analysis and Machine Intelligence*, volume 20, pages 1254–1259, 1998. [xx](#), [xxi](#), [6](#), [50](#), [74](#), [75](#), [78](#), [79](#)
- [Itt04] L. Itti. Automatic foveation for video compression using a neurobiological model of visual attention. *IEEE Transactions on Image Processing*, 13(10):1304–1318, 2004. [50](#)
- [Iza09] C. E. Izard. Emotion theory and research: Highlights, unanswered questions, and emerging issues. *Annual Review of Psychology*, 60:1–25, 2009. [15](#)
- [Jam90] W James. *The Principles of Psychology*. London : Macmillan, 1890. [5](#)
- [JHP06] C. Koch J. Harel and P. Perona. Graph-based visual saliency. In *Proceedings of Neural Information Processing Systems (NIPS)*, 2006. [xx](#), [xxi](#), [74](#), [75](#), [76](#), [77](#), [78](#), [79](#)
- [JOW<sup>+</sup>05] T. Jost, N. Ouerhani, R. Wartburg, R. Müri, and H. Hügli. Assessing the contribution of color in visual attention. *Computer Vision and Image Understanding. Special Issue on Attention and Performance in Computer Vision*, 100:107–123, 2005. [5](#), [58](#)
- [JVP11] B. Jiang, M. F. Valstar, and M. Pantic. Action unit detection using sparse appearance descriptors in space-time video volumes. In *IEEE Conference on Automatic Face and Gesture Recognition*, 2011. [42](#)
- [KBP08] I. Kotsia, I. Buciu, and I Pitas. An analysis of facial expression recognition under partial facial image occlusion. *Image and Vision Computing*, 26:1052–1067, 2008. [42](#)

- [KCT00] T. Kanade, J. F. Cohn, and Y. Tian. Comprehensive database for facial expression analysis. In *Fourth IEEE International Conference on Automatic face and Gesture Recognition (FG'00)*, pages 46–53, 2000. 23, 35, 36, 37, 39, 43, 142
- [KKD10] R.A. Khan, H. Konik, and E. Dinet. Enhanced image saliency model based on blur identification. In *25th International Conference of Image and Vision Computing New Zealand*, December 2010. 50
- [KMKB11] R. A. Khan, A. Meyer, H. Konik, and S. Bouakaz. Facial expression recognition using entropy and brightness features. In *11th International Conference on Intelligent Systems Design and Applications (ISDA)*, December 2011. 87
- [KMKB12a] R. A. Khan, A. Meyer, H. Konik, and S. Bouakaz. Exploring human visual system: study to aid the development of automatic facial expression recognition framework. In *Computer Vision and Pattern Recognition Workshop*, 2012. 69
- [KMKB12b] R. A. Khan, A. Meyer, H. Konik, and S. Bouakaz. Human vision inspired framework for facial expressions recognition. In *IEEE International Conference on Image Processing*, 2012. xxii, 42, 103, 119, 120, 124, 136
- [KMKB13a] R.A. Khan, A. Meyer, H. Konik, and S. Bouakaz. Framework for reliable, real-time facial expression recognition for low resolution images. *Pattern Recognition Letters*, 34(10):1159–1168, 2013. 132
- [KMKB13b] R.A. Khan, A. Meyer, H. Konik, and S. Bouakaz. Pain detection through shape and appearance features. In *IEEE International Conference on Multimedia and Expo (ICME)*, pages 1–6, 2013. 132
- [KP97] C. Kotropoulos and I. Pitas. Rule-based face detection in frontal views. In *IEEE International Conference on Acoustics, Speech, and Signal Processing*, pages 2537–2540, 1997. 26

- [KT04a] S. H. Kotsia and M.M. Trivedi. Robust real-time detection, tracking, and pose estimation of faces in video streams. In *International Conference on Pattern Recognition*, 2004. 30
- [KT04b] M. Kolsch and M. Turk. Analysis of rotational robustness of hand detection with a viola-jones detector. In *International Conference on Pattern Recognition*, pages 107–110, 2004. 30, 90
- [KT09] S. P. Khandait and R.C. Thool. Hybrid skin detection algorithm for face localization in facial expression recognition. In *Advance Computing Conference*, pages 398–401, 2009. 27
- [KU85] C. Koch and S. Ullman. Shifts in selective visual attention: towards the underlying neural circuitry. *Human Neurobiology*, 4:219–227, 1985. 74
- [KZP08] I. Kotsia, S. Zafeiriou, and I. Pitas. Texture and shape information fusion for facial expression and facial action unit recognition. *Pattern Recognition*, 41:833–851, 2008. 5, 40, 42, 86, 98, 99, 118
- [LBF<sup>+</sup>06] G. Littlewort, M. S. Bartlett, I. Fasel, J. Susskind, and J. Movellan. Dynamics of facial expression extracted automatically from video. *Image and Vision Computing*, 24:615–625, 2006. 5, 34, 43, 86, 98, 99, 118, 124
- [LBHW07] Y. M. Lui, J.R. Beveridge, A.E. Howe, and L.D. Whitley. Evolution strategies for matching active appearance models to human faces. In *International Conference on Biometrics: Theory, Applications, and Systems*, 2007. 30, 125
- [LBL07] G. Littlewort, M. S. Bartlett, and K. Lee. Faces of pain: automated measurement of spontaneous facial expressions of genuine and posed pain. In *9th international conference on Multimodal interfaces*, 2007. 19, 42, 123, 124, 125



- [LBP95] T. K. Leung, M.C. Burl, and P. Perona. Finding faces in cluttered scenes using random labeled graph matching. In *International Conference on Computer Vision*, pages 637–644, 1995. 27
- [LCK<sup>+</sup>10] P. Lucey, J. F. Cohn, T. Kanade, J. Saragih, Z. Ambadar, and I. Matthews. The extended cohn-kande dataset (CK+): A complete facial expression dataset for action unit and emotion-specified expression. In *IEEE Conference on Computer Vision and Pattern Recognition Workshops*, 2010. 60, 84, 94, 112, 113, 142
- [LCM<sup>+</sup>11] P. Lucey, J. F. Cohn, I. Matthews, S. Lucey, S. Sridharan, J. Howlett, and K.M. Prkachin. Automatically detecting pain in video through facial action units. *IEEE Transactions on Systems, Man, and Cybernetics, Part B: Cybernetics*, 41(3):664–674, june 2011. 124, 125, 126, 131, 137
- [LCP<sup>+</sup>11] P. Lucey, J. F. Cohn, K. M. Prkachin, P. E. Solomon, and I. Matthews. Painful data: The UNBC-McMaster shoulder pain expression archive database. In *IEEE International Conference on Automatic Face and Gesture Recognition*, pages 57–64, 2011. 8, 126, 128, 131, 153, 154
- [LDB<sup>+</sup>10] O. Langner, R. Dotsch, G. Bijlstra, D. H. J. Wigboldus, S. T. Hawk, and V. A. Knippenberg. Presentation and validation of the radboud faces database. *Cognition and Emotion*, 24:1377–1388, 2010. 152
- [Leo96] Breiman Leo. Bagging predictors. *Machine Learning*, 24:123–140, 1996. 43
- [LFCY06] S. Liao, W. Fan, A. C. S. Chung, and D. Yeung. Facial expression recognition using advanced local binary patterns, tsallis entropies and global appearance features. In *IEEE International Conference on Image Processing*, 2006. 42
- [LFT10] Y. Lin, B. Fang, and Y. Tang. A computational model for saliency maps by using local entropy. In *AAAI Conference on Artificial Intelligence*, 2010. 72

- [LQI11] Z. Li, S. Qin, and L. Itti. Visual attention guided bit allocation in video compression. *Image and Vision Computing*, 29:1–14, 2011. 50
- [LSKG98] M. Lyons, Akamatsu S, M. Kamachi, and J. Gyoba. Coding facial expressions with gabor wavelet. In *In 3rd International Conference on Automatic Face and Gesture Recognition.*, 1998. 148
- [LSP06] S. Lazebnik, C. Schmid, and J. Ponce. Beyond bags of features: spatial pyramid matching for recognizing natural scene categories. In *IEEE Conference on Computer Vision and Pattern Recognition*, 2006. 92
- [LVB<sup>+</sup>93] M. Lades, J. C. Vorbrüggen, J. Buhmann, J. Lange, C. Malsburg, R. P. Würtz, and W. Konen. Distortion invariant object recognition in the dynamic link architecture. *IEEE Transactions on Computers*, 42:300–311, 1993. 34
- [Man84] G. Mandler. *Mind and body: Psychology of emotion and stress*. W.W. Norton and Company. New York., 1984. 21
- [MB98] A. R. Martinez and R. Benavente. The AR face database. Technical report, Computer Vision Center (CVC), Barcelona, 1998. 149
- [MB10] H. Mekami and S. Benabderrahmane. Towards a new approach for real time face detection and normalization. In *International Conference on Machine and Web Intelligence*, pages 455–459, 2010. 26, 30
- [MB11] S. Moore and R. Bowden. Local binary patterns for multi-view facial expression recognition. *Computer Vision and Image Understanding*, 115(4):541 – 558, 2011. 110
- [Mit97] Tom M. Mitchell. *Machine Learning*. McGraw-Hill Science, 1997. 40
- [MKH<sup>+</sup>07] G. Michael, K. Kristian, H. Helen, N. Clifford, S. Bjorn, R. Gerhard, and M. Tobias. On the necessity and feasibility of detecting a drivers emotional state while driving. In *Affective Computing and*

- Intelligent Interaction*, Lecture Notes in Computer Science, pages 126–138. 2007. 22
- [MP98] H. Moon and P.J. Phillips. The FERET verification testing protocol for face recognition algorithms. In *Third IEEE International Conference on Automatic Face and Gesture Recognition*, 1998. 24
- [MR73] A. Mehrabian and J. Russell. A measure of arousal seeking tendency. environment and behavior. *Environment and Behavior*, 5:5:315–333., 1973. 21
- [MR06] M. M. Monwar and S. Rezaei. Appearance-based pain recognition from video sequences. In *International Joint Conference on Neural Networks*, pages 2429–2434, 2006. 125, 131
- [MR08] M. Monwar and S. Rezaei. Video analysis for view-based painful expression recognition. In *IEEE International Joint Conference on Neural Networks*, pages 3619–3626, 2008. 125, 131
- [MZ03] Y. F. Ma and H. J. Zhang. Contrast-based image attention analysis by using fuzzy growing. In *11th ACM International Conference on Multimedia*, pages 374–381, 2003. 50, 75
- [NCWB08] M. Nusseck, D. W. Cunningham, C. Wallraven, and H. H. Bülthoff. The contribution of different facial regions to the recognition of conversational expressions. *Journal of vision*, 8:1–23, 2008. 64, 65
- [NH98] A.V. Nefian and III Hayes, M.H. Face detection and recognition using hidden markov models. In *IEEE International Conference on Image Processing*, volume 1, pages 141–145 vol.1, 1998. 30
- [OAVE93] B. Olshausen, C. Anderson, and D. Van Essen. A neurobiological model of visual attention and invariant pattern recognition based on dynamic routing of information. *Neuroscience*, 13:4700–4719, 1993. 6, 50

- [OFG97] E. Osuna, R. Freund, and F. Girosi. Training support vector machines: an application to face detection. In *IEEE Conference on Computer Vision and Pattern Recognition*, pages 130–136, 1997. 30
- [OP99] T. Ojala and M. Pietikäinen. Unsupervised texture segmentation using feature distributions. *Pattern Recognition*, 32:477–486, 1999. 36, 107
- [OPH96] T. Ojala, M. Pietikäinen, and D. Harwood. A comparative study of texture measures with classification based on featured distribution. *Pattern Recognition*, 29:51–59, 1996. 36, 106, 107
- [OPM02] T. Ojala, M. Pietikäinen, and T. Mäenpää. Multiresolution gray-scale and rotation invariant texture classification with local binary patterns. *IEEE Transaction on Pattern Analysis and Machine Intelligence*, 24:971–987, 2002. xxii, 36, 106, 107, 108, 136
- [Pan09] M. Pantic. *The Encyclopedia of biometrics*, volume 6, chapter Facial Expression Analysis. 2009. xvii, 16
- [Par74] F. I. Parke. *A parametric model for human faces*. PhD thesis, Department of Computer Science, University of Utah, 1974. 13
- [PK08] S. Park and D. Kim. Spontaneous facial expression classification with facial motion vector. In *IEEE Conference on Automatic Face and Gesture Recognition*, 2008. 124
- [Plu80] R. Plutchik. *Emotion: A psychoevolutionary synthesis*. Harper and Row, New York., 1980. 19
- [PLZP11] T. Pfister, X. Li, G. Zhao, and M. Pietikäinen. Recognising spontaneous facial micro-expressions. In *International Conference on Computer Vision*, pages 1449–1456, 2011. 139
- [POP98] C. P. Papageorgiou, M. Oren, and T. Poggio. A general framework for object detection. In *International Conference on Computer Vision*, pages 555–562, 1998. 30

- [PP06] M. Pantic and I. Patras. Dynamics of facial expression: recognition of facial actions and their temporal segments from face profile image sequences. *IEEE Transactions on Systems, Man, and Cybernetics*, 36:433–449, 2006. 38, 124
- [PPNH06] M. Pantic, A. Pentland, A. Nijholt, and T. Huang. Human computing and machine understanding of human behavior: A survey. In *ACM International Conference on Multimodal Interfaces*, 2006. 2, 9, 38, 39
- [Prk92] K. Prkachin. The consistency of facial expressions of pain: a comparison across modalities. *Pain*, 51:297–306, 1992. 126, 154
- [PS08] K. Prkachin and P. E. Solomon. The structure, reliability and validity of pain expression: Evidence from patients with shoulder pain. *Pain*, 139:267–274, 2008. 126, 154
- [PS10] G.A. Poghosyan and H. G. Sarukhanyan. Decreasing volume of face images database and efficient face detection algorithm. *Information Theories and Applications*, 17, 2010. 36
- [PVRM05] M. Pantic, M. F. Valstar, R. Rademaker, and L. Maat. Web-based database for facial expression analysis. In *IEEE International Conference on Multimedia and Expo*, 2005. 24, 39, 61, 143
- [QL08] M. Qi and Z. Liming. Saliency-based image quality assessment criterion. In De-Shuang Huang, II Wunsch, DonaldC., DanielS. Levine, and Kang-Hyun Jo, editors, *Advanced Intelligent Computing Theories and Applications. With Aspects of Theoretical and Methodological Issues*, volume 5226 of *Lecture Notes in Computer Science*, pages 1124–1133. Springer Berlin Heidelberg, 2008. 50
- [Qui93] J. R. Quinlan. *C4.5: Programs for Machine Learning*. Morgan Kaufmann, 1993. 44

- [RBK96] H.A. Rowley, S. Baluja, and T. Kanade. Neural network-based face detection. In *IEEE Conference on Computer Vision and Pattern Recognition*, pages 203–208, 1996. 30
- [RCB02] U. Rajashekar, L. K. Cormack, and A.C Bovik. Visual search: Structure from noise. In *Eye Tracking Research & Applications Symposium*, pages 119–123, 2002. 6, 49, 50
- [Rus80] J. Russell. A circumplex model of affect. *Journal of Personality and Social Psychology*, 39:1161–1178., 1980. 21
- [Rus95] J Russell. Facial expression of emotion: What lies beyond minimal universality. *Psychological Bulletin*, 118:379–391, 1995. 21
- [SBR10] K. Scherer, T. Banziger, and E. Roesch, editors. *A Blueprint for Affective Computing*. Oxford University Press, 2010. 2, 9, 21
- [Sca98] B. Scassellati. Eye finding via face detection for a foveated, active vision system. In *15th Nat. Conf. Artificial Intelligence*, pages 969–976, 1998. 28
- [SF96] D. Saxe and R. Foulds. Toward robust skin identification in video images. In *International Conference on Automatic Face and Gesture Recognition*, pages 379–384, 1996. 27
- [SGM09] C. Shan, S. Gong, and P. W. McOwan. Facial expression recognition based on local binary patterns: A comprehensive study. *Image and Vision Computing*, 27:803–816, 2009. xxii, 33, 35, 36, 37, 41, 42, 106, 115, 116, 117, 119, 120, 136
- [Sin95] P. Sinha. *Perceiving and Recognizing Three-Dimensional Forms*. PhD thesis, M. I. T., Cambridge, MA, 1995. 28
- [Sir93] S.A. Sirohey. Human face segmentation and identification. Technical Report CS-TR-3176, University of Maryland, USA., 1993. 27

- [SSBW92] M. Sayette, D. Smith, M. Breiner, and G. Wilson. The effect of alcohol on emotional response to a social stressor. *Journal of Studies on Alcohol*, 53:541–545, 1992. 9
- [STR<sup>+</sup>05] V. Setlur, S. Takagi, R. Raskar, M. Gleicher, and B. Gooch. Automatic image retargeting. In *4th International Conference on Mobile and Ubiquitous Multimedia*, pages 59–68, 2005. 50
- [SW63] C. E. Shannon and W. Weave. *The Mathematical Theory of Communication*. University of Illinois Press, 1963. 72
- [Tia04] Y. Tian. Evaluation of face resolution for expression analysis. In *Computer Vision and Pattern Recognition Workshop*, 2004. xxii, 34, 35, 86, 98, 99, 101, 118, 119, 120, 136
- [TKC01] Y. Tian, T. Kanade, and J. F. Cohn. Recognizing action units for facial expression analysis. *IEEE Transactions on Pattern Analysis and Machine Intelligence*, 23:97–115, 2001. 19
- [TKCis] Y. Tian, T. Kanade, and J. F. Cohn. *Handbook of Face Recognition*. Springer, 2005, Chapter 11. Facial Expression Analysis. 23, 33
- [TP91] M. Turk and A. Pentland. Eigenfaces for recognition. *Journal of Cognitive Neuroscience*, 3:71–86, 1991. 30
- [TSW<sup>+</sup>95] J. K. Tsotsos, M. C. Scan, W. Y. K. Wai, Y. Lai, N. Davis, and F. Nufflo. Modeling visual attention via selective tuning. *Artificial Intelligence*, 78:507–545, 1995. 6, 49
- [TTUP13] A Tanveer, J. Taskeed, and C. Ui-Pil. Facial expression recognition using local transitional pattern on gabor filtered facial images. *IETE Technical Review*, 30(1):47–52, 2013. 98, 99, 117, 118
- [Val08] Michel Francois Valstar. *Timing is everything, a spatio-temporal approach to the analysis of facial actions*. PhD thesis, Imperial College, 2008. xvii, 17, 18, 19, 21

- [Vap98] Vladimir N. Vapnik. *Statistical Learning Theory*. Wiley-Interscience, 1998. 41
- [VJ01] P. Viola and M. Jones. Rapid object detection using a boosted cascade of simple features. In *IEEE Conference on Computer Vision and Pattern Recognition*, 2001. xviii, 30, 31, 32, 33, 35, 36, 72, 85, 90, 96, 111, 113, 124, 127
- [VP06] M. Valstar and M. Pantic. Fully automatic facial action unit detection and temporal analysis. In *Computer Vision and Pattern Recognition Workshop*, 2006. 38, 39
- [VP10] M.F. Valstar and M. Pantic. Induced disgust, happiness and surprise: an addition to the MMI facial expression database. In *International Language Resources and Evaluation Conference*, 2010. xxii, 113, 122, 123, 146
- [VPAC06] M.F. Valstar, M. Pantic, Z. Ambadar, and J.F. Cohn. Spontaneous vs. posed facial behavior: automatic analysis of brow actions. In *Proceedings of the 8th international conference on Multimodal interfaces, ICMI '06*, pages 162–170, New York, NY, USA, 2006. ACM. 122
- [VPP05] M.F. Valstar, I. Patras, and M. Pantic. Facial action unit detection using probabilistic actively learned support vector machines on tracked facial point data. In *IEEE Conference on Computer Vision and Pattern Recognition Workshop*, pages 76–84, 2005. 5, 38, 39, 99, 121, 124
- [Wal06] F. Wallhoff. Facial expressions and emotion database. [www.mmk.ei.tum.de/~waf/fgnet/feedtum.html](http://www.mmk.ei.tum.de/~waf/fgnet/feedtum.html), 2006. 84, 86, 94, 100, 121, 147
- [WBG87] F. Weiss, G. Blum, and L. Gleberman. Anatomically based measurement of facial expressions in simulated versus hypnotically induced affect. *Motivation and Emotion*, 11(1):67–81, 1987. 122



- [WCX11] W. Wang, W. Chen, and D. Xu. Pyramid-based multi-scale lbp features for face recognition. In *International Conference on Multimedia and Signal Processing (CMSP)*, volume 1, pages 151 – 155, 2011. 110
- [WO06] J. Whitehill and C.W. Omlin. Haar features for FACS AU recognition. In *Automatic Face and Gesture Recognition*, 2006. 36
- [WS00] G. Wyszecki and W. S. Stiles. *Color Science: Concepts and Methods, Quantitative Data and Formulae*. Wiley-Interscience, 2000. 72, 76
- [WWJ13] Ziheng Wang, Shangfei Wang, and Qiang Ji. Capturing complex spatio-temporal relations among facial muscles for facial expression recognition. In *IEEE Conference on Computer Vision and Pattern Recognition*, pages 3422–3429, 2013. 5
- [WY07] J. Wang and L. Yin. Static topographic modeling for facial expression recognition and analysis. *Computer Vision and Image Understanding*, 108:19–34, 2007. 155
- [Yan11] Peng Yang. *Facial expression recognition and expression intensity estimation*. PhD thesis, New Brunswick Rutgers, The State University of New Jersey, 2011. 41, 43
- [YH94] G. Yang and T. Huang. Human face detection in a complex background. *Pattern Recognition*, 27:53–63, 1994. 26
- [YKA02] Ming-Hsuan Yang, D. Kriegman, and N. Ahuja. Detecting faces in images: a survey. *IEEE Transactions on Pattern Analysis and Machine Intelligence*, 24:34–58, 2002. 26, 28, 30
- [YLM10] P. Yang, Q. Liu, and D. N. Metaxas. Exploring facial expressions with compositional features. In *IEEE Conference on Computer Vision and Pattern Recognition*, 2010. 5, 36, 43, 85, 86, 96, 98, 99, 113, 117, 118
- [Yng70] V. H. Yngve. On getting a word in edgewise. In *Papers from the Sixth Regional Meeting of the Chicago Linguistic Society*, pages 567–578. Chicago Linguistic Society, 1970. 2, 14

- [Zha06] L. Zhaoping. Theoretical understanding of the early visual processes by data compression and data selection. *Network: computation in neural systems*, 17:301–334, 2006. 5, 134
- [ZHF<sup>+</sup>06] Z. Zeng, Y. Hu, Y. Fu, T. S. Huang, G. I. Roisman, and Z. Wen. Audio-visual emotion recognition in adult attachment interview. In *Proceedings of the 8th international conference on Multimodal interfaces*, 2006. 3
- [ZJ05] Y. Zhang and Q. Ji. Active and dynamic information fusion for facial expression understanding from image sequences. *IEEE Transactions on Pattern Analysis and Machine Intelligence*, 27:699–714, 2005. 38, 39, 124
- [ZLY<sup>+</sup>12] Lin Zhong, Qingshan Liu, Peng Yang, Bo Liu, Junzhou Huang, and D.N. Metaxas. Learning active facial patches for expression analysis. In *IEEE Conference on Computer Vision and Pattern Recognition*, pages 2562–2569, 2012. 5
- [ZP07] G. Zhao and M. Pietikäinen. Dynamic texture recognition using local binary patterns with an application to facial expressions. *IEEE Transaction on Pattern Analysis and Machine Intelligence*, 29:915–928, 2007. 5, 36, 37, 42, 86, 98, 99, 106, 118, 124
- [ZPRH09] Z. Zeng, M. Pantic, G.I. Roisman, and T.S. Huang. A survey of affect recognition methods: Audio, visual, and spontaneous expressions. *IEEE Transactions on Pattern Analysis and Machine Intelligence*, 31:39–58, 2009. 2
- [ZZ06] Z. Zhang and J. Zhang. Driver fatigue detection based intelligent vehicle control. In *18th International Conference on Pattern Recognition*, volume 2, pages 1262–1265, 2006. 124
- [ZZH09] J. Zhang, Q. Zhang, and J. Hu. Rgb color centroids segmentation (CCS) for face detection. *ICGST International Journal on Graphics, Vision and Image Processing*, 9:1–9, 2009. 27